ABSTRACT

Title of Thesis:	INSIGHTS INTO BENTHIC MACROINVERTEBRATE ECOLOGY IN THE NORTHERN BERING AND SOUTHERN CHUKCHI SEAS FROM STABLE ISOTOPE ANALYSIS
	Emma Mackenzie Green, Master of Science, 2022
Thesis Directed By:	Dr. Lee W. Cooper Marine-Estuarine and Environmental Science

In the Pacific Arctic Region, the northern Bering Sea and southern Chukchi Sea support large and diverse communities of benthic macroinvertebrates that provide an important link to the pelagic communities and marine mammals that rely on the benthic populations for food. While the abundance and biomass of these benthic macroinvertebrates are well

documented, little is known about how benthic macroinvertebrates interact with each other and how these interactions are affected by climate change. I measured the stable isotope composition (bulk δ^{15}N and δ^{13}C values) of similar species collected in 2014, 2016, 2017, and 2021 in the northern Bering and southern Chukchi Seas. Although there was little change over time in either δ^{15}N or δ^{13}C values, both stable isotope ratios were significantly different between stations with differing production phenologies. The southern Chukchi Sea (a productive set of sites with high chlorophyll concentrations throughout the summer) had lower δ^{15}N values and higher δ^{13}C values, while the northern Bering Sea site with production mostly associated with the period of sea ice breakup had higher δ^{15}N values and lower δ^{13}C values. This pattern was observed across similar species and feeding types. The higher δ^{15}N values in the northern Bering Sea could be due to an extra step in the food chain from bacterial reworking. The contrast between these two regions in δ^{13}C might indicate higher primary production in the southern Chukchi Sea compared to the northern Bering Sea. The differing food web dynamics between these two sites highlight the benthic diversity across small scales and similar organisms in Pacific Arctic food webs.

INSIGHTS INTO BENTHIC MACROINVERTEBRATE ECOLOGY IN THE NORTHERN BERING AND SOUTHERN CHUKCHI SEAS FROM STABLE ISOTOPE ANALYSIS

by

Emma Mackenzie Green

Thesis submitted to the Faculty of the Graduate School of the
University of Maryland, College Park, in partial fulfillment
of the requirements for the degree of
Master of Science
2022

Advisory Committee:
Professor Lee W. Cooper, Chair
Professor Jacqueline M. Grebmeier
Associate Professor Ryan J. Woodland

Acknowledgements

I would first like to thank and acknowledge my primary advisor, Dr. Lee Cooper. He was patient with my many questions and kept me on a focused path. Both Lee and Dr. Jacqueline Grebmeier supported me when I accepted my position outside of the polar realm in my final year of graduate school, and I am so grateful. I also want to thank Jackie and Lee for pushing me out of my Maryland comfort zone and bringing me on two trips to the Arctic. Although they have both been to Alaska, Canada, and the Arctic many times, they still took the time to show me all their favorite places and tourist attractions.

I would also like to acknowledge the fellow Grebmeier-Cooper lab members. Christina Goethel welcomed me to CBL and has always taken the time to support my work and be a resource on all things graduate school. As a non-traveler, I am so thankful for her patience and support while packing and traveling. Stephanie Soques and Alicia Clarke welcomed me into the sorting lab and southern Maryland with open arms, and I am so grateful for their friendship. Brittany Clark, Meghan Music, and Joanna Snellings were also so supportive during my graduate career. Cédric Magen was an integral part of my time at CBL. Even though he was not my advisor, he took on the role on many occasions: patiently teaching me to run the IRMS, taking my calls about my mess-ups on nights and weekends, and pestering me to write.

Outside of the Grebmeier-Cooper lab, my committee member, Ryan Woodland has continued to mentor and support me along with all the other professors

and students at CBL. Nina Santos has been so instrumental in my time at CBL. She spent hours working with me on the mass spectrometer, made sure I was taken care of while writing, and encouraged me every step of the way. I am so grateful for her friendship and guidance.

The St. Mary's River Watershed Association board and Bob Lewis have been so supportive and accommodating while I've worked to finish up my thesis and graduate school. I would also like to acknowledge and thank my family, especially my parents, my partner for encouraging me to apply and stick with graduate school, and my friends for supporting me and coming to visit southern Maryland.

I would not be in graduate school without my undergraduate professor and thesis advisor, Dr. Bob Paul. He insisted that I run my undergraduate thesis samples at CBL with Lee despite my attempts to take the easy way out. Those samples led me to work with Lee on this project.

Data collection was a collaborative process conducted by the Grebmeier-Cooper Laboratory with assistance from the crews and science parties of the Canadian Coast Guard Ship Sir Wilfrid Laurier. The principal investigators for our laboratory and the Distributed Biological Observatory are Jacqueline Grebmeier and Lee Cooper. Within the Grebmeier-Cooper Laboratory, Christina Goethel, Jacqueline Grebmeier, and Lee Cooper collected the environmental and biological samples onboard the CCGS Sir Wilfrid Laurier. At the laboratory, Stephanie Soques and Alicia Clarke analyzed the sediment grain size and prepared the sediment for stable isotope and total organic carbon and nitrogen analysis. The Grebmeier-Cooper

laboratory also sorted and identified the benthic macroinvertebrates for biomass and abundance analysis. I'd like to thank the entire Grebmeier-Cooper laboratory for their efforts.

Table of Contents

List of Tables

List of Figures

1 Introduction

1.1 Pacific Arctic Region and the Distributed Biological Observatory

The Pacific Arctic region encompasses the Bering Sea, Chukchi Sea, Eastern Siberian Sea, and Beaufort Sea (Figure 1). The region is influenced by the northward inflow of Pacific Ocean water into the Arctic Ocean through the Bering Strait (Woodgate, 2005; Figure 1). The Bering Strait connects the Bering and Chukchi Seas and is the only connection between the Arctic Ocean and the Pacific Ocean. The water column and benthic fauna are supported by open water production in the summer and large, episodic blooms along the marginal ice zone as ice retreats in the spring. Zooplankton are not mature enough during the early season ice retreat to consume the bloom along the marginal ice zone. Therefore, much of the bloom along the marginal ice zone sinks to the benthos (Bluhm & Gradinger, 2008). For example, in the Chukchi Sea, about 60% of the primary production in the water column is transported to the benthos or to an adjacent basin (Campbell et al., 2009). The large flux of organic material to the benthos in certain regions of the Pacific Arctic has allowed benthic macroinvertebrate populations to achieve high biomass and abundance. These areas where high benthic macroinvertebrate biomass and

abundance cluster have been termed “hot spots” (Grebmeier et al., 2015).

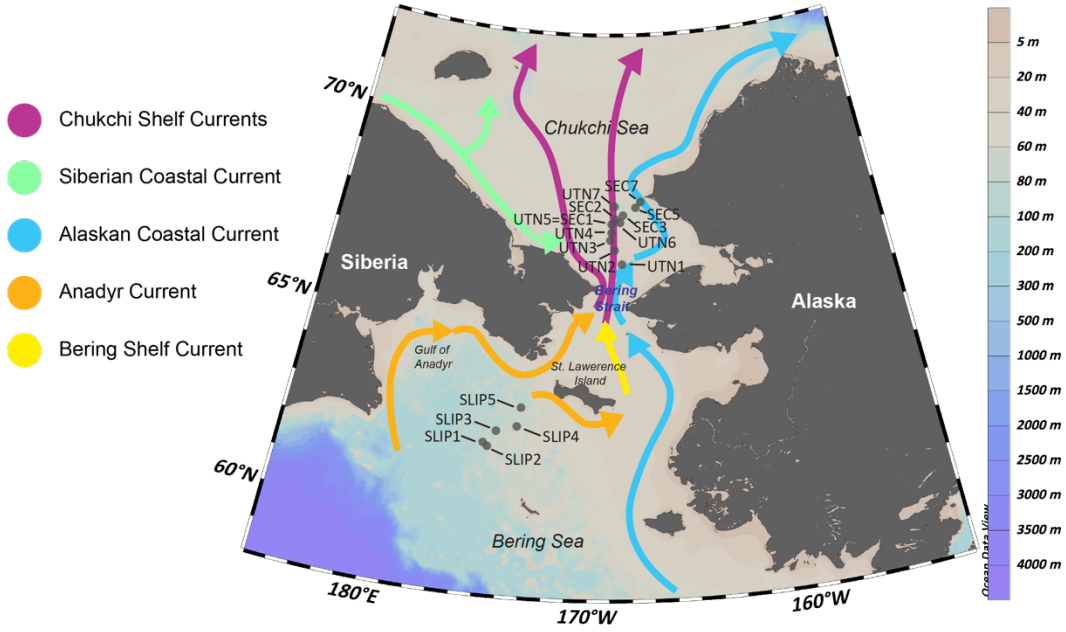

Figure 1. Map of the Pacific Arctic Region with stations addressed in this study and depth profile (m). Surface currents are simplified from maps in Danielson et al. (2020), Sibbon et al. (2020), and Stabeno et al. (2018)

Climate change impacts in the Pacific Arctic are on-going. For example, the Pacific Arctic region is experiencing declines in sea ice extent with projections of later freezing and earlier breakup of sea ice increasing the ice-free period by ten days per decade under median climate scenarios (Lebrun et al., 2019). Ice thickness (Lindsay & Schweiger, 2015), and the average age of the ice where multiyear ice is present (Meier, 2021) are also declining. The northward transport of Pacific water through the Bering Strait is increasing and winter water is freshening (Woodgate, 2018). At the same time and as a part of a feedback loop with many triggers (Stuecker et al., 2018), the surface air temperature is rising at almost twice the rate of the rest of

the globe. This phenomenon is referred to as polar amplification (Bekryaev et al., 2010).

In response to these biophysical stressors, the Pacific Arctic marine fauna distributions are changing (reviewed in Moore & Stabeno, 2015). The changes in sea ice, light penetration, and flow through the Bering Strait are expected to increase primary production in the Pacific Arctic (Grebmeier, 2012). Some studies suggest that increases in primary production have already begun (Frey, 2021; Lewis et al., 2020) while others have observed no trend in the chlorophyll *a* biomass record (Cooper & Grebmeier, 2022). With projected increases in open water primary production and warming seawater temperatures, there is concern that the tight pelagic-benthic coupling of the past will weaken and reduce the abundance and biomass of the underlying benthic macroinvertebrates. The shift from a benthic-dominated arctic system to a pelagic-dominated subarctic system with demersal fish, significant zooplankton grazing, and predatory invertebrates is already underway in the northern Bering Sea (Grebmeier, et al., 2006a).

To track these changes, researchers visit Distributed Biological Observatory (DBO) hot spots each year and gather biological, chemical, and physical oceanographic data (https://dbo.cbl.umces.edu/; Figure 2). As a part of this program, benthic macroinvertebrate samples are collected and sorted by taxon as a part of a long-term change detection array. In recent years, the benthic macroinvertebrate biomass and abundance have been shifting. The northern Bering Sea (DBO 1) and

Southern Chukchi Sea (DBO 3) have experienced the most change in the types and number of benthic macroinvertebrates present (Grebmeier et al, 2018).

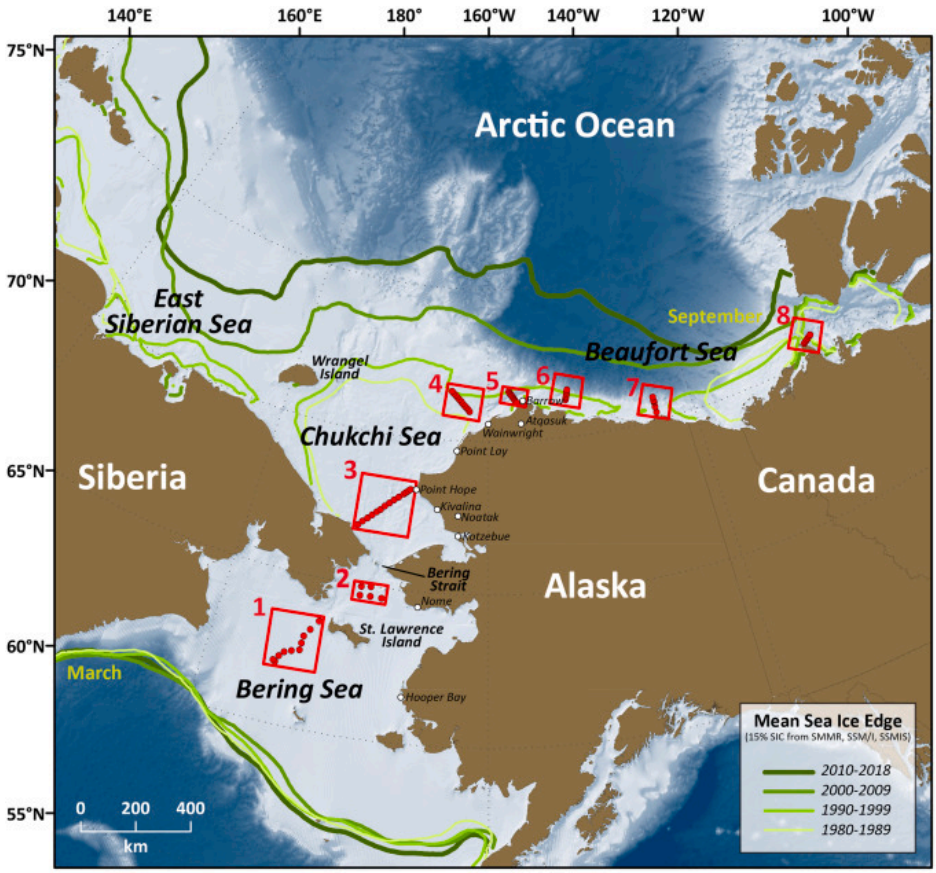

Figure 2. Map of Distributed Biological Observatory (DBO) stations with mean sea ice edge over time periods listed in the legend. Figure courtesy of Karen Frey.

While the biomass and abundance of benthic macroinvertebrates in the Pacific Arctic are well described in the region, their food webs have received less attention. Stable isotopes of nitrogen and carbon can shed insight into the feeding strategies, trophic positions (TP), and food web dynamics of organisms. Metabolism generally favors lighter isotopes and leaves the heavier isotopes to be assimilated into tissue (isotopic fractionation). This isotopic fractionation leads to stepwise increases in the

ratio of heavy to light isotopes of nitrogen as organisms move up the food web (DeNiro & Epstein, 1981; Minagawa & Wada, 1984). The ratio of heavy to light carbon isotopes does not increase significantly at each trophic level and instead provide information about the source of carbon at the base of the food web (Parker, 1964). Stable isotope ratios of carbon and nitrogen (expressed as $\delta^{13}C$ and $\delta^{15}N$ values) are used to determine food web structure and trophic patterns (reviewed in Fry, 2008; Peterson & Fry, 1987) and will be used in this study to assess the feeding behaviors of benthic macroinvertebrates in the Pacific Arctic.

1.2 Study sites within the Distributed Biological Observatory

The two broad study locations evaluated in this thesis are the northern Bering Sea (DBO 1) and southern Chukchi Sea (DBO 3; Figure 2). The northern Bering and southern Chukchi Sea have the highest net community production in the Arctic Ocean at about 200 – 400 g C m^{-2} yr^{-1} (Arrigo et al., 2008; Hill et al., 2018). Both regions lie on the broad continental shelf and are influenced by serval currents that flow generally in the northward direction (Danielson et al., 2020; Figure 1). Shallow shelves, immature zooplankton at the time of sea ice melt (Grebmeier et al., 2006b), and the high percentage of diatoms (Lalande et al., 2021) allow most of the production to go ungrazed (Cooper et al., 2002). The large pulses of organic matter support large and diverse communities of benthic macroinvertebrates (Grebmeier, et al., 2006b). The timing of the sea ice melt and the subsequent ice edge bloom differs between the two regions. In the northern Bering Sea, the sea ice begins retreating in

late April and is diminished by mid-May. In the southern Chukchi Sea, sea ice retreat begins in late May and is complete by the middle of June (Frey et al., 2015).

1.2.1 Northern Bering Sea

The annual primary production in the northern Bering Sea ranges from 250 – 470 $gCm^{-2}yr^{-1}$, and the particulate organic matter (POM) export to the benthos is on average 44 $gC\ m^{-2}yr^{-1}$ (Grebmeier et al., 2006b). One of the most distinct features of the northern Bering Sea is the bottom water cold pool (Barnes & Thompson, 1938). Brine rejection creates dense, cold water that sinks and remains at depth (Wyllie-Echeverria & Wooster, 1998). The density of this cold water maintains temperatures of less than 2 °C throughout the year. The cold pool extends from the western Gulf of Anadyr (Figure 1) and its eastern boundary varies from year to year (Clement Kinney et al., 2022). The cold pool boundary acts as a barrier for subarctic species that are unable to withstand the cold temperature (Mueter & Litzow, 2008). However, the cold pool is expected to shrink in response to declines in sea ice (Clement Kinney et al., 2022). In the northern Bering Sea, like the Arctic as a whole, bottom water temperatures and air temperatures are increasing, and the ice melt has been occurring earlier in the spring (Grebmeier, 2006b).

This study addresses one of the more productive regions within the cold pool, the reoccurring polynya south of St. Lawrence Island. This polynya forms from the southern forcing of first year ice away from St. Lawrence Island. The flow of ice to the south and brine rejection causes a winter polynya with open water to form

(Schumacher et al., 1983). The increased sediment deposition from the slowdown within baroclinic currents helps support a large benthic macroinvertebrate community (Grebmeier & Cooper, 1995). The area's high benthic biomass and productivity has also been attributed to export of algal biomass from ice edge blooms and can vary due to ice edge bloom dynamics (Cooper et al., 2012). This region is influenced by the Anadyr Water (AW) which brings in nutrients and high salinity (32.5 to 33.8 ppt; Figure 1; Coachman et al., 1975; Danielson et al., 2020). However, when the prevailing northerly winds are strong, the AW is restricted to the west and the ice edge bloom can be smaller resulting in less productivity (Cooper et al., 2012).

The benthic macroinvertebrate population in this region is dominated by nuculanid, nuculid, and tellinid bivalves with maldanid polychaetes increasing in abundance at the more southern stations. While the overall region is experiencing declines in benthic biomass, the decline is driven by the southern stations with the northern stations experiencing no significant changes. In recent years, the dominant taxa by biomass have changed from nuculanid bivalves to maldanid polychaetes in the southern stations (SLIP1, 2, and 3; Figure 1; Grebmeier et al., 2018). These shifts have impacts on the upper trophic levels such as marine mammals and seabirds. Walruses (*Odobenus rosmarus divergens*) and spectacled eiders (*Somateria fisheri*) prey on benthic macroinvertebrates, especially nuculanid and tellinid bivalves. Both walruses and spectacled eiders have shifted their habitat range in response to changes to their prey population (Jay et al., 2014; Lovvorn et al., 2005).

1.2.2 Southern Chukchi Sea

The northward transport of Pacific water through the Bering Strait heavily influences the southern Chukchi Sea. These Pacific currents from several water masses (see Danielson et al., 2020 for detailed description of water masses) bring nutrients, fresh water, and heat into the southern Chukchi Sea (Figure 1; Woodgate et al., 2015). Nitrate fluxes from the Bering Strait flowing from February to May supports the spring bloom in the southern Chukchi Sea (Zheng et al., 2021). However, as the water flows through the Bering Strait during late spring and summer, many of the nutrients are depleted (Danielson et al., 2020). The summer bloom is supported by the remaining advection of nutrients from the Bering Strait and vertical mixing (Zheng et al., 2021). Fresher waters from the Alaskan coast (Alaskan Coastal Current) in the east and colder, saltier water from the Siberian coast (Siberian Coastal Current) to the west create an east to west salinity gradient (Figure 1; Coachman et al., 1975; Woodgate et al., 2015).

Advection of nutrients and primary production along with the vertical mixing support some of the highest benthic biomass in the Pacific Arctic Region (Grebmeier et al., 2018). The overall benthic macroinvertebrate biomass has been increasing, but these increases are concentrated at UTN5 and UTN1 (Figure 1; Grebmeier et al., 2018). The benthos in the southern Chukchi Sea is dominated by bivalves (Grebmeier et al., 2018), but two of the most prominent bivalves in the region have experienced opposite trajectories. *Macoma calcarea* has been increasing in biomass and abundance while another bivalve, *Serripes sp.* is declining after reaching a peak

abundance around 2011 (Goethel, 2021). The coastal stations in this time series are less closely studied, but generally have lower biomass than those stations located farther to the west (Grebmeier et al., 2015). In the southern Chukchi Sea, gray whales (*Eschrichtius robustus*) rely on ampeliscid amphipods (Grebmeier et al., 2015) and other amphipods (Moore et al., 2022). Walruses rely on the bivalves like *Macoma calcarea* (Jay et al., 2014). Like walruses and spectacled eiders in the Bering Sea, gray whale distributions are correlated with high abundances of their favored amphipod prey items (Moore et al., 2022).

The formal DBO 3 region does not include the station, UTN1 (https://dbo.cbl.umces.edu/; Figure 3), but UTN1 is included in this study. UTN1 has been included in DBO region assessments (Cooper & Grebmeier, 2022; Grebmeier et al., 2018; Waga et al., 2020) and has yearly (apart from 2009) historical time series measurements of benthic macroinvertebrate populations and environmental parameters dating back to 1998. Since 1998, the sand dollar, *Echinarachnius parma*, has dominated UTN1's benthic macroinvertebrate biomass. The sand dollar dominance is unique among the southern Chukchi Sea stations (Grebmeier et al., 2018). However, a PhD dissertation (Stoker, 1978) measured benthic macroinvertebrate biomass in 1973 and found that the tellinid bivalve, *Macoma calcarea*, was dominant at that time. UTN1's historical record and unique benthic macroinvertebrate population dynamics was persuasive for including this station in my thesis.

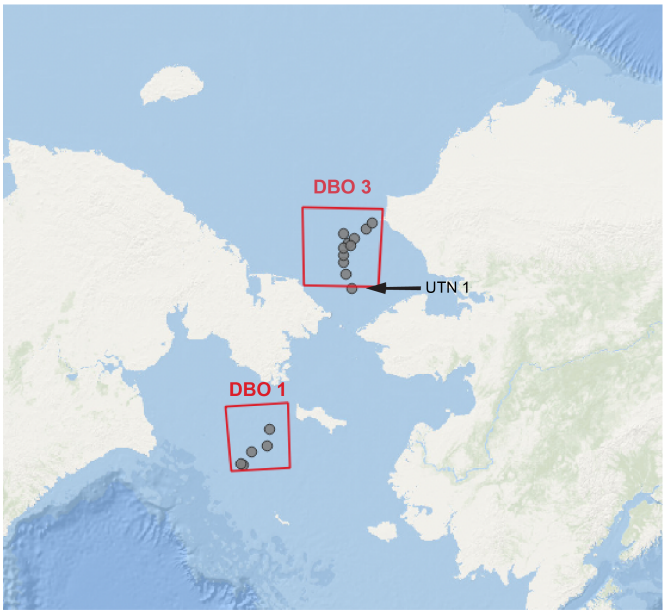

Figure 3. DBO 1 and 3 bounding boxes (red) with stations addressed in this study (gray). UTN1 is labeled as it is not a part of the Distributed Biological Observatory (DBO) study sites.

1.3 Stable Isotope Analysis

Bulk stable isotope analysis of benthic taxa from the northern Bering Sea and southern Chukchi Sea regions were analyzed as described below:

1.3.1 Standard ellipse area and Layman metrics

Hutchinson (1978) proposed that the fundamental or ecological niche can be represented by an n-dimensional hypervolume of environmental variables where the organism could survive. Environmental variables are plotted on two axes: bionomic and scenopoetic. The binomic axis encompasses the resources than an organism utilizes, and the scenopoetic is the habitat in which the organism resides (Hutchinson,

1978). This study utilizes one type of ecological niche, the trophic niche, which describes where an organism fits in a food web. Because the stable isotopes of nitrogen and carbon represent both the resources (bionomic) that an organism relies on (δ^{15}N) and the habitat (scenopoetic) in which it resides (δ^{13}C), the ecological niche can be represented in δ-space on a biplot of δ^{15}N and δ^{13}C as an 'isotopic niche.' While not equivalent to the trophic niche, the isotopic niche can be a proxy for trophic niche (Newsome et al., 2007). The isotopic niches of organisms can be compared to determine whether one organism is more of a generalist or a specialist than another (Bearhop et al., 2004).

The isotopic niche of an organism or community can be quantified using a graphical approach. The total area the stable isotopes occupy on the graph is calculated by measuring the convex hull around all data points on a stable isotope biplot (Layman et al., 2007). However, convex hulls are sensitive to sample size and do not account for the natural variability common in ecological systems. The R package, *SIBER,* can be used to account for these shortcomings by employing standard ellipse areas (SEA) and Bayesian statistics (Jackson et al., 2011). SEA is similar to the use of standard deviation in univariate data analysis. An SEA contains only 40% of the data, making it more robust to differences in sample sizes compared to a convex hull that captures the entire data set (Batschelet, 1981). However, there is still some bias due to sample size in SEAs, so the corrected standard ellipse area (SEA_C) can be used.

SEA_C is calculated as follows:

$$\mathbf{SEA_C} = \mathbf{SEA}(\boldsymbol{n}-\mathbf{1})(\boldsymbol{n}-\mathbf{2})^{-\mathbf{1}} \quad \text{(Equation 1)}$$

where *n* is the sample size.

The *SIBER* package also employs Bayesian statistics to further reduce the bias in sample size and sampling decisions. Bayesian statistics uses priors or prior distributions to calculate conditional probability. Priors account for previous research or knowledge and can be categorized as either uninformative or informative. After the prior distribution is established, the distribution of the observed data is incorporated into a likelihood function. Then, the prior distributions and likelihood functions are combined to calculate a posterior distribution (reviewed in van de Schoot et al., 2021). A Markov chain Monte Carlo (MCMC) simulation iteratively draws several samples from this posterior distribution. With these samples or iterations of the posterior distribution, uncertainty can be calculated around our SEA estimates and SEAs can be compare statistically (Jackson et al., 2011). The Bayesian estimate of SEA will be referred to as SEA_B in this thesis.

Some important caveats in the quantification of niche space using bulk stable isotope analysis should be noted. The isotopic niche is not a direct measure of ecological or trophic niche and instead is a proxy for trophic niche (Newsome et al., 2007). For accurate assessments of niche space, the tissue turnover rate of the nitrogen and carbon must be short enough to capture the variability in diet (Bearhop et al., 2004). Additionally, isotopic niches of a group cannot differentiate between within-individual and within-group niche space (Matich et al., 2021). For example, a

group with a large isotopic niche area could be comprised of generalist individuals capable of utilizing a wide range of resources or specialist individuals that are utilizing unique resources. A larger isotopic niche space could also be due to variations in the $\delta^{13}C$ and $\delta^{15}N$ at the base of the food web and not the species themselves (Matich et al., 2021) or these variations can be due to variations in TDFs (Hussey et al., 2012). Niche width and Layman metrics (see below) can also be affected by growth and nutritional status (Gorokhova, 2018) or physiological stress (Karlson et al., 2018).

Even with these caveats, niche space can be a powerful tool in determining whether a species is more of generalist, when individuals in a group utilize a variety of resources and have a large ecological niche, or specialist, when individuals in a group utilize similar resources and have a small ecological niche (Hutchinson, 1957, 1978). These concepts are useful under climate change scenarios because generalists tend to be more resilient to disturbances than specialists (Bartley et al., 2019; Jiguet et al., 2006).

Bayesian statistics are also employed for community-wide metrics of food web structure (Jackson et al., 2011). Layman et al (2007) described six quantitative metrics that are widely used to describe trophic structures (Abrantes et al., 2014; Hansen et al., 2018; Vaudo & Heithaus, 2011). These “Layman metrics” quantify communities in $\delta^{13}C$ - $\delta^{15}N$ biplot space.

The Layman metrics are as follows:

1. **Range of δ^{15}N (RN)** is calculated by subtracting the maximum δ^{15}N value in a community from the minimum δ^{15}N value. As trophic position increases, δ^{15}N values increase in a stepwise manner. Therefore, larger RNs are indicative of a longer food web.
2. **Range of δ^{13}C (RC)** is the difference between the largest (least negative) δ^{13}C value and the smallest (most negative) δ^{13}C value in a community. δ^{13}C values are relatively stable within the food web and can be used to determine the basal resources. In a community with many basal resources, the RC is larger than in a community with fewer basal resources.
3. **Total area (TA)** is the convex hull around a community in stable isotope biplot space. As discussed above, the convex hull is very sensitive to sample size, so this study uses the SEA_B of the community.
4. **Mean distance to centroid (CD)** measures the trophic diversity in a community. The Euclidean distance between the location of a species in the δ^{13}C-δ^{15}N biplot and the location of the community's centroid or mean is calculated and then averaged. If species within a community are farther from the mean (larger CD), there is more diversity in δ^{13}C and δ^{15}N values and therefore, more trophic diversity.
5. **Mean nearest neighbor distance (MNND)** is similar to CD, but instead of measuring the distance from one organism to mean, MNND measures the Euclidean distance between one organism and the closest organism in isotope space. These distances are averaged across the community. If MNND is small,

the community has more trophic redundancy and overlap than if MNND is large.

6. **Standard deviation of nearest neighbor distance (SDNND)** is measure of the evenness of species. SDNND takes the standard deviation of the distance between the two closest organisms in isotope space (Layman et al., 2007).

Like the total area of a group, community total areas are sensitive to sample size even when the sample size is large (Syväranta et al., 2013). RN and RC have the same shortcoming with just one outlier increasing the range in isotope values. CD, MNND, and SDNND are less sensitive to sample size (Layman et al., 2007), but MNND can increase with the number of species and SDNND can underestimate the evenness of a community when sample size is small (Brind'Amour & Dubois, 2013). These metrics also do not incorporate uncertainty (Jackson et al., 2011). Therefore, I used the R package, *SIBER*, to calculate Layman metrics with Bayesian statistics for the communities addressed in this study (Jackson et al., 2011).

1.3.2 Trophic position and food web dynamics

Stable isotopes can also be used to estimate trophic position (TP) and gain insight into the food web dynamics of a system (reviewed in Fry, 2008). Trophic position of organisms within a community can provide information about how energy is transferred from the primary producers up to the predators (Levine, 1980). The TP of an organism can change based on a change in the organism's diet or a change in the diet of another organism lower in the food chain (Moosmann et al., 2021). When

TPs are calculated for a community of organisms using $\delta^{13}C$ and $\delta^{15}N$ values, the food web length can be measured (Perkins et al., 2014). Longer food web lengths are associated increased ecosystem size and higher productivity at the base of the food web (Takimoto & Post, 2013).

An appropriate trophic discrimination factor (TDF) needs to be established to calculate the trophic position of an organism or food web length using stable isotopes. TDF is the stepwise increase in $\delta^{15}N$ and $\delta^{13}C$ from prey to consumer (Minagawa & Wada, 1984). Meta-analyses have found that TDFs are around 3.4 ‰ for $\delta^{15}N$ and 0.4 ‰ for $\delta^{13}C$ (McCutchan, et al., 2003; Post, 2002), but TDFs can vary from species to species or due to differing diets (reviewed in Caut et al., 2009). For example, starvation can decrease TDFs (Tamelander et al., 2006), and the quality of the protein can also impact the TDF (Florin et al., 2011). Inaccurate TDFs (Barton et al., 2019) or TDFs based on differing baselines (Iken et al., 2010) can have major implications on the apparent trophic position of Arctic species.

Although to the best of my knowledge, there have not been any laboratory studies that directly measured the trophic discrimination factor for Arctic benthic macroinvertebrates, there are several studies that have measured TDFs in the field. Hobson and Welch (1992) found an average trophic enrichment of 3.8 ‰ for $\delta^{15}N$ in Lancaster Sound between both polars bears (*Ursus maritimus*) and their prey, ring seals (*Phoca hispida*), as well as copepods (*Calanus hyperborea*) and POM (Hobson & Welch, 1992). McTigue and Dunton (2014) estimated the TDF for benthic macroinvertebrates using the suspension feeder, *A. macrocephela*, and POM in the

northern Chukchi Sea. They found a $\delta^{15}N$ TDF of 3.4 ‰ and a $\delta^{13}C$ TDF of 0.6 ‰. Using $\delta^{15}N$ values from nine studies with 241 benthic samples, Hoondert et al (2021) found an average TDF of 3.4 (± 0.00 SE) in the Alaskan Beaufort and Chukchi Seas. However, they also found that the variation in TDF between replicate benthic samples was higher than the benthic samples collected.

1.4 Study Objectives and Hypotheses

The goal of this study is to explore food web dynamics in the northern Bering Sea and southern Chukchi Sea, how these food webs differ, and whether these food webs have changed over time using bulk stable isotope analysis.

My objectives and hypotheses are as follows:

1. Objective: Determine how food webs differ between the northern Bering Sea and the southern Chukchi Sea.

   Hypothesis: The northern Bering Sea will exhibit less direct pelagic-benthic coupling than the southern Chukchi Sea, where production is sustained over a longer seasonal period (Grebmeier and Cooper, 2016)

2. Objective: Analyze shifts in food webs from 2014 to 2021

   Hypothesis: The organisms sampled from 2021 will have less sea ice algae influence in their diet than the organisms sampled from 2014 due to the decrease sea ice persistence in 2021 (Frey et al., 2014).

3. Objective: Determine whether the organisms that are thriving have different diets from those that are declining.

Hypothesis: Thriving species will be those with larger standard ellipse areas indicating a more generalist diet (Bartley et al., 2019; Kortsch et al., 2015)

2 Materials and Methods

Benthic macroinvertebrates were collected each year in July at Distributed Biological Observatory sites in the southern Chukchi Sea and the northern Bering Sea as a part of the core DBO effort (Principal Investigators: Jacqueline M. Grebmeier and Lee W. Cooper). During research cruises on the Canadian Coast Guard Ship (CCGS) Sir Wilfrid Laurier (SWL) in 2014, 2015, 2016, 2017, and 2021, select benthic macroinvertebrates were collected and identified for stable isotope analysis. After identification in the field, they were frozen in the field, and subsequently freeze dried at the Chesapeake Biological Laboratory in Solomons, Maryland, U.S.A. They were generally analyzed as whole body samples for the stable isotope composition of organic carbon and nitrogen, expressed as $\delta^{13}C$ and $\delta^{15}N$ values. These values were compared between sites and among years.

2.1 Sample Collection

2.1.1 Sediments

Surface sediments were collected using a weighted van Veen grab with a 0.1 m^2 surface area at each station annually on DBO cruises coincident with benthic macroinvertebrate sample collection as part of the core DBO effort (Figure 2). The

top 1 cm of surface sediment was sampled from the trap door of the grab before the grab was opened to limit mixing with sub-surface sediments. Samples were frozen and returned to the Chesapeake Biological Laboratory in Solomons, Maryland, USA for analysis. Sediment analysis followed standardized practices presented in Cooper et al (2002) and Grebmeier et al (2018). Briefly, this included drying the sediments and subsampling 2 g of the dried sediments. These subsamples were acidified with 4 mL of 1 N HCl to remove $CaCO_3$. After two hours of reaction, the pH was assayed. The addition of HCl continued until sediments had a pH below 2. At this point, the samples were dried in an oven at 60 °C for 24 – 48 hours, and then ground with a mortar and pestle for isotopic analyses.

2.1.2 Particulate organic matter (POM)

POM samples were collected at UTN2 and UTN5=SEC1 in 2016 and SLIP1, SLIP5, UTN2, and UTN5=SEC1 in 2015 (see Figure 1). POM collection coincided with the collection of benthic macroinvertebrates and sediment onboard the CCGS Sir Wilfrid Laurier in July. Samples were obtained by filtering 0.2- 2 L of water from the chlorophyll *a* maximum onto pre-combusted Whatman GF/F glass fiber filters. In 2015, SLIP1 and SLIP5 samples were collected at 50 m, and UTN2 and UTN5=SEC1 were collected at 15 m. In 2016, the UTN2 samples were collected at 35 m and UTN5=SEC1 were collected at 15 m. Filters were dried and frozen on board the ship and then returned to the Chesapeake Biological Laboratory.

2.1.3 Benthic macroinvertebrate collection

Benthic macroinvertebrates were collected using the same van Veen grab used to collect surface sediments. The contents of the grab were sieved through a 1 mm screen and rinsed with seawater to remove sediments. Benthic macroinvertebrates of representative taxa were removed and kept in ambient temperature seawater and then identified under a stereomicroscope shipboard (personal communication, Monika Kędra [2014-2017] or Christina Goethel [2021]). Macroinvertebrate samples were subsequently frozen and returned to the Chesapeake Biological Laboratory in Solomons, Maryland, USA where they were stored in a -20 °C freezer until they were freeze-dried for 48 hours in a VirTis Lyo-Centre benchtop lyophilizer. The samples that were collected from 2014 to 2017 were returned to the -20 °C freezer after freeze-drying to limit moisture re-absorption. Prior to analysis, samples were re-dried at 60 °C overnight before homogenization by grinding using a mortar and pestle.

Once dried, bivalve shells were measured for length to the nearest 0.1 mm using Capri 15 cm stainless steel digital calipers. Length was defined as the maximum distance from the anterior to posterior axis (Gaspar et al., 2001). After length measurement, soft tissue was extracted from the bivalves. If bivalves or gastropods were large enough (e.g. *Yoldia hyperborea*, *Serripes sp*., *Mya sp.*, Naticidae) their foot (muscle tissue) was removed, and both the foot and the remaining body parts of the organism were analyzed separately for $\delta^{15}N$ and $\delta^{13}C$ values. For all other organisms, the whole organism or the partial specimen available was used. Nine samples were homogenized composites of multiple organisms from the same species.

All dried samples were ground using a mortar and pestle and placed in a pre-muffled vial.

Most of our study organism tissues (bivalves, polychaetes, and amphipods) are not significantly calcified apart from brittle stars (Class: Ophiuroidea). Brittle stars are heavily calcified with high-magnesium calcite (Wood et al., 2010). Before acidification, four out of the five brittle stars were measured for $\delta^{15}N$ values as de-calcification using acid can affect the $\delta^{15}N$ values of the samples (Mateo et al., 2008). Drops of 1 M HCl treatment were applied to the sample until the sample stopped bubbling. Then, the sample was placed in the drying oven at 60 °C until excess moisture was removed. The samples were not rinsed with deionized water due to its effects on $\delta^{13}C$ and $\delta^{15}N$ (Mateo et al., 2008). All other organism soft tissues were not acidified before analysis. Organism feeding types were categorized using the taxonomic and feeding guild classification outlined in Macdonald et al (2010).

2.2 Stable isotope analysis

Macroinvertebrate samples were weighed into 4 x 6 mm tin capsules. Sediment and POM samples were weighed into larger tin capsules of various sizes. Most samples (except for POM collected in 2015) were analyzed at the Chesapeake Biological Laboratory using a Costech ESC 4010 Elemental Analyzer (EA) coupled to a continuous flow Delta V Plus Isotope Ratio Mass Spectrometer (Thermo Scientific) run in a continuous flow mode. The POM samples collected in 2015 were analyzed at the Centre for Stable Isotope Research and Analysis in Göttingen,

Germany using a µEA/EA (Eurovector) coupled to a continuous flow Delta V Plus Isotope Ratio Mass Spectrometer (Thermo Scientific).

Isotopic results are expressed using the standard delta notation:

$$\boldsymbol{\delta X}(‰) = \frac{\boldsymbol{R_{Sample} - R_{Standard}}}{\boldsymbol{R_{Standard}}} \times \mathbf{1000} \qquad \textbf{(Equation 2)}$$

where X is the ^{13}C and ^{15}N of the sample or standard and R is the $^{13}C/^{12}C$ or $^{15}N/^{14}N$ of the sample or standard. Values are expressed as per mil (‰).

$\delta^{15}N$ value calculations are in reference to the international reference standard, atmospheric N_2, and $\delta^{13}C$ value calculations are in reference to the international reference standard, Vienna Pee Dee Belemnite. Internal standards were run alongside samples to determine analytical error. Analytical error was less than 0.05 ‰ for $\delta^{13}C$ values and less than 0.1 ‰ for $\delta^{15}N$ values.

2.3 Statistical analyses

All statistical analysis were undertaken in R Studio with R Version 4.2.0 (R Core Team, 2022). Visualizations were produced in R Studio (R Core Team, 2022), Ocean Data View (Schlitzer, 2022), or ArcMap (*ArcMap*, 2020). I considered the following variables in my analyses: location, year of sampling, feeding type, phylum or group (i.e. Bivalves, Polychaetes, Amphipod, Echinodermata, etc.), and size (either the length of the bivalve or the dry weight). Stable isotope biplots of $\delta^{13}C$ and $\delta^{15}N$ (Fry, 2006) were made to visualize the results.

Similar functions were used to test for differences between groups, communities, years, methods, etc. Prior to testing the null hypothesis of no significant difference, groups were assessed for normality using the Shapiro-Wilks test of normality (Shapiro & Wilk, 1965) with the function shapiro.test() in the base R package, *stats*. When the p-value was significant (Shapiro-Wilks test: $P < 0.05$) indicating a non-normal distribution of the dataset, the non-parametric Wilcoxon rank-sum test was used to compare two groups. When the dataset was normally distributed (Shapiro-Wilks test: $P > 0.05$), Welch's two-sample t test was used. I used the functions wilcox.test() and t.test() for the Wilcoxon rank-sum test and Welch's two sample t-test, respectively. Both are base R functions (R Core Team, 2022).

When comparing more than two groups, homogeneity of variances was tested along with tests for normality as Analysis of Variance (ANOVA) models are more sensitive to differences in variances than Welch's t-tests (Delacre et al., 2017). The distribution of each group's data was assessed for normality using the same methods for two groups. Homogeneity of variances was assessed with Levene's tests (Levene, 1960) using the function levene_test() from the R package, *rstatix* (Kassambara, 2021). When assumptions of normality and homogeneity of variances were met, an ANOVA test was conducted with the function aov() in base R (R Core Team, 2022). If significant differences were detected between any of the groups, a pairwise t-test was conducted with Bonferroni p-value adjustments (R Core Team, 2022). When the assumption of normal distributions was not met, I used the non-parametric Kruskal Wallis test (Kruskal & Wallis, 1952) followed by the non-parametric pairwise

Wilcoxon rank sum test. The Kruskal-Wallis tests were performed with the function, kruskal.test(), and the pair-wise comparisons were made with the function, pairwise.wilcox.test() in base R (R Core Team, 2022). When the assumption of homogeneity of variances was not met, I used the Welch one-way ANOVA test with the function welch_anova_test() in the *rstatix* package (Kassambara, 2021). If assumptions of equal variances were not met, then the standard deviations were pooled. If the variances were equal across groups, I did not pool the standard deviations.

2.3.1 Clustering

Stations were clustered into groups using the following R package programs (*italicized*): *cluster* for the clustering (Maechler et al., 2022), *factoextra* for visualizing the clusters (Kassambara & Mundt, 2020), *clustertend* to determine the clustering tendency of the dataset (Wright et al., 2022), and *dendextend* for comparing the dendrograms of various calculations (Galili, 2015). Environmental and spatial (Latitude and Longitude) variables were averaged for each station from 2014 – 2018 and normalized to a common scale. Environmental and spatial data for the cruises and stations used in this study are available through the Arctic Data Center (Cooper et al., 2019a, 2019b, 2019c, 2022; Nobre & Vagle, 2019a, 2019b). These data can be accessed through: https://arcticdata.io/catalog/portals/DBO/Data. Biological parameters were not included in the clustering analysis.

Briefly, environmental variables were collected as follows. Bottom water temperature and salinity were collected with a CTD (Conductivity, Temperature, and Depth; Sea-Bird SBE25.33 mounted on a SBE32 Carousel 12-bottle water sampler with 8-L bottles). Nutrient samples (silicate, ammonium, phosphate, and nitrite + nitrate) were collected from the overlying bottom water at each station and year. They were filtered, frozen on board, and analyzed by the Nutrient Analytical Services Laboratory (NASL) at CBL in Solomons, Maryland, USA. Water column chlorophyll *a* (bottom water and integrated) was collected by filtering 250 mL of seawater collected with the CTD through 25 mm GFF filters. The filters were frozen and stored in 10 mL of 90% acetone for 24 h in the dark. Sediment chlorophyll *a* (1-cm^3*)* was collected from the trap door of the van Veen grab using the same methods as the sediment collected for stable isotope analysis. The sediment samples were then treated with 10 mL of 90% acetone and incubated for 12 h in the dark. Chlorophyll *a* (sediment, integrated, and bottom water) was measured with a Turner Designs 10-AU field fluorometer. Two independent samples of sediment chlorophyll *a* were averaged. Sediment grain size samples were also collected from the trap door of the van Veen grab. Samples were dried, weighed, and sieved through 0-4 phi sized sieves. Percent of the total sediment at each grain size was calculated and the 0-4 phi percentages were averaged to obtain the percent silt and clay (see Grebmeier et al., 1989 for more detailed methods).

Before clustering, it is important to determine whether the given dataset tends to cluster because clustering algorithms will always produce clusters even when there

are none. The tendency of the dataset to cluster was determined with the Hopkins statistic (Hopkins & Skellam, 1954). The Hopkins statistic is calculated dividing the sum of the nearest neighbor distances in the data set by the sum of a uniformly distributed data set's nearest neighbor distances plus the data set's nearest neighbor distances (Adolfsson et al., 2019). I used the function get_clust_tendency() from the *factoextra* package to calculate the Hopkins Statistic (Kassambara & Mundt, 2020).

Standardized Euclidean distance was used to calculate the dissimilarity matrix because all variables were numeric and continuous, and this method considers all variables with equal weights. Euclidean dissimilarity matrixes quantify the difference between each station using the shortest distance between the points on a coordinate plane. This matrix was used for hierarchical clustering. Agglomerative hierarchical clustering was used as it tends to perform better on smaller datasets than divisive hierarchical clustering (Weigand et al., 2021). In hierarchical agglomerative clustering, each data point begins as its own cluster. Then, the two closest points (smallest Euclidean distance between them) are placed into a cluster. The result is one cluster with two points and several clusters with only one point. The process is repeated until all points are in one cluster (Mehta et al., 2020).

However, Euclidean distance can only measure the distance between two points so a linkage method must be used to "link" the points into clusters. The agglomerative coefficient, which measures the strength of the clustering structure, was calculated for several linkage methods, and the method with the highest agglomerative coefficient was used (Kaufman & Rousseeuw, 2005). The chosen

method was compared to the clusters produced from the other methods using the Fowlkes-Mallows Index (FM Index; Fowlkes & Mallows, 1983).

The dendrogram produced by agglomerative hierarchical clustering was split into clusters based on the gap statistic (Tibshirani et al., 2001). After the clusters were determined, the methods were repeated after dropping spatial variables to ensure that the clusters were based on similarities in the environmental characteristics of the stations and not just their locations. Then, the clusters were visualized by their principal components using principal component analysis (PCA). PCA reduces the variation in a multivariable data set into principal components. These principal components contain most of the variation from the original variables. Plots of two principal components can be used to visualize and validate patterns or clusters in the data (Jolliffe, 2002).

2.3.2 Tissue type

When both the muscle tissue and the remaining portion of the body were analyzed for their $\delta^{13}C$ and $\delta^{15}N$ values, I compared the stable isotope values of the different body parts with the paired version of the tests mentioned in the beginning of Section 2.3. The organisms included in this analysis were bivalves and gastropods (e.g. *Yoldia hyperborea*, *Serripes sp*., *Mya sp.*, Naticidae).

2.3.3 Trophic position

TP was estimated for each organism. When both muscle and body tissue for an organism were analyzed for $\delta^{15}N$ and $\delta^{13}C$ values, the muscle tissue were used to estimate trophic position.

The software package *tRophicPosition* in R utilizes Bayesian models to incorporate variability in TDFs, baselines, and estimates of TP (Quezada-Romegialli et al., 2019). This package also allows for multiple baselines and the use of TDFs for both $\delta^{13}C$ and $\delta^{15}N$. One drawback of using Bayesian statistics is the large sample size needed ($n \geq 8$; Quezada-Romegialli et al., 2019). The samples in this study were not collected in large enough quantities for all samples to undergo Bayesian trophic position calculations. For samples with inadequate sample sizes, the traditional method of only using $\delta^{15}N$ of one baseline was used. Both methods were used for samples with adequate sample sizes for Bayesian TP estimations. I used a two source full baseline model which accounts for the TDF of $\delta^{13}C$ and $\delta^{15}N$ for Bayesian TP estimates (Quezada-Romegialli et al., 2019).

After calculation using Bayesian approaches, I used the traditional method of calculating trophic position with the $\delta^{15}N$ value of organic materials in sediment as the baseline:

$$\mathbf{TP} = \frac{\boldsymbol{\delta^{15}N_{consumer} - \delta^{15}N_{sediment}}}{\mathbf{3.4}} + \mathbf{1} \qquad \textbf{(Equation 3)}$$

where $\delta^{15}N_{consumer}$ is the $\delta^{15}N$ value of the benthic macroinvertebrate, $\delta^{15}N_{sediment}$ is the mean $\delta^{15}N$ value of the sediment for the year and cluster the benthic

macroinvertebrate was collected from, 3.4 is the δ^{15}N TDF, and 1 is the TP of the baseline.

The traditional method of estimating TP was used to calculate the TP for all benthic macroinvertebrates. When the Bayesian method was employed, the consumer TP results of the Bayesian and traditional methods of estimating TP were compared.

2.3.4 Standard ellipse areas of taxonomic families

The R package *SIBER* (Jackson et al., 2011) was used to determine the standard ellipse area of organisms that met the sample size criteria of ten or more samples when categorized by cluster and taxonomic family. Samples from all years were pooled for this analysis. The coding sequences followed the vignettes "Introduction to SIBER", "Comparing communities", and "Comparing groups" by Andrew Jackson (2014). These vignettes are available at https://cran.r-project.org/web/packages/SIBER/vignettes/.

2.3.5 Community metrics

Community metrics were calculated for clusters with appropriate sample size ($n > 50$) following the vignette for *SIBER* (Jackson et al., 2011), "Comparing communities." Groups within communities were defined by feeding type.

2.3.6 Sediment δ^{13}C and δ^{15}N value trend analysis

I used the nonparametric Mann-Kendall trend test (Kendall, 1975; Mann, 1945) to test for monotonic upward or downward trends in sediment $\delta^{13}C$ and $\delta^{15}N$ values over time.

2.3.7 Abundance and Biomass

Abundance and biomass time series data were used to calculate the abundance of organisms per feeding type. The available abundance measurements include data from 1998-2018. Four grabs were collected at each station using the same methods of collection as the benthic macroinvertebrates used for stable isotope analysis. Organisms were sorted and identified at the University of Tennessee, Knoxville (1998-2008) and Chesapeake Biological Laboratory (2009-2017). Abundance and biomass data are available for 2012 through 2015 from the Arctic Data Center (Grebmeier & Cooper, 2019a, 2019b, 2019c, 2019d). All other data were provided by Jacqueline M. Grebemier.

For comparisons of feeding types across regions, all organisms that were categorized by Macdonald et al (2010) as having one of the following feeding characteristics: suctorial parasite, detritivore, scavenger, or predator (apart from the grazer/detritivore Cumacea) were grouped together as "Detritivore/Predator/Scavenger." Biomass is expressed as grams of carbon per meter squared using the conversions of formalin-preserved wet weight (g) to carbon dry weight in Stoker (1978) and Grebmeier et al (1989). Benthic macroinvertebrate biomass and abundance were averaged among four grabs and normalized the data to

abundance per square meter. Abundance and biomass data were not evaluated extensively as a part of this thesis as these data are evaluated in other studies (see Grebmeier, 2012; Grebmeier et al., 2015, 2018).

3 Results

3.1 Clustering

Different types and quantities of organisms were collected at each station and during each cruise. In some cases, sample sizes were too small for statistical analyses. Clustering was performed on sixteen stations where benthic macroinvertebrates were sampled for this study to reach sample sizes large enough for analyses (see Figure 1 for stations). Environmental and spatial variables included in the clustering model were Latitude, Longitude, depth (m), bottom water temp (°C), salinity, silicate (µmol/L), ammonium (µmol/L), phosphate (µmol/L), nitrite + nitrate (µmol/L), $\delta^{18}O$ (‰), bottom water chlorophyll *a* (µg/L), integrated chlorophyll *a* (mg/m^2), sediment chlorophyll *a* (mg/m^2), percentage of sediment greater or equal to 5 phi (silt and clay), sediment total organic carbon (%), and sediment total organic nitrogen (%).

All variables were averaged for each station from 2014-2019 and 2021. Then, these variables were standardized to a common scale with a mean of 0 and a standard deviation of 1 to give each variable relatively equal weight. The Hopkins Statistic was significant (H = 0.69) which indicates that the dataset tends to cluster. The agglomerative coefficient was used to determine the best linkage method for hierarchical clustering. The agglomerative coefficient measures the strength of the

clustering structure with higher values indicating more clustering structure (Kaufman & Rousseeuw, 2005). The agglomerative coefficient was calculated for four of the most common linkage methods: complete linkage, single linkage, average linkage, and Ward's minimum variance distance. The Ward's minimum variance distance method had the highest agglomerative coefficient (0.86) of the four methods tested.

The clusters produced from the Ward's method were compared to the clusters produced from the other three methods using the FM index, which assesses the similarity between two sets of clusters. The FM index is reported on a scale of 0 to 1 with an index of 1 indicating that the clusters are the same and 0 indicating that they are completely different (Fowlkes & Mallows, 1983). The FM index between the clusters for Ward's minimum distance method compared to the other three most common linkage methods (complete, single, and average). The FM Index of Ward's minimum variance distance method compared to complete and average linkage methods was 1 indicating that all three linkage methods produced the same clustering structure. For single linkage compared to Ward's minimum distance, the FM Index was 0.74. The single linkage method grouped all Chukchi Sea stations together but split the northern Bering Sea stations into two groups (SLIP4 in one group and all others in another group; Figure 1). I used the clustering structure produced from Ward's minimum distance, complete, and average linkage methods.

The optimal number of clusters was three as determined by the gap statistic and a visualization of the dendrogram. The gap statistic compares the log normalized intra-cluster sums of squares at each number of clusters to a distribution without

clustering. The number of clusters is the smallest number of clusters in which the gap between the actual dataset and the simulated dataset is positive (Tibshirani et al., 2001). After the clusters were established, I visualized the clusters using principal component analysis. A scree plot was used to determine the optimal number of principal components (Holland, 2019). The first principal component explained 53.9 % of the variance in the data and the second principal component explained 31.4 %. After the second principal component, the variance explained by each subsequent principal component sharply declined with the third principal component explaining only 5.6 % of the variance between clusters (Figure 4). Therefore, two principal components were used in the visualization (Figure 5). Visualization of the clusters using principal component analysis confirmed the clustering results from agglomerative hierarchical clustering (Figure 5).

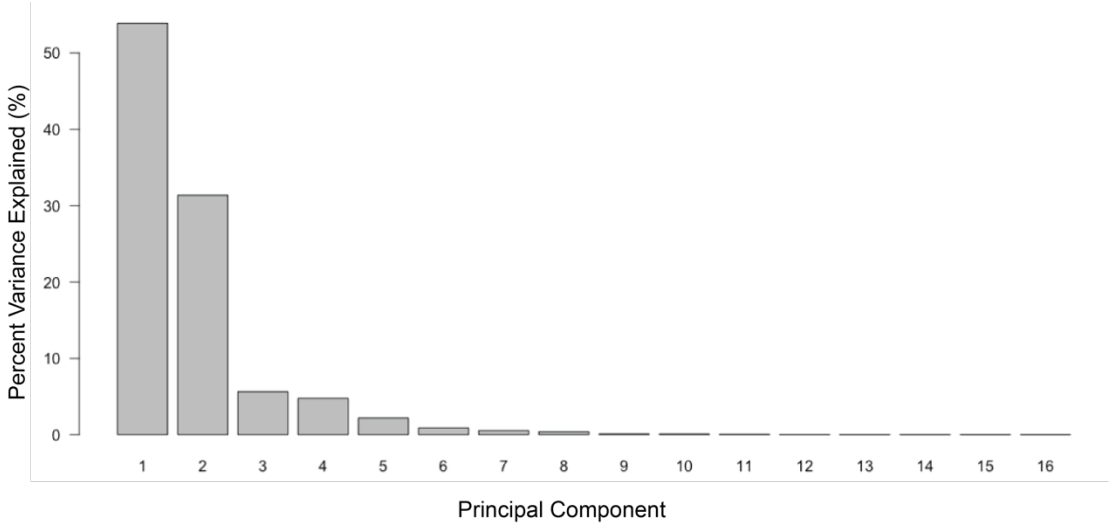

Figure 4. Scree plot representing the percent variance (%) accounted for by each principal component.

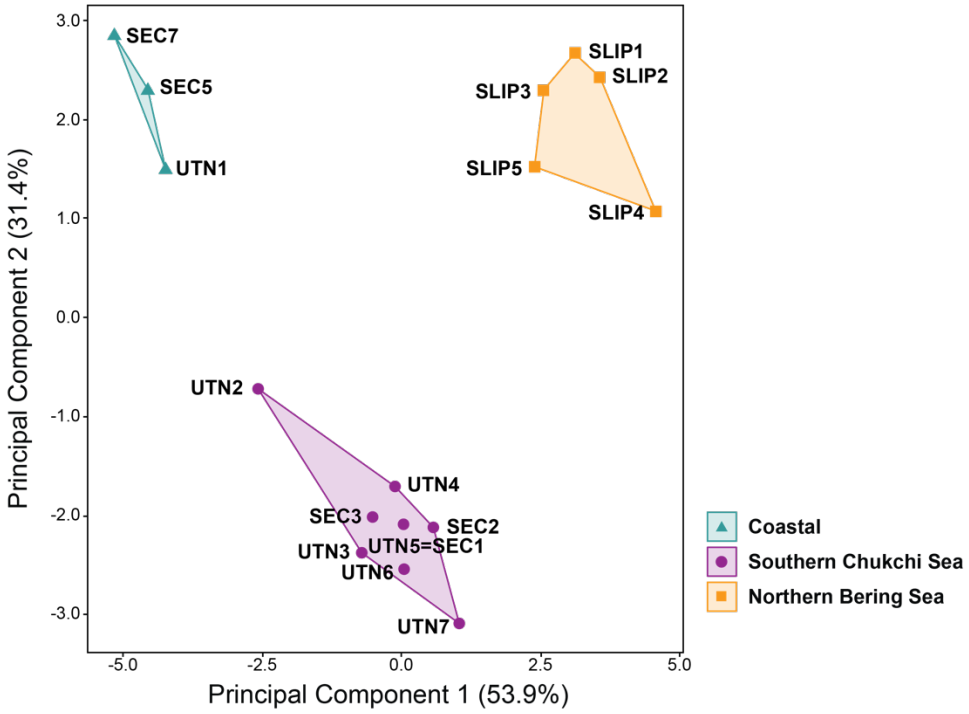

Figure 5. First and second principal components of environmental parameters that influenced the clustering of stations.

The clusters generally followed spatial structure apart from the southernmost station in the Chukchi Sea (UTN1) which clustered with the northernmost stations (SEC5 and SEC7; Figure 6). The northern Bering Sea stations all clustered together while the southern Chukchi Sea stations were split into two groups (Figure 6). Both water column and sediment conditions differed among clusters (Table 1). The coastal stations were the shallowest, the northern Bering Sea stations were the deepest, and the southern Chukchi Stations were intermediate. Bottom water temperature (in July) was highest in the coastal stations and lowest in the northern Bering Sea. Bottom water salinity was highest in the southern Chukchi stations while coastal stations had fresher bottom water than the other two clusters. The northern Bering Sea and

southern Chukchi Sea stations had higher bottom water nutrients than the coastal stations across all nutrient parameters. Bottom water $\delta^{18}O$ values were also measured. The ratio of ^{18}O to ^{16}O can be used to trace the sources of seawater. Melted sea ice is more enriched in ^{18}O than precipitation and run off (Dansgaard, 1964). However, the differences between $\delta^{18}O$ (ratio of ^{18}O to ^{16}O compared to a standard and scaled to per mil notation) are not large enough for any inference on distinctions between study sites. Bottom water chlorophyll *a* (µg/L) and integrated chlorophyll a (mg/m^2) were highest in the southern Chukchi Sea and lowest in the coastal stations (Table 1).

Sediment characteristics included silt and clay content (% ≥ 5 phi), chlorophyll *a*, and total organic carbon and nitrogen (Table 1). Northern Bering Sea and southern Chukchi Sea stations had higher silt and clay content (% ≥ 5 phi) while the coastal stations had coarser sediments. Sediment chlorophyll *a* was highest in the southern Chukchi Sea stations and lowest in the coastal stations (Table 1). Total organic carbon (TOC; %) in sediments was highest in the northern Bering Sea while total organic nitrogen (TON; %) in the sediments did not vary by more than 0.1 % between the study areas.

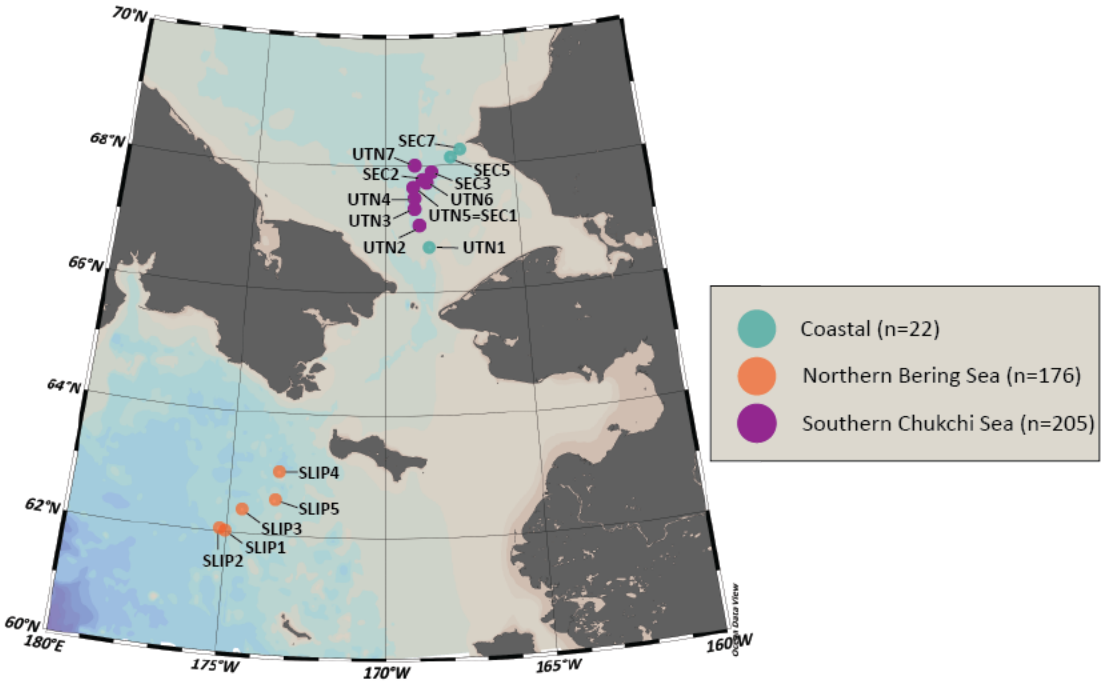

Figure 6. Map of stations clustered by environmental parameters with number of benthic macroinvertebrate samples collected within each cluster (n).

Table 1. Mean (± SD) environmental parameters of station clusters (NBS: northern Bering Sea; SCS: southern Chukchi Sea). Means were calculated by averaging the environmental parameters for each year and station (2014-2019 and 2021). Temperature, nutrient concentrations, salinity, and $\delta^{18}O$ values are from samples from the bottom water.

Cluster	Depth (m)	Temp (°C)	Salinity	Silicate (µmol/L)	Nitrate + Nitrite (µmol/L)	Phosphate (µmol/L)	Ammonium (µmol/L)
Coastal	42 ± 7	4.6 ± 1.4	31.7 ± 0.5	5.95 ± 2.71	1.11 ± 0.82	0.66 ± 0.17	0.87 ± 0.32
NBS	73 ± 6	-0.8 ± 1.0	32.1 ± 0.2	39.28 ± 9.86	15.11 ± 3.24	2.07 ± 0.39	2.73 ± 1.16
SCS	51 ± 5	2.6 ± 1.4	32.6 ± 0.2	16.12 ± 10.88	10.68 ± 3.94	1.48 ± 0.37	2.73 ± 1.02

Table 1. (cont.)

Cluster	$\delta^{18}O$ (‰)	Bottom Water Chl *a* (µg/L)	Integrated Chl *a* (mg/m^2)	Sediment Chl *a* (mg/m^2)	Silt and Clay Content (% ≥ 5 phi)	Total Organic Carbon (%)	Total Organic Nitrogen (%)
Coastal	-1.6 ± 0.4	1.73 ± 1.65	48.38 ± 33.99	18.37 ± 8.94	32.8 ± 15.6	0.6 ± 0.2	0.1 ± 0.0
NBS	-1.3 ± 0.3	0.94 ± 1.31	63.39 ± 55.87	20.30 ± 9.71	78.3 ± 11.1	1.2 ± 0.3	0.2 ± 0.0
SCS	-1.0 ± 0.3	5.62 ± 4.38	277.34 ± 194.6	21.97 ± 6.39	76.5 ± 15.6	1.0 ± 0.2	0.2 ± 0.0

These regions also have distinct biological characteristics (Figure 7). In the study years when benthic macroinvertebrate biomass data were available (2014, 2015, and 2017), the southern Chukchi Sea had the highest benthic macroinvertebrate biomasses of the three clusters (Figure 7). When averaged across study years where data were available, mean abundance (number of benthic macroinvertebrates/m^2) was highest in the southern Chukchi Sea at 8,504 ± 3,314 while mean abundances in the northern Bering Sea and coastal stations were lower: 3,310 ± 1,212 and 2,739 ± 652, respectively. The northern Bering Sea had the highest number of taxonomic families present per m^2 (46 ± 6) during the study years. The southern Chukchi Sea had the lowest number of taxonomic families (33 ± 5), and the coastal stations were intermediate (42 ± 5). Shannon-Weiner Indexes (a measure of biodiversity) were similar in the coastal stations and northern Bering Sea (2.9 ± 0.3 and 2.8 ± 0.2, respectively) while the southern Chukchi Sea stations had a lower mean Shannon-Weiner Index of 1.5 ± 0.5.

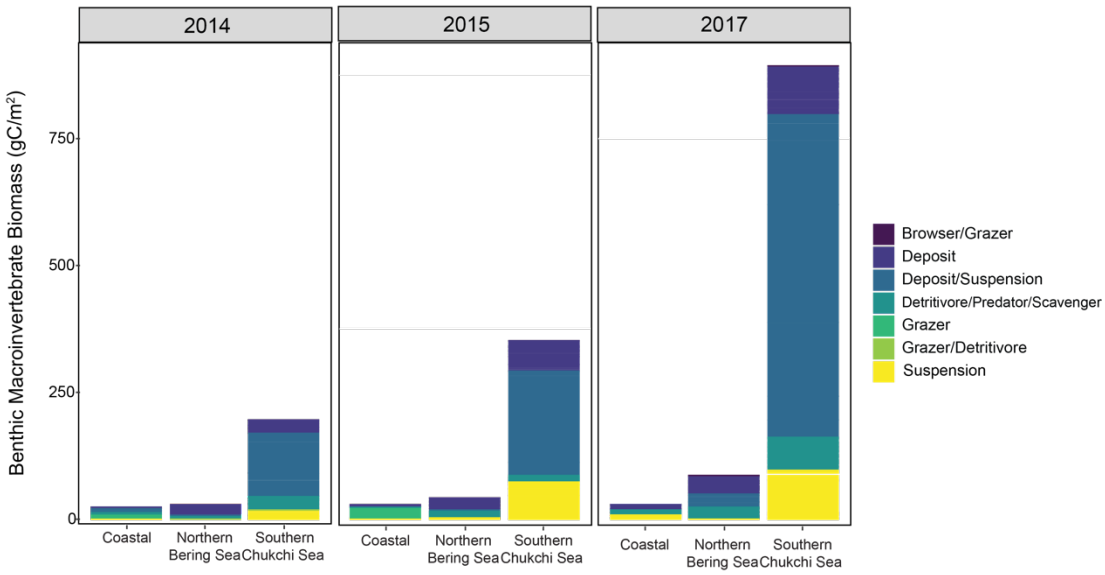

Figure 7. Benthic macroinvertebrate biomass (gC/m^2) grouped by feeding type and cluster for 2014, 2015, and 2017.

3.2 Benthic macroinvertebrates

A total of 403 benthic macroinvertebrates were analyzed for δ^{13}C and δ^{15}N values. Twenty-two benthic macroinvertebrates were from coastal stations, 176 were from the northern Bering Sea, and 205 organisms were from the southern Chukchi Sea (Figure 6). Samples were grouped based on clusters, year sampled, and taxonomic family. Five brittle stars (Echinodermata: Ophiuroidea) were analyzed for δ^{15}N values before and after acidification. The brittle stars were from the taxonomic families Ophiactidae and Ophiuridae. The mean δ^{15}N value of the brittle stars before acidification was 0.4 ‰ less than the mean after acidification. The sample error for δ^{15}N values was 0.1 ‰. Therefore, δ^{15}N values before acidification are reported for these five samples. The only brittle star sample that I did not analyze for δ^{15}N before

analysis was an Ophiuridae from the northern Bering Sea in 2017. The δ^{15}N value of that sample is not reported.

3.2.1 Tissue Type

Of the thirty-two samples in which muscle tissue could be extracted, 26 were from UTN2, five were from SEC2, and one was from UTN7 (see Figure 1 and Figure 6). The organisms were from the taxonomic families Cardiidae (bivalve; n = 22), Myidae (bivalve; n = 2), Natacidae (gastropod; n = 1), and Yoldiidae (bivalve; n = 7). I did not reject the null hypothesis that the differences between the δ^{15}N of the body and the δ^{15}N of the bivalve foot muscle were equal to zero (paired Wilcoxon rank sum test: V = 193, P = 0.190; Figure 8). However, the null hypothesis of no significant difference was rejected for δ^{13}C values (paired Wilcoxon Rank sum test: V = 40, P < 0.001; Figure 9). The mean δ^{13}C of the body was on average 1.5 ‰ lower than the mean δ^{13}C of the bivalve muscle tissue (Figure 9).

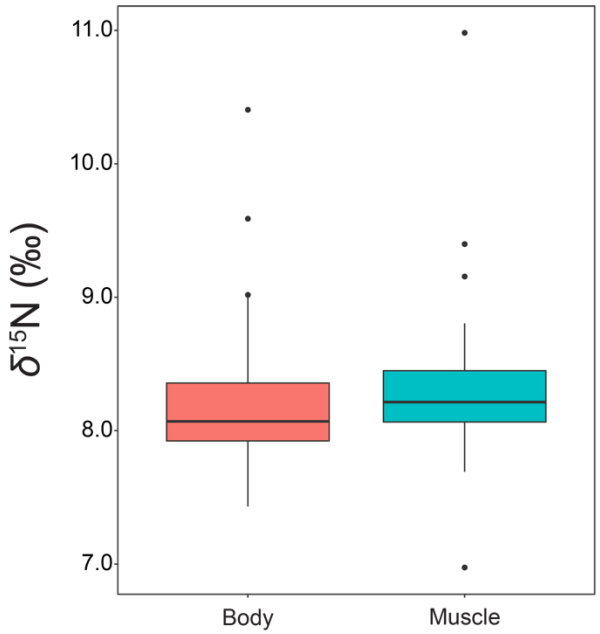

Figure 8. Box plot of the δ^{15}N values (‰) by tissue type (body or foot muscle) of 31 bivalves and one gastropod from SEC2, UTN2, and UTN7 stations with components include median (horizontal bar), interquartile range (IQR; box), 1.5*IQR (error bars) and outliers (± 1.5*IQR; black dots). The mean δ^{15}N of the body tissue was +8.3 ‰ (±0.6 SD), and the mean δ^{15}N value of the muscle tissue was +8.3 ‰ (±0.7 SD)

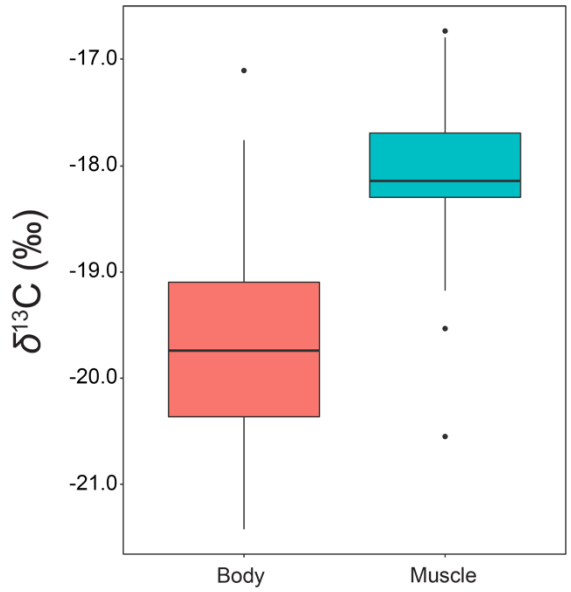

Figure 9. $\delta^{13}C$ values by tissue type (body or foot muscle) of 24 bivalves and one gastropod from SEC2, UTN2, and UTN7 stations median (horizontal bar), interquartile range (IQR; box), 1.5*IQR (error bars) and outliers (± 1.5*IQR; black dots). The mean $\delta^{13}C$ value of the body tissue was -19.6 ‰ (± 1.1 SD) and the mean $\delta^{13}C$ of the muscle tissue was -18.1 ‰ (± 0.8 SD).

3.2.2 Trophic position

I used the clusters reported in Section 3.1 to calculate the mean $\delta^{15}N$ and $\delta^{13}C$ values of the sediment for each year. In all clusters except for $\delta^{13}C$ values at coastal stations, there were significant differences between the sediment $\delta^{15}N$ and $\delta^{13}C$ values among years (Table 2). Therefore, trophic position was calculated separately for each year for both Bayesian and traditional TP calculations. The $\delta^{15}N_{sediment}$ was the average $\delta^{15}N$ value of the sediment from the cluster and year of the sample.

Table 2. Results of Kruskal-Wallis tests on the $\delta^{13}C$ and $\delta^{15}N$ values of sediment collected in different years from 2014 to 2017 and 2021.

	$\delta^{13}C$			$\delta^{15}N$		
Cluster	**chi-squared**	**df**	**P-value**	**chi-squared**	**df**	**P-value**
Northern Bering Sea	23.01	4	<0.001*	16.60	4	0.002*
Southern Chukchi Sea	23.26	4	<0.001*	25.78	4	<0.001*
Coastal	2.17	4	0.705	11.97	4	0.018*

*significant P-values (<0.05)

TDFs in the Bayesian model and in the traditional calculations of TP were calculated from data presented in McTigue and Dunton (2014). I simulated a normally distributed data set using the mean and standard deviation of the difference between in $\delta^{15}N$ and $\delta^{13}C$ values of *A. macrocephala* and phytoplankton (McTigue & Dunton, 2014). The TDF for $\delta^{15}N$ was 3.4 ‰ with an SD of 0.6 ‰, and the TDF for $\delta^{13}C$ was 0.4 ‰ with a standard deviation of 0.6 ‰. The TDF for $\delta^{15}N$ was used in both the Bayesian and traditional estimates of TP while the TDF for $\delta^{13}C$ was only used in the Bayesian estimations.

Nine families had adequate sample size for each study year and cluster ($n > 8$) for Bayesian estimation of trophic position with the R package, *tRophicPosition* (Quezada-Romegialli et al., 2019). The two baselines included in the two source full baseline model were the sediment and POM samples. The POM samples were collected in 2016 in the southern Chukchi Sea and 2015 in the northern Bering Sea. I used a lamda (baseline TP) of one for the model as both the sediment and POM sources are at the base of the food web (TP = 1). The model was run with an uninformative prior, 200,000 adaptive iterations before sampling, and 200,000

posterior iterations of the model. 20,000 of those iterations were discarded as "burn in" and five parallel chains were run (Quezada-Romegialli et al., 2019).

After calculation using Bayesian approaches, I used the traditional method of calculating trophic position (Equation 3). Welch's t-tests and Wilcoxon rank sum exact tests were used to compare Bayesian and tradition methods of estimating TP for the nine groups where sample size was adequate for Bayesian trophic position estimations. Six out of the nine groups analyzed had significantly different TPs when estimated with the different methods (Table 3). Bayesian TP estimates were greater than the estimates from traditional methods. On average, the Bayesian TP estimates were 0.5 (± 0.3 SD) greater than the traditional estimates of TP.

Table 3. Results comparing mean (± SD) trophic position (TP) calculated using the Bayesian approach with R package, *tRophicPosition*, and the traditional approach (+3.4 ‰ per trophic level). Clusters are northern Bering Sea (NBS) and southern Chukchi Sea (SCS). The test used determined the statistic presented in the table. If Welch's t-test was used, the t-statistic is reported. If the Wilcoxon rank-sum exact test was used, the Wilcoxon statistic is reported.

Cruise	Cluster	Taxonomic Family	n	Traditional TP	Bayesian TP	Test Used	Statistic	P
SWL14	NBS	Nuculanidae	13	1.5 ± 0.2	1.5 ± 0.2	t-test	23.1	0.691
SWL14	NBS	Tellinidae	17	1.2 ± 0.2	1.3 ± 0.2	Wilcoxon	177.0	0.264
SWL14	SCS	Cardiidae	17	1.3 ± 0.1	1.6 ± 0.3	Wilcoxon	224.5	0.005*
SWL14	SCS	Tellinidae	26	1.5 ± 0.4	1.9 ± 1.0	t-test	2.3	0.029*
SWL21	NBS	Maldanidae	8	2.5 ± 0.2	2.8 ± 0.5	t-test	1.8	0.095
SWL21	NBS	Tellinidae	9	0.9 ± 0.1	1.4 ± 0.6	Wilcoxon	67.5	0.014*
SWL21	SCS	Nephtyidae	9	2.3 ± 0.1	3.2 ± 1.2	Wilcoxon	63.0	0.049*
SWL21	SCS	Pectinaridae	11	2.3 ± 0.2	2.9 ± 0.5	t-test	3.77	0.002*
SWL21	SCS	Tellinidae	36	1.0 ± 0.1	1.6 ± 0.3	Wilcoxon	1243.0	<0.001*

*indicates significant p-values

3.3 Overview

3.3.1 Coastal

The cluster with the least benthic macroinvertebrate samples was the coastal cluster (Figure 6 and Figure 10). Due to limited water column production, no POM samples were collected in this region. The $\delta^{13}C$ values in the sediment ranged from -23.0 ‰ (± 1.0 SD) in 2021 to -22.2 ‰ (± 0.4 SD) in 2015 and $\delta^{15}N$ sediment values ranged from 6.1 ‰ (± 1.6 SD) in 2015 to 8.8 ‰ (± 0.5 SD) in 2021. The organism with the highest $\delta^{13}C$ and $\delta^{15}N$ values was a predatory polychaete, Family Nephtyidae, in 2015. The organism with the lowest $\delta^{15}N$ values was the deposit feeding polychaete, Family Sternaspidae, in 2021. Unidentified tunicates had the lowest mean $\delta^{13}C$ value in 2015. None of the consumer samples had large enough sample sizes for statistical analysis between years (Table 4).

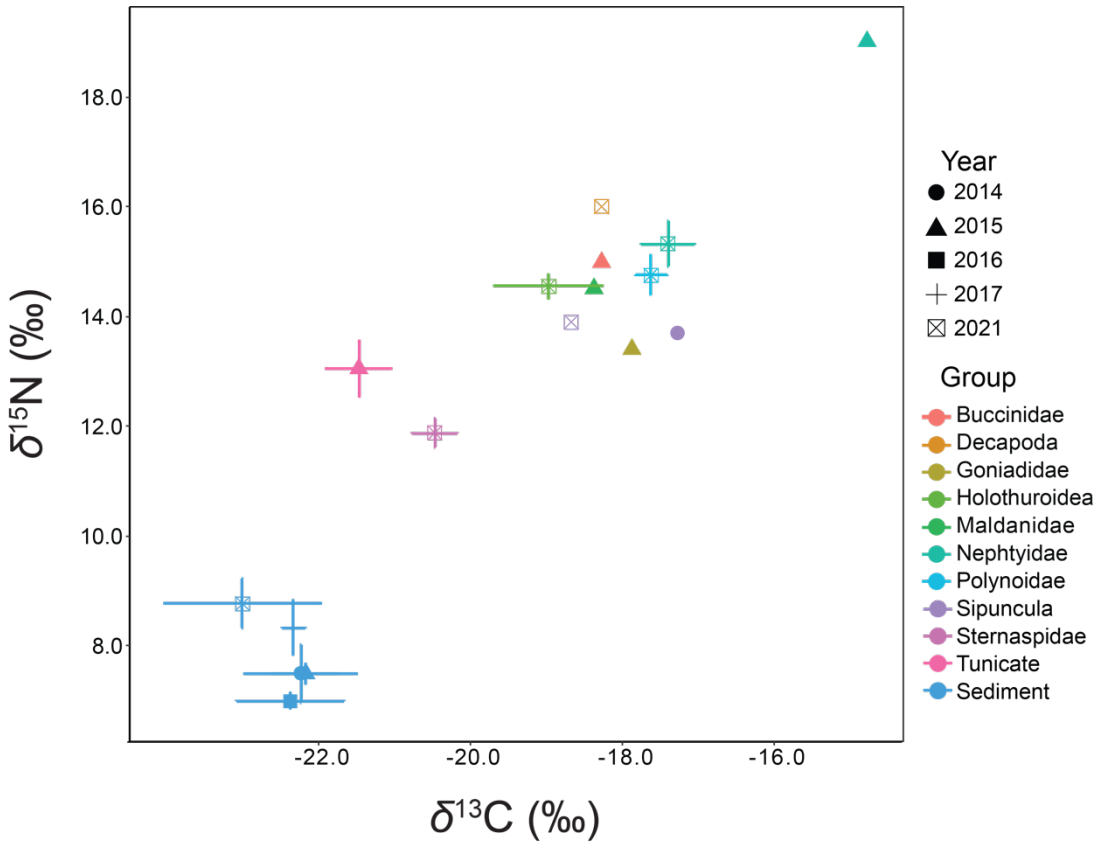

Figure 10. Mean (points) and standard deviations (error bars) $\delta^{13}C$ and $\delta^{15}N$ values (‰) of benthic macroinvertebrates and sediment collected in the coastal stations. Symbols represent the year of sampling. Benthic macroinvertebrate groups are the lowest taxonomic category the sample was identified to (phylum or taxonomic family).

Table 4. Mean stable isotope values ($\delta^{13}C$ and $\delta^{15}N$), standard deviations (±SD), number of replicates (n), and C/N (wt./wt.) of benthic macroinvertebrates (by group and taxonomic family) and sediment in the coastal stations. Feeding type is also reported using the classifications of Macdonald et al (2010). Trophic positions (TP) for benthic macroinvertebrates were calculated using mean sediment $\delta^{15}N$ values from the year of sampling.

		Coastal Stations									
				$\delta^{13}C$		$\delta^{15}N$					
Group/Family	**Feeding Type**	**Year**	**n**	**(‰)**	**±SD**	**(‰)**	**±SD**	**C/N**	**±SD**	**TP**	**±SD**
Sediment											
		2014	3	-22.3	0.7	7.5	0.5	7.4	0.1		
		2015	3	-22.2	0.4	7.5	0.2	6.6	0.3		

		2016	2	-22.4	0.7	7.0	0.1	6.7	0.9		
		2017	3	-22.4	0.2	8.3	0.5	7.1	0.3		
		2021	3	-23.0	1.0	8.8	0.5	8.1	0.6		
Echinodermata											
Holothuroidea	Browser/Grazer										
		2021	2	-19.0	0.7	14.6	0.2	4.8	0.1	2.6	0.0
Gastropoda											
Buccinidae	Scavenger										
		2015	1	-18.3		15.0		4.2		3.2	
Polychaeta											
Maldanidae	Subsurface Deposit										
		2015	1	-18.4		14.5		4.4		3.1	
Nephtyidae	Predator										
		2015	1	-14.8		19.0		3.9		4.4	
		2021	4	-17.4	0.4	15.3	0.4	4.3	0.2	2.8	0.1
Polynoidae	Predator										
		2021	2	-17.6	0.2	14.8	0.4	4.4	0.1	2.7	0.1
Sternaspidae	Suspension										
		2021	5	-20.5	0.3	11.9	0.3	4.7	0.2	1.8	0.1
Sipuncula											
	Herbivorous										
		2014	1	-17.3		13.7		4.1		2.8	
		2021	1	-18.7		13.9		4.1		2.8	
Goniadidae											
		2015	1	-17.9		13.4		3.7		2.4	
Tunicata	Suspension										
		2015	2	-21.5	0.4	13.1	0.5	5.4	0.3	2.7	0.1

3.3.2 Northern Bering Sea

The average $\delta^{13}C$ value of the sediment in the northern Bering Sea during our study period ranged from -23.3 ‰ in 2021 to -20.7 ‰ in 2016 (Table 5 and Figure

11). The lowest average sediment δ^{15}N value was in 2016 (8.6 ‰) and the highest was in 2017 (9.9 ‰). The predatory gastropod from the family Cyclinidae had the highest δ^{13}C value at -16.9 ‰ in 2015 while the lowest δ^{13}C value reported (-23.4 ‰) in 2015 was from the deposit feeding polychaetes in the family Pectinariidae. The highest δ^{15}N value was in the predatory priapulid worm (Family: Priapulidae) at 17.5 ‰ in 2015, and the lowest was the nucuilid bivalves from 2021 with a mean δ^{15}N value of 9.0 ‰.

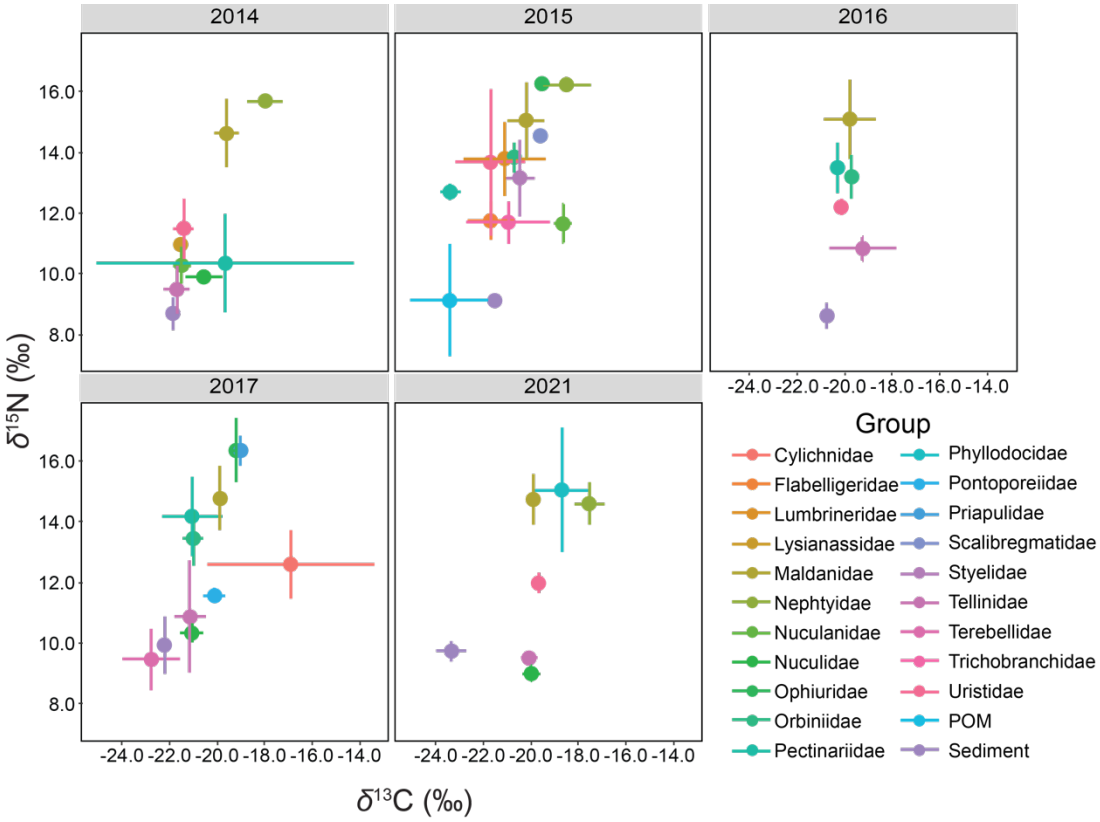

Figure 11. Mean (point) and standard deviation (error bars) of δ^{13}C and δ^{15}N values of benthic macroinvertebrates, sediment, particulate organic matter (POM) of samples collected in the northern Bering Sea. Each graph is a year in which sampling occurred. Groups represent either the baseline group (sediment or POM) or the taxonomic family. Taxonomic families with one sample per taxonomic family were excluded from these graphs for simplicity.

Table 5. Mean stable isotope values (δ^{13}C and δ^{15}N), standard deviations (±SD), number of replicates (n), and C/N (wt./wt.) of benthic macroinvertebrates (by group and taxonomic family) and isotopic baselines (POM [particulate organic matter] and sediment) in the northern Bering Sea stations. Feeding type is also reported using the classifications of Macdonald et al (2010). Trophic positions (TP) for benthic macroinvertebrates are presented using the mean δ^{15}N value of the sediment for the year of sampling.

		Northern Bering Sea									
Group/Family	**Feeding Type**	**Year**	**n**	**δ^{13}C (‰)**	**±SD**	**δ^{15}N (‰)**	**±SD**	**C/N**	**±SD**	**TP**	**±SD**
Sediment											
		2014	5	-21.9	0.1	8.7	0.5	6.2	0.3		
		2015	5	-21.5	0.1	9.1	0.2	6.4	0.2		
		2016	5	-20.7	0.2	8.6	0.4	6.3	0.1		
		2017	5	-22.2	0.2	9.9	0.9	6.5	0.2		
		2021	5	-23.3	0.6	9.7	0.3	7.8	0.2		
POM											
		2015	5	-23.4	1.6	9.1	1.8				
Amphipoda											
Lysianassidae	Scavenger										
		2014	3	-21.5	0.1	11.0	0.1	10.0	0.3	1.7	0.1
Oedicerotidae	Predator										
		2015	1	-19.1		15.8		5.3		3.0	
Pontoporeiidae	Surface Deposit										
		2017	3	-20.1	0.5	11.6	0.3	7.5	0.7	1.6	0.1
Uristidae	Scavenger										
		2014	2	-21.4	0.4	11.5	1.0	11.0	0.1	1.8	0.3
		2015	4	-21.7	1.5	13.7	2.4	9.8	2.0	2.4	0.7
		2016	2	-20.1	0.1	12.2	0.3	8.9	0.4	2.0	0.1
		2021	5	-19.7	0.3	12.0	0.3	7.8	0.4	1.6	0.1
Bivalvia											
Lyonsiidae	Suspension										
		2014	1	-20.6		10.1		5.9		1.4	
Nuculanidae	Surface Deposit										
		2014	13	-21.5	0.4	10.3	0.6	7.2	0.5	1.5	0.2
		2015	2	-18.7	0.4	11.6	0.6	4.0	0.1	1.8	0.2
		2017	1	-21.2		11.0		6.0		1.4	
Nuculidae	Subsurface Deposit										

		2014	5	-20.6	0.8	9.9	0.2	6.7	0.9	1.3	0.1
		2017	3	-21.1	0.5	10.3	0.3	7.3	[1]	1.2	0.1
		2021	5	-20.0	0.4	9.0	0.3	6.2	0.5	0.7	0.1
Tellinidae	Surface Deposit/ Suspension										
		2014	17	-21.7	0.1	9.5	0.8	8.0	0.9	1.2	0.2
		2016	3	-19.2	1.4	10.8	0.4	5.3	0.6	1.6	0.1
		2017	6	-21.1	0.7	10.9	1.9	7.6	1.2	1.4	0.5
		2021	9	-20.1	0.3	9.5	0.2	6.4	0.6	0.8	0.3
Echinodermata											
Ophiactidae	Suspension										
		2017	1	[2]		13.4		11.0		2.1	
Ophiuridae	Predator										
		2015	3	-19.5	0.3	16.2	0.2	6.0	2.3	3.1	0.1
		2017	2	-19.2	0.1	16.4	1.1	4.4	0.1	3.0	0.3
Gastropoda											
Cylichnidae	Predator										
		2017	2	-16.9	3.5	12.6	1.1	5.7	0.2	1.9	0.3
Nemertea	Predator										
		2015	1	-19.2		15.8		4.9		3.0	
		2017	1	-20.3		12.0		5.3		1.7	
Polychaeta											
Ampharetidae	Surface Deposit										
		2015	1	-23.2		12.2		9.3		1.9	
Cirratulidae	Surface Deposit										
		2015	1	-20.1		13.3		4.5		2.2	
Flabelligeridae	Surface Deposit										
		2015	2	-21.7	1.0	11.8	0.6	5.8	0.7	1.8	0.2
		2017	1	-20.5		11.5		4.8		1.6	
		2021	1	-19.4		12.8		5.1		1.9	
Goniadidae	Predator										
		2015	1	[3]		11.8		10.0		1.8	
Lumbrineridae	Subsurface Deposit/ Detritivore/										

[1] Due to a software issue, total organic carbon and nitrogen were not measured for two of the samples
[2] Sample was not acidified and was high in carbonates so only $\delta^{15}N$ value is reported
[3] Due to a software error, $\delta^{13}C$ value was not available

	Predator									
		2015	3	-21.1	1.7	13.8	1.2	6.4	2.0	2.4	0.3
	Subsurface										
Maldanidae	Deposit										
		2014	4	-19.6	0.5	14.6	1.1	5.0	0.5	2.8	0.4
		2015	5	-20.2	0.8	15.1	1.3	5.1	0.9	2.7	0.4
		2016	5	-19.8	1.1	15.1	1.3	4.8	0.5	2.9	0.4
		2017	3	-19.9	0.1	14.8	1.1	4.9	0.4	2.6	0.3
		2021	8	-20.1	0.7	14.1	2.1	5.2	0.5	2.4	0.3
Nephtyidae	Predator										
		2014	3	-18.0	0.8	15.7	0.2	3.9	0.1	3.1	0.1
		2015	3	-18.5	1.1	16.2	0.3	4.3	0.3	3.1	0.1
		2021	2	-17.6	0.6	14.6	0.7	4.2	0.1	2.4	0.1
	Detritivore/ Browser/ Predator/										
Onuphidae	Scavenger										
		2015	1	-21.9		16.6		5.3		3.2	
		2017	1	-18.8		15.5		4.4		2.8	
	Subsurface										
Orbiniidae	Deposit										
		2015	2	-20.7	0.3	13.8	0.5	5.2	0.0	2.4	0.1
		2016	2	-19.7	0.0	13.2	0.7	5.2	0.3	2.3	0.2
		2017	2	-21.0	0.4	13.4	0.9	6.2	1.4	2.2	0.2
	Subsurface										
Pectinariidae	Deposit										
		2014	2	-19.6	5.4	10.3	1.6	11	2.2	1.5	0.5
		2015	2	-23.4	0.4	12.7	0.3	8.1	1.3	2.1	0.1
		2016	2	-20.3	0.1	13.5	0.8	5.6	1.2	2.4	0.3
		2017	5	-21.1	1.3	14.2	1.3	6.0	1.3	2.4	0.4
		2021	1	-20.9		14.2		5.7		2.3	
	Predator/										
Phyllodocidae	Scavenger										
		2021	2	-18.7	1.1	15.1	2.1	5.0	0.3	2.6	0.6
	Subsurface										
Scalibregmatidae	Deposit										
		2015	2	-19.6	0.0	14.6	0.1	4.7	0.1	2.6	0.0
	Surface										
Terebellidae	Deposit										
		2017	3	-22.8	1.2	9.5	1.0	7.6	3.6	1.0	0.3
	Surface										
Trichobranchidae	Deposit										
		2015	2	-21.0	1.8	11.7	0.7	6.0	0.6	1.8	0.2

Priapulida											
Priapulidae	Predator										
		2015	1	-18.9		17.5		4.8		3.5	
		2017	2	-19.0	0.3	16.4	0.5	5.0	0.1	3.0	0.1
Tunicata											
Styelidae	Suspension										
		2015	3	-20.5	0.6	13.2	1.3	6.5	0.4	2.2	0.4

The taxonomic family, Tellinidae, had adequate sample sizes for comparison between years when the samples from 2016 and 2017 were combined into one group (Figure 12). A Welch's One-Way ANOVA test was performed on the $\delta^{13}C$ values of Tellinidae among samples collected in 2014, 2016-2017, and 2021. There were significant differences between at least two of the temporal groups ($F(2 \text{ [between group degrees of freedom]},35\text{[within group degrees of freedom]}) = 43.17$, $P < 0.001$). Pairwise t-tests were performed with Bonferroni p-value adjustments and a pooled standard deviation. These tests revealed that the differences were between the $\delta^{13}C$ values of the Tellinidae collected in 2014 and the two other groups: 2016-2017 ($P = 0.002$) and 2021 ($P < 0.001$). There were no significant differences between the Tellinidae $\delta^{13}C$ values in 2016-2017 and 2021 ($P = 0.763$). The mean Tellinidae $\delta^{13}C$ value in 2014 was -21.6 ‰ (± 0.5 SD) while the means in 2016-2017 and 2021 were more enriched, -20.5 ‰ (± 1.3 SD) and -20.1 ‰ (± 0.3 SD), respectively. The TPs were also compared temporally among Tellinidae in the northern Bering Sea using the non-parametric Kruskal-Wallis test. The test found significant differences between at least two pairs ($H(2 \text{ [between group degrees of freedom]}) = 17.20$, $P < 0.001$). Tellinidae in 2016 and 2017 had significantly higher TP (mean ± SD: 1.5 ±

0.4) than the Tellinidae in 2021 (0.8 ± 0.3; P = 0.001). The Tellinidae TP in 2014 was also significantly higher (mean ± SD: 1.2 ± 0.2) than the TP in 2021 (P = 0.004). There were no significant differences between the TPs in 2014 and 2016-2017 for the Tellinidae in the northern Bering Sea (P = 0.327; Figure 12).

Stable isotope values of $\delta^{13}C$ and $\delta^{15}N$ can vary based on the size of the organism (Fry & Arnold, 1982; Schlacher & Connolly, 2014; Villamarín et al., 2018). Length (mm) of the Tellinidae samples were measured prior to dissection analysis. The mean (± SD) lengths in 2014, 2016-2017, and 2021 were 19.9 ± 7.6 mm, 12.4 ± 5.2 mm, and 22.9 ± 7.7 mm. A Kruskal-Wallis test found there were significant differences between these lengths (H(2) = 10.0; P = 0.006). A post-hoc, pairwise, Wilcoxon rank sum test with Bonferroni multiple test corrections revealed the differences were between 2014 and 2016-2017 (P = 0.016) and between 2016-2017 and 2021 (P = 0.012). There was not a significant difference between Tellinidae length in 2014 and 2021 (P = 1.0).

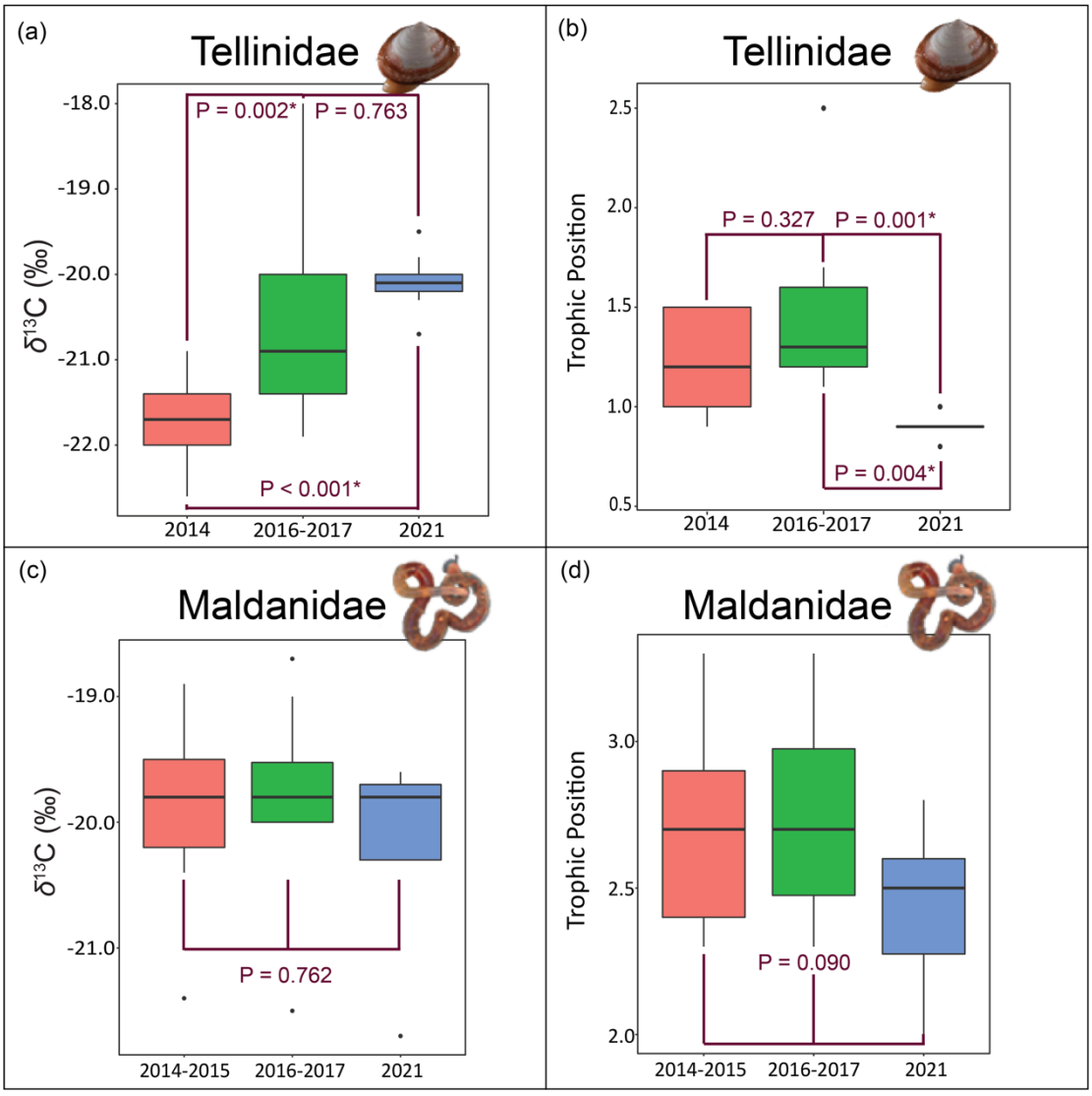

Figure 12. Boxplots of Tellinidae (a-b) and Maldanidae (c-d) δ^{13}C values (‰) and trophic position (TP) from the northern Bering Sea cluster plotted over time. Boxplot components include median (horizontal bar), interquartile range (IQR; box), 1.5*IQR (error bars) and outliers (± 1.5*IQR; black dots). P-values from time-period comparisons are reported in burgundy type with the burgundy bars indicating the groups compared. *indicates significant p-values. (a). Tellinidae δ^{13}C values (‰) plotted over time (2016 and 2017 combined to reach adequate sample size for analysis) with post-hoc Kruskal-Wallis p-value results from pairwise comparisons. (b) Tellinidae TP in three temporal categories with post-hoc Kruskal-Wallis p-value results. (c) Maldanidae δ^{13}C values (‰) plotted over time with 2014 and 2015 combined and 2016 and 2017 combined to reach adequate sample size for statistical

analysis. Kruskal-Wallis test result p-value is also reported. (d) Maldanidae TP plotted in three temporal categories with p-value result of the Kruskal-Wallis test.

The Maldanidae family also had large enough sample sizes for comparison between years when 2014 and 2015 were treated as one group and 2016 and 2017 were treated as one group (Figure 12). The non-parametric Kruskal-Wallis test was used to compare δ^{13}C values among the three groups (2014-2015, 2016-2017, and 2021). There were no significant differences among these groups for Maldanidae samples in the northern Bering Sea ($H(2) = 0.54$; $P = 0.762$). There were also no significant differences between Maldanidae TP among these temporal groups (Kruskal-Wallis test: $H(2) = 4.81$; $P = 0.090$).

3.3.3 Southern Chukchi Sea

In the southern Chukchi Sea sediment samples, the most heavy isotope depleted mean δ^{13}C value was observed in 2021 (-22.2 ‰) while the most heavy isotope enriched value was in 2016 (-21.2 ‰; Table 6; Figure 13). The most heavy isotope depleted δ^{15}N value in sediment was in 2016 (+ 7.2 ‰) and the most heavy isotope enriched value was in 2021 (+ 8.5 ‰). The organism with the highest δ^{15}N value (14.6 ‰) and the highest δ^{13}C value (-14.6 ‰) was a ribbon worm or Nemertea collected in 2021. The most negative δ^{13}C value was a Trichobranchidae polychaete from 2016 (-20.1 ‰). Trichobranchidae are surface deposit feeders (Macdonald, et al., 2010). The mean δ^{15}N value of Myidae, suspension feeding bivalves (Macdonald, et al., 2010), collected in from 2021 had the lowest δ^{15}N value (+ 7.3 ‰) of the organisms collected in the southern Chukchi Sea.

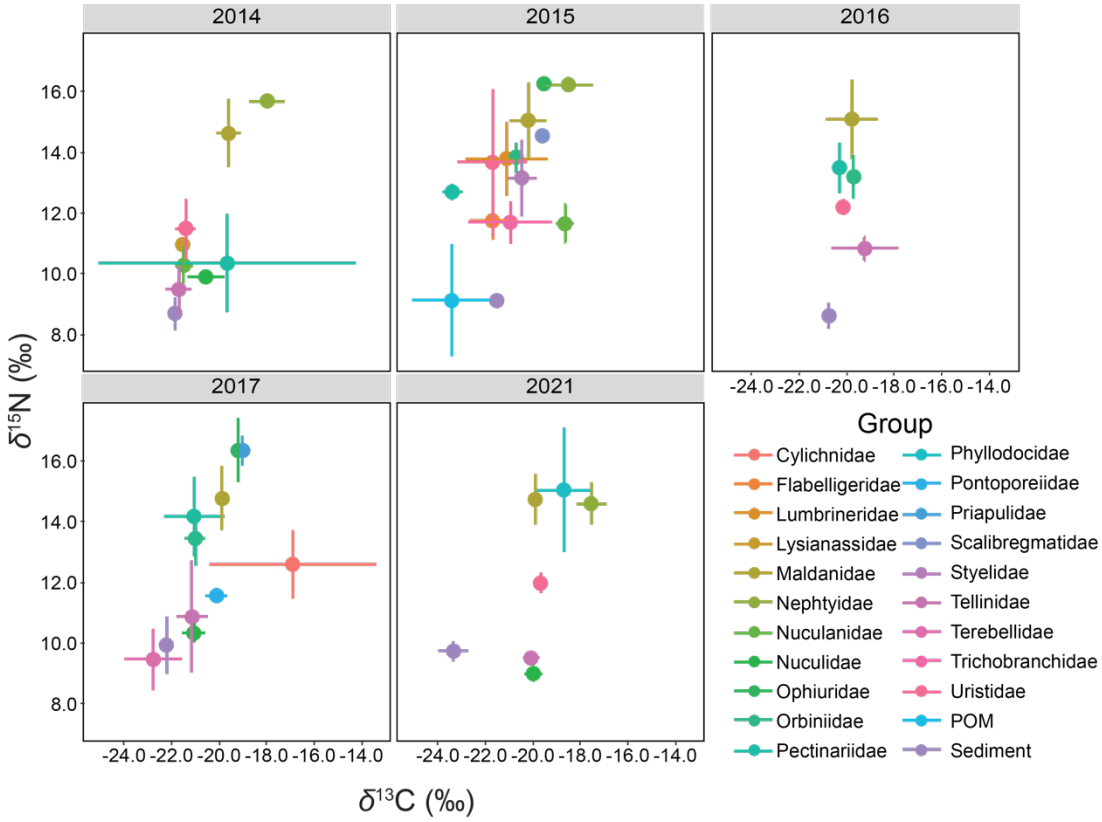

Figure 13. Mean (point) and standard deviation (error bars) of $\delta^{13}C$ and $\delta^{15}N$ values of benthic macroinvertebrates, sediment, particulate organic matter (POM) of samples collected in the southern Chukchi Sea. Each graph corresponds to a year in which sampling occurred. Groups represent either the baseline group (sediment or POM) or the taxonomic family. Taxonomic families with one sample per taxonomic family were excluded from these graphs for simplicity.

Table 6. Mean stable isotope values ($\delta^{13}C$ and $\delta^{15}N$), standard deviations (±SD), number of replicates (n), and C/N (wt./wt.) of benthic macroinvertebrates (by group and taxonomic family) and isotopic baselines (POM [particulate organic matter] and sediment) in the southern Chukchi Sea stations. Feeding types are also reported using the classifications in Macdonald et al (2010). Trophic positions (TP) for benthic macroinvertebrates are presented using the mean $\delta^{15}N$ value of the sediment for the year of sampling.

		Southern Chukchi Sea									
Group/Family	Feeding Type	Year	n	$\delta^{13}C$ (‰)	±SD	$\delta^{15}N$ (‰)	±SD	C/N	±SD	TP	±SD
Sediment											
		2014	8	-21.6	0.2	7.3	0.3	6.4	0.3		

		2015	8	-21.4	0.1	7.6	0.2	6.3	0.1		
		2016	8	-21.2	0.3	7.2	0.5	6.1	0.2		
		2017	8	-21.9	0.1	8.0	0.4	6.5	0.1		
		2021	7	-22.2	0.6	8.5	0.2	7.8	0.2		
POM											
		2015	6	-24.1	1.2	7.5	0.8				
		2016	6	-22.8	0.8	6.3	0.8				
Amphipoda											
Lysianassidae	Scavenger										
		2014	1	-19.8		9.2		9.1		1.6	
Melitidae	Detritivore										
		2017	1	-16.7		10.7		6.3		1.8	
Pontoporeiidae	Surface Deposit										
		2017	1	-19.3		9.9		6.0		1.6	
Bivalvia											
Cardiidae	Suspension										
		2014	22[4]	-18.4	0.8	8.2	0.2	6.2	1.1	1.3	0.1
		2017	1	-17.5		9.4		4.1		1.4	
Hiatellidae	Suspension										
		2017	1	-18.5		10.3		3.8		1.7	
Myidae	Suspension										
		2014	2	-18.4	0.1	7.3	0.5	5.2	1.3	1.1	0.1
		2021[5]	1	-17.2		7.9		3.8		0.8	
Nuculanidae	Surface Deposit										
		2017	2	-19.0	0.4	9.6	0.4	6.1	2.7	1.5	0.1
Nuculidae	Subsurface Deposit										
		2014	6	-19.3	0.7	10.1	0.5	6.0	0.6	1.9	0.1
		2015	2	-19.1	0.1	9.4	0.1	5.4	0.3	1.6	0.1
		2016	2	-19.2	0.9	9.6	0.7	4.3	0.0	1.6	0.2
		2017	4	-19.0	0.6	9.8	0.3	5.0	1.2	1.6	0.1

[4] Sample size for $\delta^{13}C$ values was 18. Due to a software error, four samples were not analyzed for $\delta^{13}C$ values

[5] Siphon

Tellinidae	Surface Deposit/ Suspension										
		2014	26	-18.6	0.5	8.5	0.5	6.9	2.3	1.4	0.1
		2015	6	-17.9	0.2	9.5	0.7	5.3	0.1	1.6	0.2
		2016	5	-17.6	0.1	9.7	0.6	4.6	0.2	1.6	0.2
		2017	5	-18.3	0.1	9.7	0.5	5.7	1.2	1.5	0.2
		2021	36	-19.1	0.5	8.5	0.5	5.9	0.5	1.0	0.1
Yoldiidae	Subsurface Deposit										
		2014	5	-17.9	1.1	8.4	0.4	5.0	0.8	1.4	0.1
		2017	3	-17.6	0.6	9.1	0.5	5.5	0.6	1.4	0.1
		2021	4	-17.8	0.9	8.7	0.4	4.4	0.3	1.0	0.1
Echinodermata											
Ophiuridae	Predator										
		2017	1	-17.9		13.8		5.1		2.7	
Gastropoda											
Naticidae	Predator										
		2014	1	-17.1		11.0		4.2		2.2	
		2021	1	-16.0		12.4		6.2		2.1	
Nemertea	Predator										
		2021	1	-14.6		14.6		4.1		2.8	
Polychaeta											
Ampharetidae	Surface Deposit										
		2014	4	-18.8	0.4	9.3	0.4	7.0	0.7	1.7	0.1
		2021	3	-19.4	0.4	8.7	0.3	5.5	0.5	1.1	0.1
Flabelligeridae	Surface Deposit										
		2014	1	-16.6		12.0		4.1		2.5	
		2017	1	-19.9		11.7		4.6		2.1	
Maldanidae	Subsurface Deposit										
		2016	4	-18.5	0.6	13.7	0.4	4.1	0.4	2.8	0.1
		2017	4	-18.2	0.1	12.8	0.3	4.7	0.6	2.4	0.1
Nephtyidae	Predator										
		2014	1	-15.2		13.7		4.1		3.0	
		2016	2	-16.6	0.6	14.2	0.4	3.9	0.2	3.0	0.1
		2021	9	-15.6	0.3	13.0	0.2	4.1	0.1	2.3	0.1

Opheliidae	Subsurface Deposit									
		2017	1	-20.0		11.5		4.8	2.0	
Pectinariidae	Subsurface Deposit									
		2014	6	-19.6	1.2	11.7	0.8	5.8	0.7	2.4	0.3
		2016	4	-19.6	0.4	12.9	0.4	5.0	0.5	2.6	0.1
		2017	3	-19.4	0.5	12.2	0.9	4.8	0.4	2.2	0.3
		2021	11	-19.3	0.4	12.8	0.7	5.0	0.3	2.3	0.2
Phyllodocidae	Predator/ Scavenger									
		2015	1	-17.2		14.2		5.0	2.9	
		2017	1	-17.6		11.2		5.1	2.0	
Polynoidae	Predator									
		2017	2	-17.7	1.4	12.8	3.0	4.7	1.1	2.4	0.8
Terebellidae	Surface Deposit									
		2021	2	-18.9	0.4	12.2	0.4	5.6	0.1	2.1	0.1
Trichobranchidae	Surface Deposit									
		2016	1	-20.1		12.0		5.2	2.3	
Tunicata										
Styelidae	Suspension									
		2014	1	-18.8		10.8		5.7	2.1	

Two taxonomic families had adequate sample size for comparison between years: Pectinariidae and Tellinidae (Figure 14). However, the Pectinariidae samples needed to be pooled for 2014, 2016, and 2017 to reach adequate sample sizes for comparison to the samples collected in 2021. Tellinidae samples were compared between 2014 and 2021. The Tellinidae $\delta^{13}C$ values from 2014 were significantly higher than the samples from 2021 (Welch's t-test: $T(4.5) = 4.05$; $P < 0.001$). TP estimates for Tellinidae were also significantly higher in 2014 compared to 2021 (Welch's t-test: $T(7.4) = 7.34$; $P < 0.001$). To ensure that the differences in TP and

$\delta^{13}C$ values were not due to the size of the organism, I compared the length (mm) of the Tellinidae in 2014 (mean ± SD: 26.8 ± 8.7) and 2021 (mean ± SD: 30.1 ± 5.8). There were not significant differences between the sizes of Tellinidae in 2014 and 2021 (T(46.7) = -1.72; P = 0.09). There was not a significant difference between the $\delta^{13}C$ values of Pectinariidae samples from earlier years (2014, 2016, 2017) and 2021 (Welch's t-test: T(16.9) = -0.98; P = 0.340). TP also did not vary between 2014-2017 and 2021 (Welch's t-test: T(21.9) = 1.4; P = 0.177).

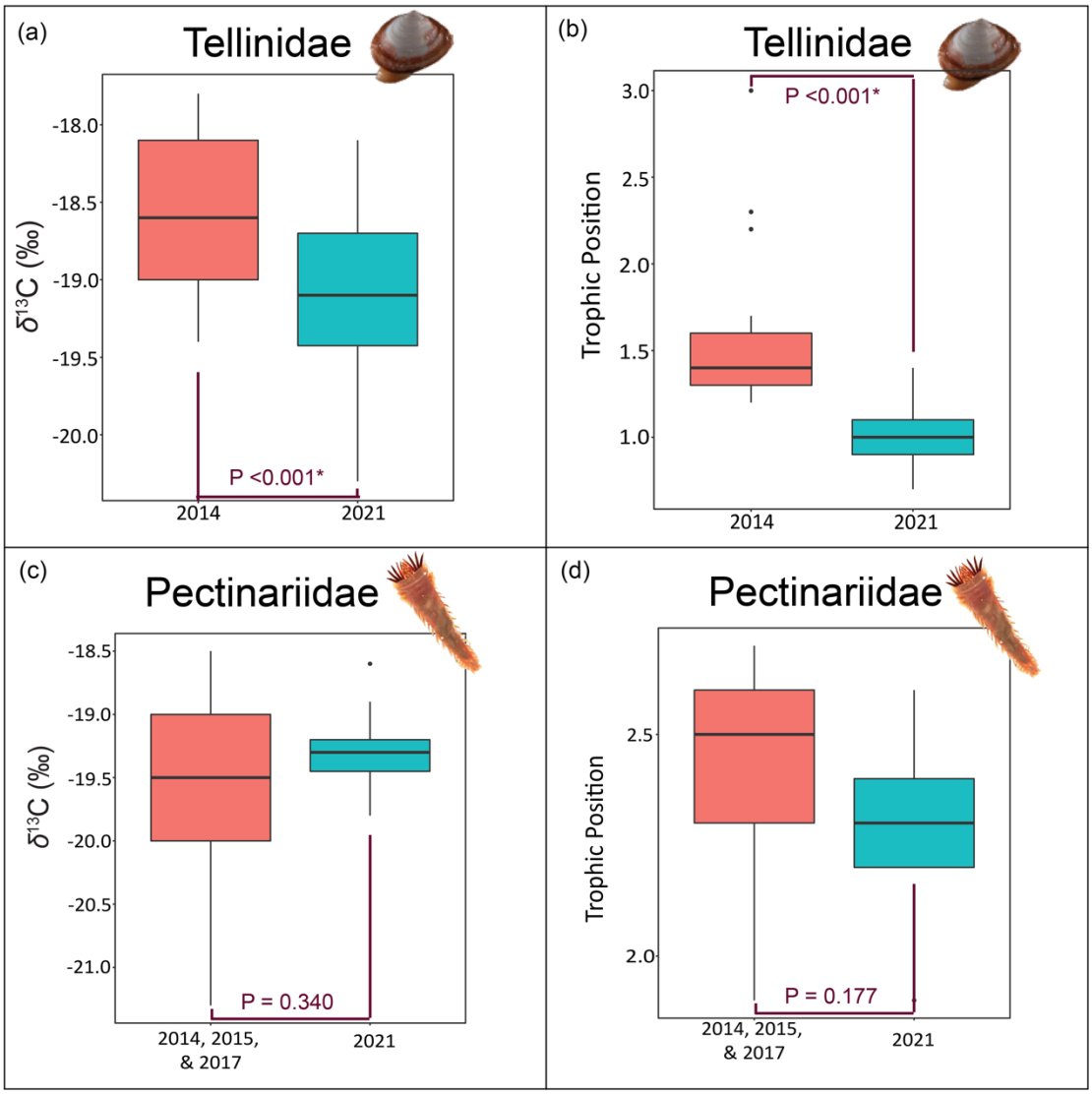

Figure 14. Boxplots of Tellinidae (a-b) and Pectinariidae (c-d) δ^{13}C values (‰) and trophic position (TP) from the southern Chukchi Sea cluster plotted over time. Boxplot components include median (horizontal bar), interquartile range (IQR; box), 1.5*IQR (error bars) and outliers (± 1.5*IQR; black dots). P-values from time-period comparisons are reported in burgundy type with the burgundy bars indicating the groups compared. *indicates significant p-values. (a). Tellinidae δ^{13}C values (‰) plotted in 2014 and 2021 with Welch's t-test p-value. (b) Tellinidae trophic position (TP) from 2014 and 2021 with Welch's t-test p-value. (c) Pectinariidae δ^{13}C values (‰) plotted in two study periods earlier years (2014, 2015, and 2017) and 2021. The p-value from the Welch's t-test comparing the two groups is also reported. (d) Pectinariidae TP in the earlier years (2014, 2015, and 2017) and 2021 with the Welch's t-test p-value.

3.4 Sediments

Mean sediment organic matter $\delta^{13}C$ and $\delta^{15}N$ values for all DBO stations during the study period (2014-2021) were plotted using Ocean Data View software (Figures 15 and 16; Schlitzer, 2022) while only the stations where benthic macroinvertebrates were collected for this study were analyzed statistically. When including all DBO stations, the $\delta^{13}C$ values of the coastal Bering Strait stations were the most enriched. The most depleted $\delta^{13}C$ values were along the coast of the northernmost stations (Figure 15). For the clusters addressed in this study, the $\delta^{13}C$ values are lowest in the coastal stations and highest in the southern Chukchi Sea with intermediate values in the northern Bering Sea for the clusters addressed in this study (Figure 15).

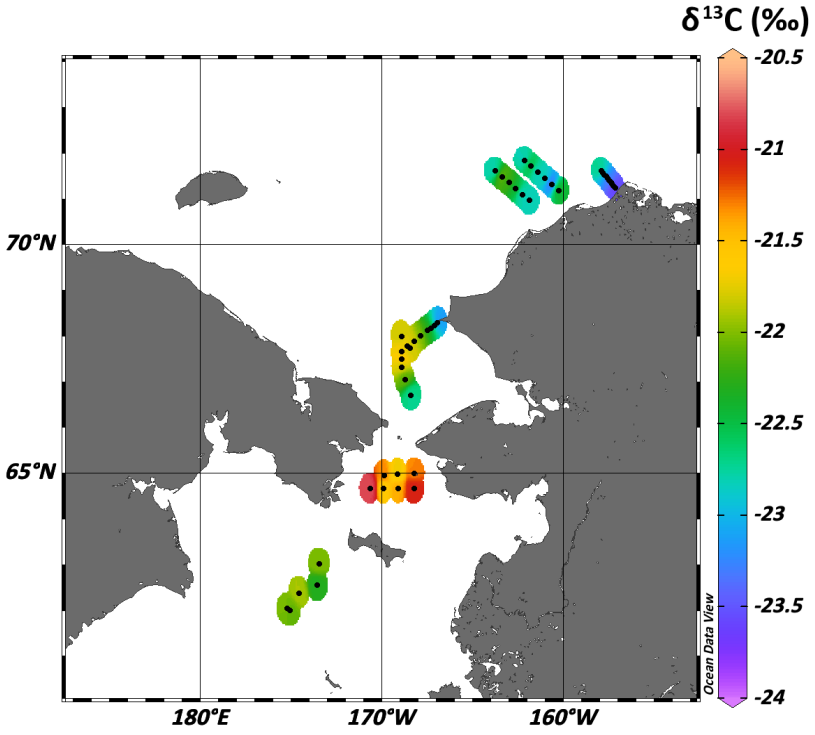

Figure 15. Sediment organic carbon $\delta^{13}C$ values interpolated using weighted means for stations over the study period (2014 - 2021). Weighted averages surrounding the measured points were estimated to 11 per mille of the Latitude and Longitude visualized in the plots.

When including all DBO stations, the lowest δ^{15}N values are found near the Alaskan coast and farthest offshore at the Barrow Canyon (DBO 5) and in the central Bering Strait stations (Figure 16). The highest δ^{15}N values were in the northern Bering Sea. For the clusters in this study, means across years in δ^{15}N are highest in the northern Bering Sea, intermediate in the southern Chukchi Sea and lowest in the coastal stations.

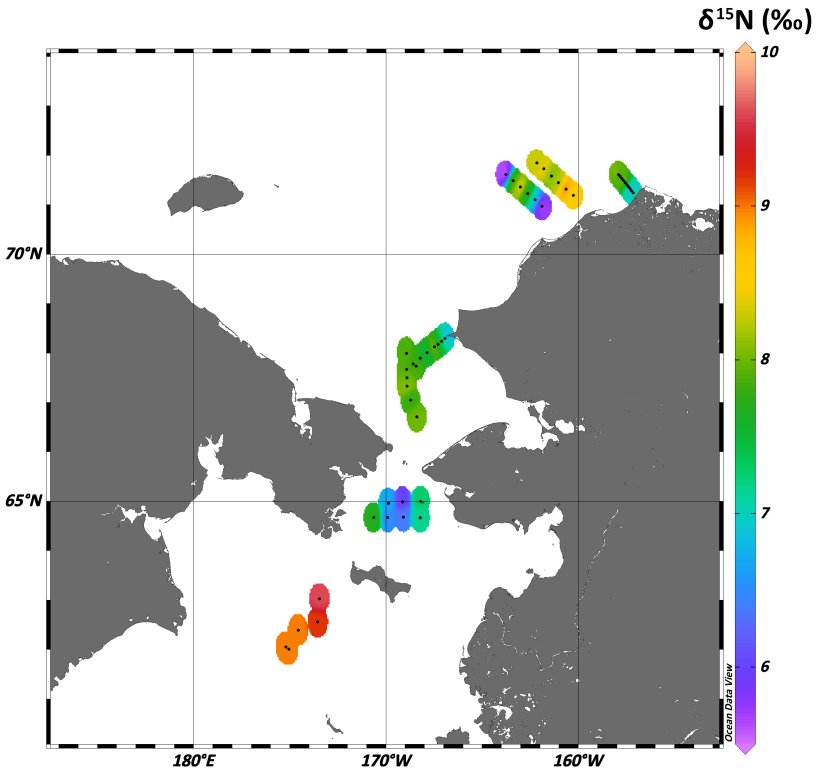

Figure 16. Sediment organic fraction δ^{15}N values interpolated using weighted means for stations over the study period (2014 - 2021). Weighted averages surrounding the measured points were estimated to 11 per mille of the Latitude and Longitude visualized in the plots.

The δ^{13}C and δ^{15}N values of the clusters addressed in this study were compared statistically (Table 7 and Table 8). There were significant differences between the sediment δ^{13}C values collected at the different clusters in 2014

(ANOVA: F(2,13) = 4.30; P = 0.037), 2015 (Kruskal-Wallis: H(2) = 8.35; P = 0.015), 2016 (ANOVA: F(2,13) = 10.97; P = 0.002), 2017 (ANOVA: F(2,13) = 16.44; P < 0.001), and 2021 (ANOVA: F(2,12) = 4.29; P = 0.039). Pairwise analyses found that these differences were between the southern Chukchi Sea and coastal station $\delta^{13}C$ values in 2014 – 2017 (Table 7). In 2016, there were significant differences between northern Bering Sea and coastal station sediment $\delta^{13}C$ values. There were also significant differences between the $\delta^{13}C$ values in the northern Bering Sea and southern Chukchi Sea in 2016.

Table 7. P-values of pairwise tests comparing $\delta^{13}C$ values among the northern Bering Sea (NBS), southern Chukchi Sea (SCS), and coastal stations.

		P-values		
Year	**Test Used**	**NBS vs SCS**	**NBS vs Coastal**	**SCS vs Coastal**
2014	T-test	0.202	0.187	0.037*
2015	Wilcoxon Rank Sum Test	0.592	0.107	0.048*
2016	T-test	0.290	0.001*	<0.001*
2017	T-test	0.002*	0.138	<0.001*
2021	T-test	0.047*	0.570	0.154

* indicates a significant P-value

There were significant differences between the organic fraction of sediment $\delta^{15}N$ values collected at the different clusters in 2014 (ANOVA: F(2,13) = 17.65; P < 0.001), 2015 (Kruskal-Wallis: H(2,13) = 10.13; P = 0.006), 2016 (Kruskal-Wallis: H(2,13) = 10.97; P = 0.002), 2017 (ANOVA: F(2,13) = 10.48; P = 0.005), and 2021 (ANOVA: F(2,12) = 26.02; P < 0.001). In all study years (2014-2017 and 2021), northern Bering Sea and southern Chukchi Sea stations had significantly different

sediment organic fraction δ^{15}N values. There were also significant differences among all three clusters in 2016. The northern Bering Sea and coastal stations had significantly different sediment organic fraction δ^{15}N values in 2014 (Table 8).

Table 8. P-values of pairwise tests comparing δ^{15}N values among the northern Bering Sea (NBS), southern Chukchi Sea (SCS), and coastal stations.

		P-values		
Year	**Test Used**	**NBS vs SCS**	**NBS vs Coastal**	**SCS vs Coastal**
2014	T-test	<0.001*	0.002*	0.521
2015	Wilcoxon Rank Sum Test	0.013*	0.107	1.00
2016	T-test	0.011*	0.002*	0.042*
2017	Wilcoxon Rank Sum Test	0.013*	0.107	0.775
2021	T-test	<0.001*	0.001	0.239

* indicates a significant P-value

3.4.1 Trend analysis

Sediment δ^{13}C and δ^{15}N values were also assessed for trends over time using the non-parametric Mann-Kendall trend test for monotonic trends (Kendall, 1975; Mann, 1945). Sediment δ^{13}C and δ^{15}N values were averaged for each cluster and year. Data were available from 2012 to 2021 with the exception of 2020. Sediment δ^{13}C and δ^{15}N values for 2020 were interpolated using cubic spine interpolation for autocorrelation assessments as they do not allow for missing data. Autocorrelation was assessed visually. There was no autocorrelation or partial autocorrelation in any of the clusters for both δ^{13}C and δ^{15}N values. The original dataset without the interpolated values for 2020 was used for the trend tests. The null hypothesis of no monotonic trend present was not rejected for either the sediment δ^{13}C or δ^{15}N values in each cluster (Table 9). These results indicate that there was not an upward or

downward monotonic trend over the time in the sediment $\delta^{13}C$ or $\delta^{15}N$ values in any of the clusters.

Table 9. Results of Mann-Kendall monotonic trend tests for mean sediment $\delta^{13}C$ and $\delta^{15}N$ values annual in each cluster (2012 – 2021). The Kendall's tau statistic and two-sided p-value are reported.

	$\delta^{13}C$		$\delta^{15}N$	
Cluster	tau	P-value	tau	P-value
Coastal	-0.278	0.348	0.500	0.076
Northern Bering Sea	-0.444	0.118	0.222	0.466
Southern Chukchi Sea	-0.389	0.175	0.389	0.175

3.5 Comparing benthic macroinvertebrates among study sites

3.5.1 Comparisons of $\delta^{15}N$ values across clusters by feeding group

Organisms were grouped by their feeding type and cluster for comparisons by feeding group. $\delta^{13}C$ values, $\delta^{15}N$ values, and TP were compared between and among clusters irrespective of the year of sampling (Figure 17 and Figure 18). Suspension and predator benthic macroinvertebrates had adequate sample sizes to be compared across all three clusters (Figure 17). Deposit feeders and organisms that both deposit and suspension feed had adequate sample sizes for comparisons between the northern Bering and southern Chukchi Sea clusters (Figure 17). Scavengers did not have adequate sample size across clusters to be compared (Figure 17). Deposit feeders in the northern Bering Sea had significantly higher $\delta^{15}N$ values (n=90, mean = 12.4 ‰, SD = 2.3) than deposit feeders in the southern Chukchi Sea (n = 75, mean = 11.0 ‰, SD = 1.8; $T(161) = 4.46$, $P < 0.001$). Invertebrates that could both suspension and

deposit feed also had significantly higher $\delta^{15}N$ values in the northern Bering Sea (n = 35, mean = 9.8 ‰, SD = 1.0) than in the southern Chukchi Sea (n = 81, mean = 8.9 ‰, SD = 1.0; T(59) = 4.6, P < 0.001; Figure 17).

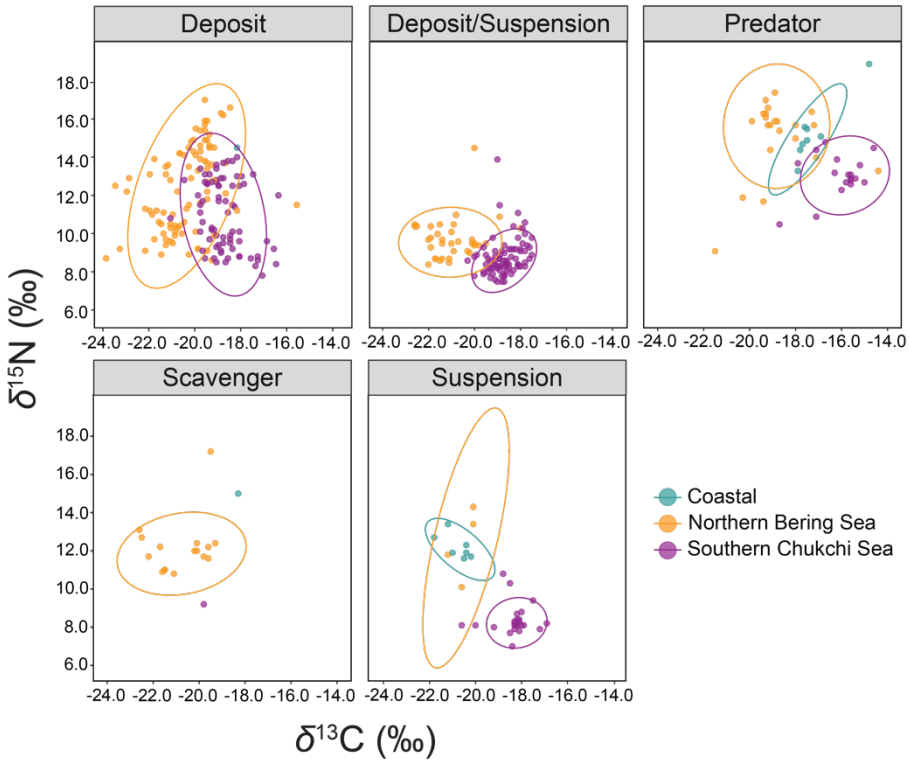

Figure 17. Stable isotope biplot of organisms collected in different locations grouped by trophic guild. Ellipses encompass 95% confidence intervals around $\delta^{15}N$ and $\delta^{13}C$ values.

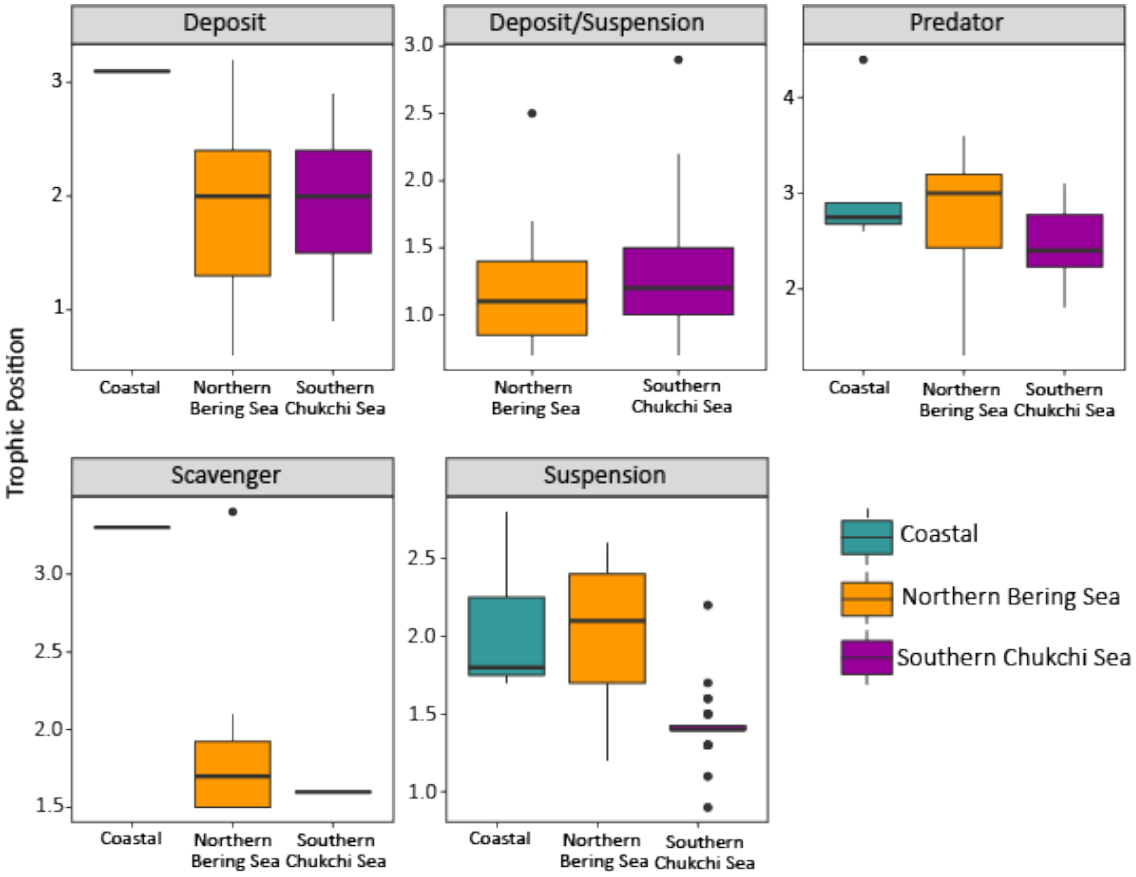

Figure 18. Box and whisker plot of invertebrate trophic positions grouped by feeding type.

For predators, all three groups had adequate sample sizes for comparison. A non-parametric Kruskal-Wallis Test was used followed by the pairwise Wilcoxon rank sum test for multiple comparisons with Bonferroni p-value adjustments to compare δ^{15}N values. There were significant differences between at least one pair of clusters in the δ^{15}N values of the predators ($H[2] = 16.73$, $P < 0.001$). These significant differences were between the δ^{15}N values of predators in the southern Chukchi Sea and the other two clusters: coastal stations ($P < 0.001$) and the northern Bering Sea stations ($P < 0.001$). No significant differences between the northern

Bering Sea and coastal stations were detected (P = 1.0). The highest average δ^{15}N value was in the coastal stations (n = 8; mean = 15.4; SD = 1.6), and the lowest δ^{15}N values were in the southern Chukchi Sea (n = 18; mean = 13.1; SD = 1.1). The northern Bering Sea had intermediate δ^{15}N values (n = 24; mean = 15.1; SD = 2.0).

Suspension feeder δ^{15}N values were compared using the non-parametric Kruskal-Wallis Test followed by the pairwise Wilcoxon rank sum test for multiple comparisons with Bonferroni p-value adjustments. Significant differences were detected between the δ^{15}N values of the suspension feeders across clusters (Kruskal-Wallis: H[2] = 24.27, P < 0.001). Northern Bering Sea suspension feeder δ^{15}N values were not significantly different from suspension feeders in the stations that clustered in the coastal category (P =1.00). However, southern Chukchi Sea suspension feeder δ^{15}N values were significantly different from both northern Bering Sea δ^{15}N values (P = 0.002) and coastal δ^{15}N values (P < 0.001). Suspension feeder δ^{15}N values were highest in the northern Bering Sea (n=5; mean=12.6 ‰; SD=1.7), intermediate in the coastal category stations (n = 7; mean = 12.2 ‰; SD = 0.6), and lowest in the southern Chukchi Sea (n = 28; mean = 8.3 ‰; SD = 0.7).

3.5.2 Comparisons of δ^{13}C values across clusters by feeding group

Deposit feeders in the northern Bering Sea had significantly lower δ^{13}C values (n = 90; mean = -20.6 ‰; SD = 1.3) than deposit feeders in the southern Chukchi Sea (n = 28; mean =- 18.9 ‰; SD = 0.9; Wilcox rank sum test: W = 738, P < 0.001). Invertebrates that could both suspension and deposit feed also had significantly lower

δ^{13}C values in the northern Bering Sea (n = 35; mean = -21.0 ‰; SD = 1.0) than in the southern Chukchi Sea (n= 28; mean = -18.7 ‰; SD =0 .6; Welch's t-test: T(45) = -11.97, P < 0.001).

I used the non-parametric Kruskal-Wallis H Test and pairwise Wilcoxon rank sum test for multiple comparisons with Bonferroni p-value adjustments without pooled standard deviations to compare predator δ^{13}C values across clusters. The predators had significantly different δ^{13}C values between at least one pair of clusters (H[2]=21.494, P < 0.001). The southern Chukchi Sea and coastal stations had similar δ^{13}C values (P = 0.08) while the northern Bering Sea δ^{13}C values were significantly different from the coastal station predators (P = 0.028) and the southern Chukchi Sea values (P < 0.001). The highest average δ^{13}C value was in the southern Chukchi Sea (n = 28; mean = -16.1 ‰; SD = 1.0) and the lowest average δ^{13}C values were in the northern Bering Sea (n = 24; mean = -18.4 ‰; SD = 2.0). The coastal category stations had intermediate δ^{13}C values (n = 8; mean = -17.2 ‰; SD = 1.0).

Suspension feeder δ^{13}C values were significantly different between at least one pair of clusters (Kruskal-Wallis: H[2] =16.04, P < 0.001). The northern Bering Sea had similar δ^{13}C values for suspension feeders as were observed at the coastal stations (P = 0.662) and the southern Chukchi Sea stations (P = 0.167). The southern Chukchi Sea and coastal stations were significantly different (P < 0.001). Suspension feeder δ^{13}C values were highest in the southern Chukchi Sea (n = 28; mean = -18.3; SD = 0.8), intermediate in the northern Bering Sea stations (n = 5; mean = -19.3; SD = 2.7), and lowest in the coastal stations (n = 7; mean = -20.8; SD = 0.6). The sample

sizes in this test were as small as n = 5 so I am hesitant to draw conclusions from these results.

3.5.3 Comparison of feeding guild trophic position by cluster

Trophic position for each invertebrate was calculated for all organisms using Equation 3. Invertebrates were grouped by trophic guild and their trophic positions were compared (Figure 18). For predators and suspension feeders, all three clusters had large enough sample sizes for comparison. I did not reject the null hypothesis that the mean trophic positions of deposit feeders in the northern Bering Sea (mean = 1.9, sd = 0.7) and southern Chukchi Sea (mean = 1.9, sd = 0.5) were equal (Welch's T-test: T[159] = -0.29, P = 0.77). I also did not reject the null hypothesis of equal means in the suspension and deposit feeders between the northern Bering Sea (mean = 1.2, sd = 0.4) and southern Chukchi Sea (mean = 1.3, sd = 0.4; Welch's T-Test: T[62] = -1.11, P = 0.269).

There were significant differences detected between at least two of the clusters in predator TP values (H[2] = 6.7; P = 0.47). However, none of the pairs were significantly different in the pairwise Wilcoxon rank sum test (northern Bering Sea vs. coastal: P = 1.00, northern Bering Sea vs. southern Chukchi Sea: P = 0.059, southern Chukchi Sea vs. coastal: P = 0.070).

Significant differences in suspension feeder TP were detected between at least two of the pairs of clusters on (H[2] = 21.56, P < 0.001). The southern Chukchi Sea suspension feeders had significantly different trophic positions from the coastal

stations ($P < 0.001$) and the northern Bering Sea ($P = 0.004$). There were no significant differences between suspension feeding trophic positions in the coastal stations and northern Bering Sea ($P = 1.00$). Suspension feeders in the coastal stations and the northern Bering Sea had equal mean trophic positions (mean = 2.0, sd = 0.4). The southern Chukchi Sea suspension feeders had a lower mean TP at 1.3 (sd = 0.2).

3.6 Community metrics

For Layman metric calculations, all study years were pooled across clusters. The coastal stations did not have a large enough sample size for community wide metrics. Group sample sizes that are less than ten can cause bias in the estimates of convex hull total area (Jackson et al., 2011). Therefore, feeding guilds with less than ten samples per cluster were combined with other groups or dropped from the analysis. Three feeding groups in the northern Bering Sea (deposit, deposit/suspension, and predator/scavenger) and four groups in the southern Chukchi Sea (deposit, deposit/suspension, suspension, and predator/scavenger) were used in this analysis.

I used an uninformative Wishart prior with a sigma of two (McCarthy, 2007). Model parameters were 20,000 iterations, 1,000 discarded distributions, and ten thinned posteriors to fit the model for Layman Metrics. Two parallel chains were run. The number of posterior distributions of the first community that were less than the posterior distributions of the second community were divided by the total number of posterior distributions to compare the results of each Layman metric (see the

"comparing communities" from https://cran.r-project.org/web/packages/SIBER/vignettes/ for code). Four thousand posterior distributions of community Layman metrics were generated.

Layman metrics were larger in the southern Chukchi Sea than northern Bering Sea except for nearest neighbor distance (NND; Table 10). All total area posterior distributions (100 %) for northern Bering Sea were smaller than the posterior distributions from the southern Chukchi Sea. The δ^{15}N range was larger in the southern Chukchi Sea than the northern Bering Sea in 72% of the distributions, and the δ^{13}C range was larger in 100% of the distributions. Centroid distance (CD) was also larger in the southern Chukchi Sea than the northern Bering Sea in 98.7% of the distributions. The northern Bering Sea mean nearest neighbor distance posterior distributions (MNND) were greater than the southern Chukchi Sea for 99.4 % of the distributions. The standard deviation of the nearest neighbor distance (SDNND) was greater in the southern Chukchi Sea with 99.8 % of the distributions larger than those in the northern Bering Sea.

Table 10. Layman metrics (Layman et al., 2007) from the northern Bering Sea and southern Chukchi Sea benthic macroinvertebrate samples.

Cluster	δ^{13}C Range	δ^{15}N Range	Total Area (‰^{2})	CD	MNND	SDNND
Northern Bering Sea	1.3 ± 0.2	4.2 ± 0.2	0.8 ± 0.3	1.6 ± 0.1	2.1 ± 0.1	0.4 ± 0.2
Southern Chukchi Sea	2.5 ± 0.2	4.4 ± 0.3	4.1 ± 0.7	1.9 ± 0.1	1.6 ± 0.1	1.2 ± 0.2

3.7 Standard ellipse area (SEA)

Benthic macroinvertebrates were pooled across years to reach an adequate sample size for SEA_B. None of the samples from the coastal category stations fit the criterion of more than ten samples per taxonomic family (Table 4). Six families from the northern Bering Sea and six families from the southern Chukchi Sea met this criterion (Tables 5 and 6). I fit Bayesian multivariate ($\delta^{13}C$ and $\delta^{15}N$) normal distributions around each group. I ran 20,000 iterations of the model, discarded 1,000 of the first values, thinned the distribution by 10, and ran two parallel chains of the model. I fit the ellipses using an inverse Wishart prior with a sigma of two (McCarthy, 2007). Posterior distributions were compared for each pair of organisms by calculating the percent of the standard ellipse area posterior distributions that were larger than another organism (Jackson et al., 2011). Four thousand posterior distributions of SEA_B were calculated for each taxonomic family (Figure 19). When families were analyzed for their SEA in both the northern Bering Sea and the southern Chukchi Sea (Nuculidae, Pectinariidae, and Tellinidae), the families from the northern Bering Sea had larger TAs and SEAs (Table 11; Figure 19). The proportion of posterior distribution samples SEA_Bs that were larger in the northern Bering Sea than in the southern Chukchi Sea was 82.7%, 100%, and 100% for Nuculidae, Pectinariidae, and Tellinidae, respectively.

Pectinariidae in the northern Bering Sea had the largest total area, SEA, SEA_C, and SEA_B across all families and the two regions (Table 11). Pectinaridae SEA_B estimates were larger than the other families in 100% of the distributions except for

one family. The only exception was Uristidae where Pectinaridae posterior distributions of SEA_B were higher for 95.9 % of the distributions. Maldanidae SEA_Bs were larger than Nuculanidae and Nuculidae for 81% and 99% of the distributions, respectively.

Of the southern Chukchi Sea stations, Tellinidae had the largest total area, SEA, SEA_C, and SEA_B (Table 11). Nuculidae had the smallest SEA_B mode in the southern Chukchi Sea. In the southern Chukchi Sea, the Tellinidae SEA_Bs were larger than Cardiidae in 99.8% of the distributions. While Pectinariidae SEA_Bs were larger in the northern Bering Sea, they were the second largest in the southern Chukchi Sea. The smallest reported SEA_B mode was in Nephytidae in the southern Chukchi Sea.

Table 11. Group metrics of total area (TA) in carbon and nitrogen stable isotope space, standard ellipse area (SEA), corrected standard ellipse area (SEA_C), and posterior distribution estimates of Bayesian Standard ellipse areas (SEA_B) of mode and lower and upper limits of 95% credibility intervals. Clusters are the northern Bering Sea (NBS) and southern Chukchi Sea (SCS). TA, SEA, SEA_C, and SEA_B are derived from the area occupied in $\delta^{13}C$ and $\delta^{15}N$ value (‰) bi-plot space and are expressed in per mille squared (‰^{2}).

Cluster	Family	TA (‰^{2})	SEA (‰^{2})	SEA_C (‰^{2})	Lower Limit	Mode (‰^{2})	Upper Limit
NBS	Maldanidae	12.0	2.7	2.8	1.8	2.7	4.1
NBS	Nuculanidae	5.4	2.0	2.2	1.2	2.0	3.4
NBS	Nuculidae	2.6	1.1	1.2	0.6	1.0	2.0
NBS	Pectinariidae	30.2	11.5	12.7	5.6	10.9	20.2
NBS	Tellinidae	15.0	3.5	3.6	2.5	3.5	4.9
NBS	Uristidae	12.0	5.7	6.2	3.0	5.4	9.9
SCS	Cardiidae	2.9	0.9	0.9	0.6	0.8	1.4
SCS	Nephtyidae	1.6	0.7	0.7	0.4	0.7	1.3
SCS	Nuculidae	1.9	0.8	0.9	0.5	0.8	1.4
SCS	Pectinariidae	5.8	1.7	1.8	1.1	1.7	2.5
SCS	Tellinidae	10.4	1.9	1.9	1.5	1.9	2.3

SCS	Yoldiidae	2.6	1.2	1.3	0.6	1.1	2.1

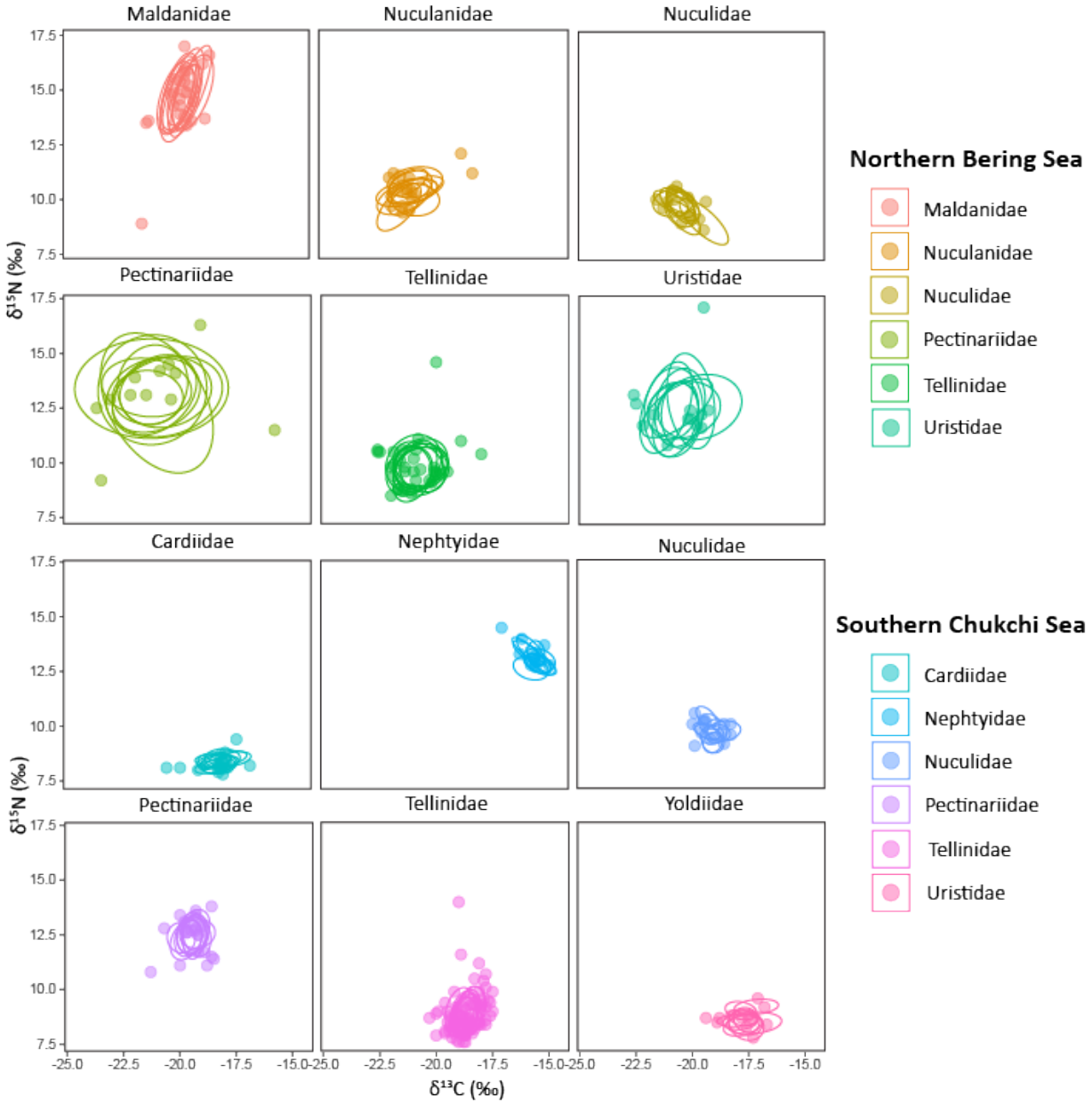

Figure 19. Bayesian standard ellipse areas of six taxonomic families from the northern Bering Sea (top two rows) and six taxonomic families from the southern Chukchi Sea (bottom two rows). Ten independently calculated ellipses are plotted around the raw δ^{15}N and δ^{13}C values of the invertebrates.

SEA estimates of consumers do not account for the variability at the base of the food web (Layman et al., 2012; Newsome et al., 2007). A large isotopic niche or SEA of an organism could reflect more variability in basal resources and not a larger isotopic niche. In this study, organisms grouped by taxonomic family were pooled across years furthering the bias in estimates of SEA. I subtracted posterior distributions (SEA_B) of the sediment collected at all study years from the posterior distributions of the consumers to correct for the bias in baseline sediment. These corrected estimates ($SEA_{B\text{-corrected}}$) were averaged and compared. This method is similar to methods used in other stable isotope studies such as Catry et al (2016), who subtracted the basal resource $\delta^{13}C$ and $\delta^{15}N$ values from the raw consumer $\delta^{13}C$ and $\delta^{15}N$ values, and Warry et al (2016), which normalized Layman metrics to the basal $\delta^{13}C$ and $\delta^{15}N$ values. In the northern Bering Sea, the mean sediment SEA_B size across all years was 1.8 ± 0.3 ‰^{2}. In the southern Chukchi Sea, the mean sediment SEA_B size was 0.6 ± 0.1 ‰^{2}.

4 Discussion

4.1 Clustering

Three distinct clusters emerged from the environmental parameters of the stations where benthic macroinvertebrates were collected in this study (Figure 5). These clusters persisted when tested under three different linkage methods (complete linkage, average linkage, and Ward's minimum variance distance). The northern Bering Sea stations clustered together even when the spatial variables (Latitude and

Longitude) were removed from the analysis. This result was expected because the remainder of the samples were in the Chukchi Sea which differs from the northern Bering Sea in hydrodynamic conditions, primary productivity, and sediment characteristics (see Section 1.2).

The Chukchi Sea stations clustered into two groups: the southern Chukchi Sea stations and coastal stations. While UTN1 is somewhat distant from the coast, the other two stations in this region, SEC5 and SEC7 are relatively close to the coast (Figure 6), and share coastal characteristics at UTN1. For example, UTN1 is the shallowest of the stations with a mean depth of 35 m (± 0.5 SD). It also had higher July mean temperatures (4.0 ± 0.9 °C), lower salinity (31.9 ± 0.3), and less silt and clay in the sediments (52.1 ± 19.8 %) than the southern Chukchi stations sampled as part of this study (Temperature: 2.9 ± 1.2 °C, Salinity: 32.6 ± 0.2, silt and clay content [≥ 5 phi]: 79.1 ± 10.7 %; Table 1). UTN1 also had $\delta^{13}C$ values that more closely resembled the coastal stations than the other Chukchi sea stations (-22.5 ± 0.5 ‰). Because UTN1's environmental parameters more closely resembled the two coastal stations, I classified UTN1 as a coastal station despite its separation from the stations closest to the Alaska coast.

4.2 Stable isotope analysis

One of the main challenges in this study is the limited $\delta^{13}C$ and $\delta^{15}N$ values for basal food resources for each of the study regions and years. When all food sources are measured for a community, the $\delta^{13}C$ and $\delta^{15}N$ values at the base of the food web

can be used to estimate trophic position or mixing models of what an organism is consuming. Presumably, there are three basal resources available to these benthic macroinvertebrates: organic matter in the sediments, POM, and sea ice algae. POM was only measured as a part of this study in 2015 in the northern Bering Sea and 2015 and 2016 in the southern Chukchi Sea. In addition, in 2010, POM $\delta^{13}C$ and $\delta^{15}N$ values were made available by Dr. Katrin Iken, University of Alaska Fairbanks (personal communication). In both the northern Bering Sea and southern Chukchi Sea, the POM values differed in both $\delta^{13}C$ and $\delta^{15}N$ values between years (Figure 20). There was also no standard offset between the POM and sediment $\delta^{15}N$ values to estimate POM $\delta^{15}N$ for the years when POM wasn't collected. Therefore, using POM as a baseline for years when POM was not collected was not advisable.

The other basal resource, sea ice algae, was not measured as a part of this study because ice melt occurred before collection in July. However, other studies have found that sea ice algae $\delta^{13}C$ values are isotopically distinct from other isotopic end-members in the Pacific Arctic. $\delta^{13}C$ values in ice algae tend to be enriched compared to POM or sediment due to inorganic carbon limitations in interstitial spaces as photosynthesis proceeds (Lovvorn et al., 2005; McTigue & Dunton, 2017; North et al., 2014). The $\delta^{13}C$ and $\delta^{15}N$ values from Lovvorn et al (2005) are isotopically distinct from our other samples (Figure 20).

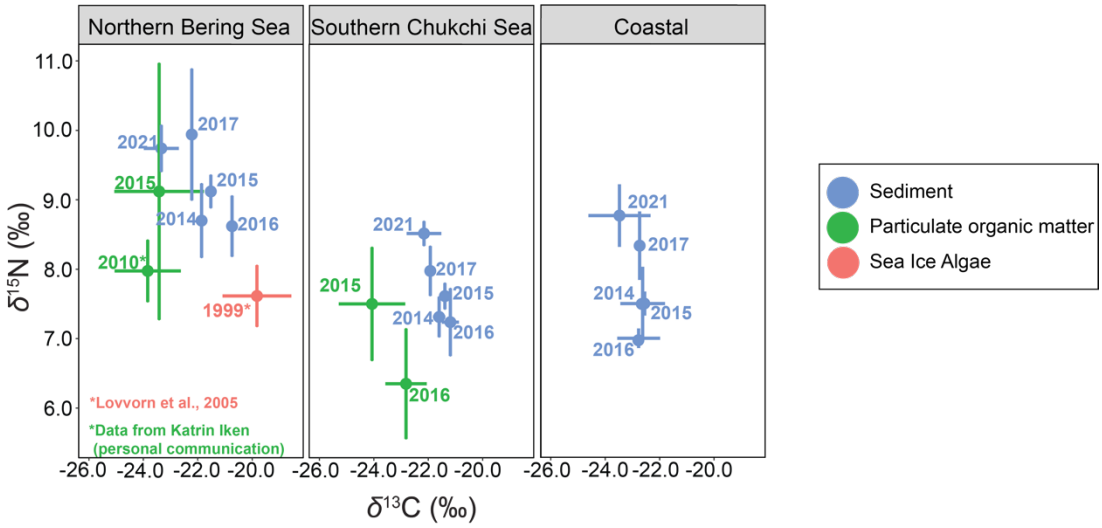

Figure 20. Mean (circle) and SD (error bars) $\delta^{13}C$ and $\delta^{15}N$ values of basal food web resources in each cluster. Sea ice algae $\delta^{13}C$ and $\delta^{15}N$ values are from Lovvorn et al (2005).

4.2.1 Estimating trophic position

There are several methods of calculating trophic position including the traditional method (Equation 3), a two baseline mixing model (Post, 2002), or Bayesian estimations (Quezada-Romegialli et al., 2019). Stable isotope mixing models quantify proportions of food sources in an organism's diet based on the stable isotope signatures of end-members and the organism's tissues. These models require analyzing stable isotope values of all basal production and that the consumer falls within the food sources' range in $\delta^{13}C$ – $\delta^{15}N$ biplot space after corrections for TDF (reviewed in Phillips et al., 2014). For deposit and suspension feeding organisms such as Tellinidae, the two main food sources available are the organic matter in the sediment and POM. However, Tellinidae stable isotope values did not fall within these food sources in $\delta^{13}C$ – $\delta^{15}N$ biplot space (Figure 21). I found similar patterns for the other plots generated across years and consumers. These results suggest a missing

enriched $\delta^{13}C$ end-member. Similar studies in the Pacific Arctic (Iken et al., 2010; Lovvorn et al., 2005; McTigue & Dunton, 2014; Tu et al., 2015) have also cited higher $\delta^{13}C$ values than would be expected with the end-members collected. Without POM collected in all years and meeting the assumptions for mixing models, it was not practical to calculate trophic position using the two-baseline model.

Bayesian estimations require a sample size of $n \geq 8$ for each consumer (Quezada-Romegialli et al., 2019). Only nine taxonomic families met this requirement. I used these nine taxonomic families to compare the traditional and Bayesian trophic position estimations. Both Bayesian and traditional TP estimates require TDFs. TDFs were not measured as a part of this study, but McTigue and Dunton (2014) determined a TDF of 3.4 ‰ for similar benthic macroinvertebrates in the northeastern Chukchi Sea. The $\delta^{15}N$ TDF was estimated using the amphipod, *Ampelisca macrocephela*, and phytoplankton (the particulates that were retained on a 20 μm filter; McTigue and Dunton, 2014). *A. macrocephela* are suspension feeding amphipods that generate a posterior to anterior feeding current to forage on diatoms. This current can also trap surface sediments in this process (Highsmith & Coyle, 1990). I used the $\delta^{15}N$ TDF determined in McTigue and Dunton (2014) and

calculated δ^{13}C TDF based on the mean and SD presented in the paper for the Bayesian model.

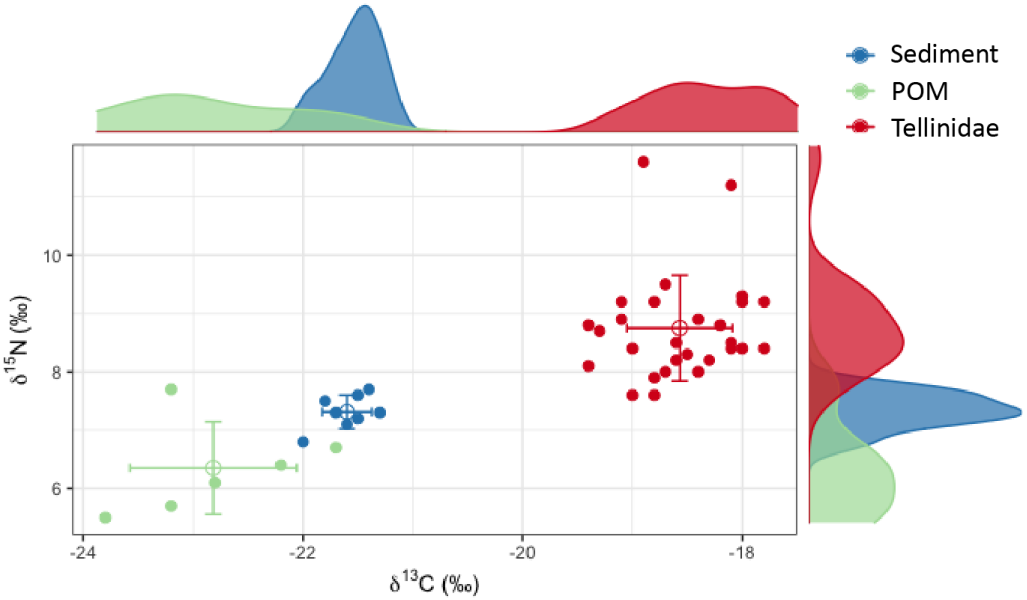

Figure 21. Stable isotope biplot (δ^{13}C vs. δ^{15}N) of the taxonomic family Tellinidae samples collected in the southern Chukchi Sea in 2014 and food sources (sediment and POM [Particulate organic matter]). Centroid (circle) ± standard deviations (error bars) are also shown for each end-member and the consumer. Smoothed density estimates are also included on the outside of each axis. This plot was generated using the R package, *tRophicPosition* (Quezada-Romegialli et al., 2019).

The Bayesian estimates of TP included the sediment collected at the year and cluster of the benthic macroinvertebrate and POM. The POM collected in 2015 for the northern Bering Sea and in 2016 for the southern Chukchi Sea was used to represent POM for all years, since it was not measured each year. In the traditional estimations of TP, sediment was used as a baseline along with the mean δ^{15}N TDF of 3.4 ‰ from McTigue and Dunton (2014). While using sediment organic matter as a baseline has its limitations for suspension feeders, the stable isotope content of the organic fraction of surface sediments was measured at each station and year.

Additionally, North et al (2014) found that while POM and ice algae $\delta^{13}C$ and $\delta^{15}N$ values varied between late summer and spring in the northern Bering Sea, sediment $\delta^{13}C$ and $\delta^{15}N$ values remained relatively constant on a seasonal basis.

There were significant differences between the traditional approach of estimating trophic position and the Bayesian approach of estimating trophic position for six of the nine organisms. All Bayesian estimations of TP were lower than the traditional method of estimating TP. The lower TP is due to the inclusion of POM isotope signatures and the $\delta^{13}C$ value TDF in the Bayesian model. The significant differences presented in this comparison do not invalidate the traditional TPs calculated for the remainder of the organisms. The analytical error associated with the $\delta^{15}N$ measurement in this study was ± 0.1 ‰ and many of the standard deviations calculated through Bayesian statistics were much higher (Table 3). When accounting for the standard deviation of both methods of calculating TP and the analytical error, the traditional and Bayesian approaches yielded similar results. Therefore, while the differences between Bayesian and traditional approaches yielded statistically significant results, these differences may not be ecologically significant.

The benthic macroinvertebrates studied here are primary consumers and therefore, should have trophic positions greater than two. However, for many of the samples, the trophic position estimates were less than two (Table 3) both using the traditional method and the Bayesian method. In the northern Bering Sea, Terrebellidae in 2017 had a TP of 1.0 indicating that the mean Terrebellidae $\delta^{15}N$ value was equal to the mean $\delta^{15}N$ value of the sediment organic matter. Nuculidae

and Tellinidae had TPs of less than 1 in 2021 in the northern Bering Sea. In the southern Chukchi Sea, Tellinidae and Yoldiidae had a TP of 1.0 in 2021, and Myidae had a TP of less than 1.0 in 2021. Nuculidae, Terrebellidae, and Yoldiidae are deposit feeders while Myidae is a suspension feeder. Tellinidae bivalves can both suspension and deposit feed. In the Myidae and Tellinidae, the TP of less than one can be attributed to not including POM (suspension feeders primary food resource) in the TP calculations, but the Terrebellidae, Nuculidae, and Yoldiidae presumably feed on organic matter in the sediments. The TP of less than one in the deposit feeders suggest that the organisms fed on another basal resource or earlier in the season when the sea ice was melting. These TPs of less than one may also be due to inaccurate estimations of TDF due to other artifacts.

4.2.2 Whole body and muscle tissue comparison

Different tissue types have different stable isotope turnover times, which can affect the $\delta^{13}C$ and $\delta^{15}N$ values of the organism. Muscle tissues tend to integrate stable isotope signatures of the food source slowly (on the order or weeks to months) while blood, liver, and stomach stable isotope signatures change more rapidly (Bond et al., 2016; Martínez del Rio & Carleton, 2012; Tieszen et al., 1983). Some samples were large enough to have their muscle tissue separated from other soft tissues. These samples included two *Mya* sp., one Naticidae, 22 *Serripes* sp., and seven *Yoldia* sp. Both the muscle tissue and body tissue were analyzed for $\delta^{13}C$ and $\delta^{15}N$ values. While there were no significant differences between the $\delta^{15}N$ of the muscle versus

body tissue in our samples (Figure 8), the $\delta^{13}C$ of the body was on average 1.5 ‰ less than the muscle tissue (Figure 9).

Two possible explanations for the differences in the $\delta^{13}C$ values between the muscle and body tissues are changes in the source primary producers that the bivalves and gastropod fed on during the longer integration time of the muscle tissue versus the shorter integration time in the body tissue or the higher lipid content contained in body tissue compared to muscle tissue. In a 42 day isotopic enrichment study of *Nuculana radiata* and *Macoma moesta*, Weems et al (2012) found that the muscle tissue had little to no heavy isotope enrichment in ^{13}C over the course of the experiment while $\delta^{15}N$ values became enriched in the heavy isotope.

To determine the isotopic turnover time in our study organisms, I used the formula from a literature review (Vander Zanden et al., 2015) of 11 invertebrate muscle tissues and 44 invertebrate whole-body tissues. I used the weights of the organisms where muscle tissue could be extracted to calculate the isotopic half-life of the invertebrate whole body and muscle tissue in this study. The half-life calculated for the average weight of the organisms was 3.6 days for muscle tissue and 3.4 days for body tissue. This equates to a turnover rate of about 0.07 % day^{-1} for body tissue and 0.05 % day^{-1} for muscle tissue. Given this small difference between turnover rate and the results of Weems et al (2012), it is likely that the differences in $\delta^{13}C$ between tissue types reflects the higher lipid content in the body tissue rather than a switch in basal resource feeding type. Lipids tend to lower the $\delta^{13}C$ values of the tissues (Post et al., 2007).

4.3 Do food web dynamics differ between the northern Bering Sea and southern Chukchi Sea?

4.3.1 Sediment Organic Matter

At the base of the food web, the lowest sediment $\delta^{13}C$ values and highest C/N ratios were in 2021 for all clusters. The coastal stations and southern Chukchi Sea also had the highest $\delta^{15}N$ values in 2021. The highest northern Bering Sea $\delta^{15}N$ values in the sediment were in 2017 (Tables 4-6). The lowest $\delta^{13}C$ values, highest C/N ratios, and highest $\delta^{15}N$ values (in two of the clusters) in 2021 could indicate a change in hydrodynamics (Iken et al., 2010), primary production (Gu et al., 1996), or microbial processes (Casciotti, 2016). Despite this one year shift, there were no monotonic trends detected over time in sediment $\delta^{13}C$ or $\delta^{15}N$ organic matter values in any of the clusters (see section 3.4.1).

The lower $\delta^{13}C$ values in the coastal stations across years (mean = -22.4 ‰, sd = ± 0.6) compared to the southern Chukchi Sea (mean = -21.6 ‰, sd = ± 0.5) stations could be due to terrestrial inputs. Terrestrial organic matter $\delta^{13}C$ values generally range between -30 ‰ to -23 ‰ while marine organic matter ranges are between -24 ‰ to -18 ‰ (Fry & Sherr, 1984). This is primarily due to the fractionation associated with CO_2 dissolving into water (Peterson & Fry, 1987). However, the C/N ratios are not entirely consistent with terrestrial inputs. C_3 terrestrial plants have higher C/N ratios than marine algae and POM (reviewed by Lamb et al., 2006). The C/N ratios in the coastal stations were higher than the southern Chukchi Sea in only 2014 and

2017. The lower C/N ratios in the other years could be due to phytoplankton community structure variations or other variables such as lower nutrients in the coastal stations compared to the southern Chukchi Stations, which would tend to increase C/N ratios (reviewed in Martiny et al., 2013). The more heavy isotope depleted $\delta^{13}C$ values along the coast are most likely due to terrestrial influence as another study found higher terrestrial influence in essential amino acids near SEC5 and SEC 7 compared with the remainder of the southern Chukchi Sea (Zinkann et al., 2022).

The sediment $\delta^{13}C$ organic matter values were lower in the northern Bering Sea (mean = -21.9 ‰, sd = ± 0.9) compared to the southern Chukchi Sea (mean = -21.6 ‰, sd = ± 0.5) when values were averaged across years (Figure 15). The higher $\delta^{13}C$ values in the southern Chukchi Sea could be attributed to the higher annual primary productivity in the southern Chukchi Sea compared with the northern Bering Sea (Grebmeier et al., 2006). When primary productivity rates are higher, phytoplankton do not discriminate against ^{13}C as much as when primary productivity rates are lower. The increase in ^{13}C in the phytoplankton leads to higher $\delta^{13}C$ values (Fry & Sherr, 1984). Dunton et al (1989) also found this trend when comparing $\delta^{13}C$ values of the Bering Sea to the southern Chukchi Sea.

In all study years, the sediment $\delta^{15}N$ values in the northern Bering Sea were significantly higher than the $\delta^{15}N$ values in the southern Chukchi Sea (Table 8). Kędra et al (2019) also found higher bivalve $\delta^{15}N$ values for compound specific amino acid stable isotopes in the northern Bering Sea compared to the southern

Chukchi Sea. Currents in the southern Chukchi Sea are stronger than the northern Bering Sea due to the flow through the Bering Strait (Grebmeier et al., 2015) which supplies the the southern Chukchi Sea with "new" nitrogen (Walsh et al., 1989). Nitrogen that has not been reworked by bacteria or primary producers tends to be more depleted in ^{15}N. Dentrification can also effect residual $\delta^{15}N$ values. Denitrification elevates the $\delta^{15}N$ values in the residual source pool because of the large fractionation associated with the conversion of NO_3 to N_2 (reviewed by Casciotti, 2016). Both regions have high rates of denitrification with large nitrogen deficits compared to the rest of the world's oceans (Chang & Devol, 2009; Henriksen et al., 1993; McTigue et al., 2016; Tanaka et al., 2004; Zhuang et al., 2022). The higher $\delta^{15}N$ values in the northern Bering Sea indicate the likelihood of a more detrital-based food web with higher denitrification rates and nitrogen recycling than in the southern Chukchi Sea (Figure 22).

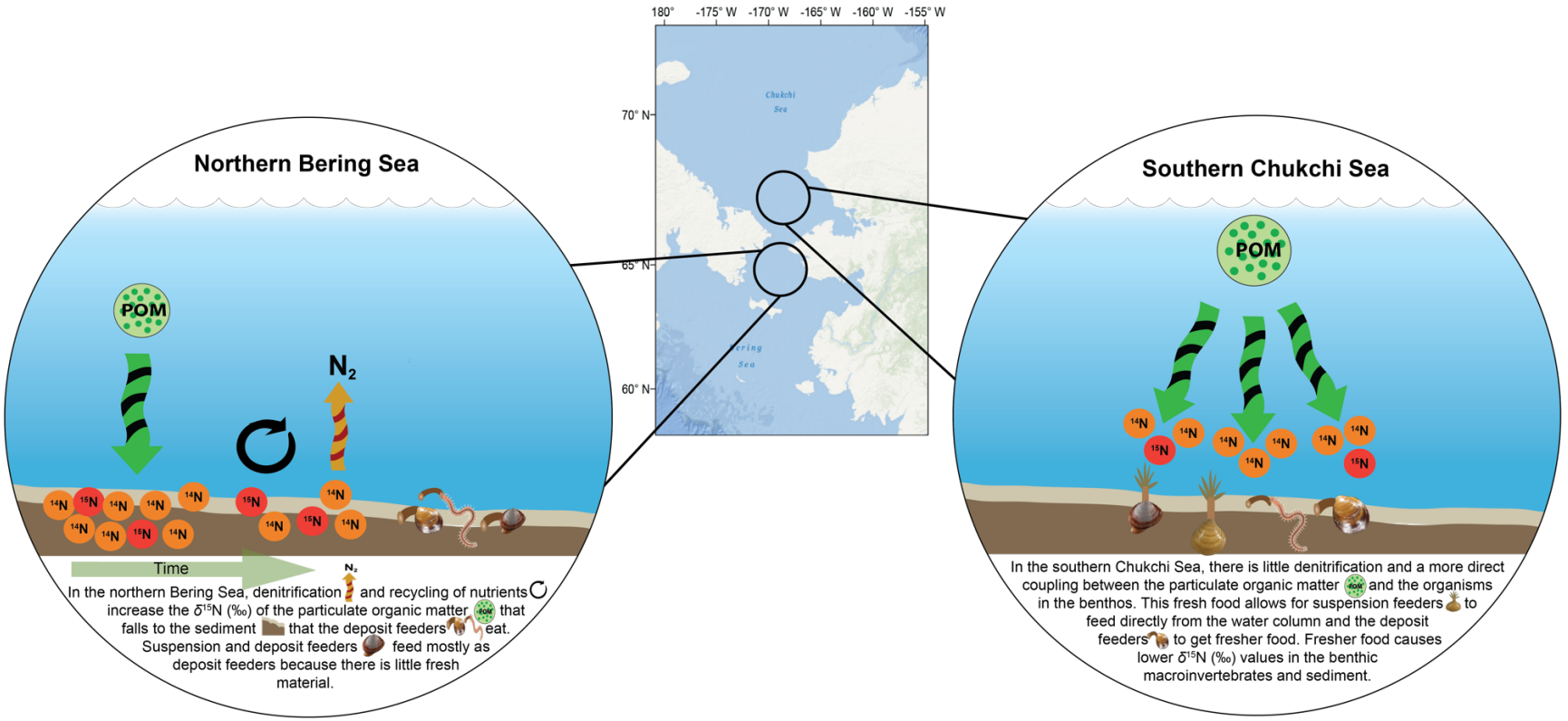

Figure 22. Conceptual diagram detailing the processes that might be leading to the higher δ^{15}N values in the northern Bering Sea compared with the southern Chukchi Sea. Symbols courtesy of the Integration and Application Network (ian.umces.edu/media-library).

These patterns also indicate a higher degree of pelagic-benthic coupling in the southern Chukchi Sea than in the northern Bering Sea. As bacteria and phytoplankton take up the nitrogen in the water column and sediment, they preferentially consume the ^{14}N in the organic matter and leave the heavier ^{15}N behind (Peterson, 1999). This kinetic fractionation leaves higher $\delta^{15}N$ values in the sediment. In the more productive southern Chukchi Sea, the sediment $\delta^{15}N$ values are lower possibly due to the more direct pelagic-benthic coupling compared to the northern Bering Sea where nutrients are recycled in the sediment. Dunton et al (1989) found a similar pattern where the $\delta^{13}C$ values in benthic consumers in the Chukchi Sea more closely resembled the zooplankton $\delta^{13}C$ values than in the northern Bering Sea. These similar $\delta^{13}C$ values in the benthic and pelagic communities indicate tighter pelagic-benthic coupling in the southern Chukchi Sea with a more detrital-based food web in the northern Bering Sea (Dunton et al., 1989). This theory is further supported by the larger number of suspension feeders in the southern Chukchi Sea relative to the northern Bering Sea. While from 1998 – 2018, the northern Bering Sea benthic macroinvertebrates were dominated by deposit feeders, the southern Chukchi Sea station had substantially more suspension feeders (Figure 23). This pattern is also apparent in the biomass data for the study years (Figure 7)

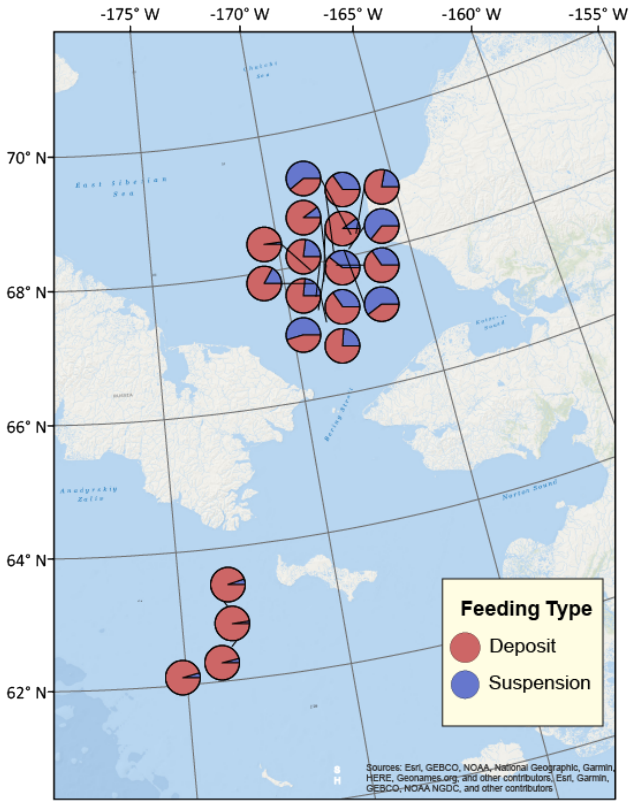

Figure 23. Abundance of deposit and suspension feeding benthic macroinvertebrates in the northern Bering Sea and the southern Chukchi Sea. Counts of organisms were aggregated into 1° cells and averaged over from 1998 - 2018.

In summary, the higher δ^{15}N values in the northern Bering Sea are likely due to denitrification and recycling of nutrients in the sediments while in the southern Chukchi Sea, there is more direct coupling of the water column POM to benthic macrobenthic organisms (Figure 22). This detrital-based food web may be beneficial to the stability of the benthic organisms in the northern Bering Sea. Rooney and McCann (2012) used data from Sánchez and Olaso (2004) to argue that the food webs that rely on energy derived from detritus (more than 50%) tend to be more diverse than food webs that rely on phytoplankton. I observed this pattern in our dataset. Coastal stations and northern Bering Sea stations had higher Shannon-Weiner

diversity indexes (mean ± SD: 2.3 ± 1.1 and 2.8 ± 0.3, respectively) than the Southern Chukchi Sea (1.2 ± 0.6) for the study years where biodiversity data was available (2014, 2015, and 2017).

4.3.2 Benthic Macroinvertebrates

The higher baseline δ^{15}N and lower δ^{13}C values in the northern Bering Sea compared with the southern Chukchi Sea were also observed in the deposit, deposit and suspension feeders, and predatory benthic macroinvertebrates (Figure 17). These three feeding guilds had higher δ^{15}N values in the northern Bering Sea than the southern Chukchi Sea. Deposit and deposit/suspension feeders had significantly lower δ^{13}C values in the northern Bering Sea compared to the southern Chukchi Sea. There were significant differences between the predator δ^{13}C values in the northern Bering Sea and southern Chukchi Sea. However, when accounting for the standard deviations of the mean, these distributions overlap, providing less confidence that significant differences extend to that feeding guild. There were also significant differences among suspension feeder δ^{13}C and δ^{15}N values in the southern Chukchi Sea, but again the standard deviations of the mean overlap. Additionally, the sample sizes were drastically different among groups (coastal: n = 7, northern Bering Sea: n = 5, southern Chukchi Sea: n = 28) so caution is advised in drawing inferences from these results.

Stable isotope signatures of consumers are largely dependent on the stable isotope signatures of the source, but TP values account for the differences in δ^{15}N

source values (Layman et al., 2012). Therefore, I compared the trophic positions across feeding guilds (Figure 17). There were no significant differences between the trophic position of deposit, deposit/suspension, and predator feeding organisms in the southern Chukchi and northern Bering Sea. There were significant differences in suspension feeder TP between the southern Chukchi Sea and northern Bering Sea, but again, small sample sizes limit interpretation. The differences among feeding types in δ^{13}C and δ^{15}N values but not TP values indicate that the source δ^{13}C and δ^{15}N values differ between these two sites but not the overall feeding strategies of similar benthic macroinvertebrates. These findings suggest that the differences in δ^{13}C and δ^{15}N values between the benthic macroinvertebrates in the northern Bering and southern Chukchi Sea can be attributed to the changes in the baseline δ^{13}C and δ^{15}N values of the sediment and not changes in feeding behavior.

4.3.3 Community-wide Layman metrics

Layman metrics (Layman et al., 2007) were used to assess the overall community structure in the northern Bering and southern Chukchi Seas (Table 10). The total sample size of benthic macroinvertebrates in the coastal stations was not large enough for community-wide assessments (Table 4). Layman metrics were calculated using Bayesian statistics as these metrics can be highly influenced by outliers and sample size when raw δ^{13}C and δ^{15}N values are used (Jackson et al., 2011; Layman et al., 2007). The δ^{15}N range was larger (4.4 ± 0.3) in the southern Chukchi Sea than the northern Bering Sea (4.2 ± 0.2) indicating that the southern

Chukchi Sea has a longer food web (Layman et al., 2007). However, the difference between these ranges are small and standard deviations of the means overlap. The $\delta^{13}C$ range was larger in the southern Chukchi Sea (2.5 ± 0.2) than the northern Bering Sea (1.3 ± 0.2) which is indicates there are more basal resources at the base of the food web in the southern Chukchi Sea (Layman et al., 2007). The increase in basal resources could be due to the later ice break up in the Chukchi Sea than the Bering Sea (Grebmeier et al., 2015) leading to persistence of ice algae $\delta^{13}C$ signals in the Chukchi Sea benthic macroinvertebrates.

TA and CD measure the degree of trophic diversity in the community (Layman et al., 2007). TA is calculated using the Bayesian SEA of the entire community (Jackson et al., 2011) and CD measures the Euclidean distance to the "centroid" or mean position of the community on a $\delta^{13}C$ and $\delta^{15}N$ biplot (Layman et al., 2007). The larger TA and CD in the southern Chukchi Sea (mean ± SD; TA: 4.1 ± 0.7, CD: 1.9 ± 0.1) compared to the northern Bering Sea (mean ± SD; TA: 0.8 ± 0.3, CD: 1.6 ± 0.1) indicate more trophic diversity in the southern Chukchi Sea community (Table 10). Larger trophic diversity in a community has been associated with the ecosystem resilience (Alp & Cucherousset, 2022; Kuiper et al., 2015).

The MNND and SDNND results were contradictory. MNND was larger in the northern Bering Sea than the southern Chukchi Sea, but SDNND was smaller in the northern Bering Sea than in the southern Chukchi Sea. Both MNND and SDNND metrics measure the degree of trophic redundancy in a community (Layman et al., 2007). When MNND is smaller, there is more overlap in isotopic space indicating

more redundancy in the system. When MNND is large, there is less "species packing" and more distinct isotopic niches (Layman et al., 2007). The MNND was larger in the northern Bering Sea (2.1 ± 0.1) than the southern Chukchi Sea (1.6 ± 0.1) indicating less trophic redundancy in the northern Bering Sea (Table 10). SDNND is the standard deviations of these means. If the SDNND is lower there is a relatively even distribution of species in isotopic biplot space. If it is higher, there is a more uneven distribution of species. The SDNND was smaller in the northern Bering Sea (0.4 ± 0.2) than in the southern Chukchi Sea (1.2 ± 0.2; Table 10). These apparently contradictory results may be a consequence of including suspension feeders in the southern Chukchi Sea, but not in the northern Bering Sea. Although Jackson et al (2011) found that increasing the number of groups in a community did not influence Layman metrics, MNND is more sensitive to sample size than SDNND (Layman et al., 2007).

With the exception of MNND, all Layman metrics were higher in the southern Chukchi Sea than the northern Bering Sea. These findings suggest that the southern Chukchi Sea has more basal sources, trophic levels, and trophic diversity than the northern Bering Sea.

4.4 Were there shifts in food web dynamics from 2014 to 2021?

The nonuniform and small sample sizes of benthic invertebrates collected across years and study sites did not allow for robust analyses of food web shifts across years. However, for certain taxonomic families, there were large enough

sample sizes to analyze differences across years or groups of years. In the northern Bering Sea, Tellinidae δ^{13}C values and TP were compared among 2014, 2016-2017, and 2021 and Maldanidae were compared between 2014-2015 and 2016-2017. In the southern Chukchi Sea, Tellinidae and Pectinariidae were assessed for temporal differences. Pectinariidae samples were pooled for 2014, 2016, and 2017 and compared to samples collected in 2021. Tellinidae samples were compared between 2014 and 2021. While only three taxonomic families were analyzed for temporal trends, these families are some of the most dominant macroinvertebrates in the Pacific Arctic benthos.

The δ^{13}C values and TP values of two taxonomic families of polychaetes, Pectinariidae in the northern Bering Sea and Maldanidae in the southern Chukchi Sea, did not vary significantly over time. However, in both the northern Bering Sea and southern Chukchi Sea, Tellinidae δ^{13}C values and TP changed over time. In the northern Bering Sea, the 2014 Tellinidae δ^{13}C values were significantly lower than the δ^{13}C values of the Tellinidae collected in later years (2016-2017 and 2021), and TP estimates were significantly lower in 2021 than the earlier study periods (Figure 12; 2016-2017 and 2014).

Body size can impact the stable isotope values of organisms due to the faster isotopic turnover rates during early growth stages (Fry & Arnold, 1982) or due to shifts in diets (Schlacher & Connolly, 2014; Villamarín et al., 2018). I tested whether these shifts in TP and δ^{13}C values were based on size by comparing the lengths of the Tellinidae shell among study periods in the northern Bering Sea. Size of the shell did

vary significantly between study periods, but these differences in length did not align with the differences in $\delta^{13}C$ values and TP. Length was not significantly different between 2021 and 2014, but the 2016 – 2017 samples were significantly smaller in size than in 2014 and 2021. If the differences in $\delta^{13}C$ values and TP were due to the size of the organism, I would expect to see the same temporal trends in $\delta^{13}C$ values and TP. The differences in $\delta^{13}C$ values in 2014 also did not align with sediment organic matter sample $\delta^{13}C$ values. The lowest $\delta^{13}C$ values in the sediment were in 2021, but the lowest $\delta^{13}C$ values in Tellinidae were in 2014 (Table 5 and Figure 12).

There were also differences among study periods in Tellinidae TP and $\delta^{13}C$ values in the southern Chukchi Sea stations. The mean $\delta^{13}C$ value was significantly higher in 2014 (-18.6 ‰ ± 0.5) than in 2021 (-19.1 ‰ ± 0.5). The trophic position of Tellinidae was significantly higher in 2014 (1.5 ± 0.4) than in 2021 (1.0 ± 0.1). As in the northern Bering Sea stations, I tested for differences in length among years. There was not a significant difference between the length of the Tellinidae samples in 2014 and 2021. However, in the southern Chukchi Sea, the differences between $\delta^{13}C$ values could be attributed to higher sediment organic matter $\delta^{13}C$ values in 2014 relative to 2021. The differences in TP cannot be attributed to differing baseline values as TP is corrected for the $\delta^{15}N$ of the baseline sediment. In both the southern Chukchi Sea and northern Bering Sea, Tellinidae TPs were lower in 2021 than the earlier study periods.

My original hypothesis for shifts in food webs was that the benthic macroinvertebrates from 2014 would have more sea ice algae in their diets than those

from 2021 (see Section 1.5). Sea ice algae $\delta^{13}C$ and $\delta^{15}N$ values were not measured as a part of this study, but other studies have found that sea ice algae $\delta^{13}C$ values are isotopically distinct from other isotopic end-members in the Pacific Arctic (Figure 20). $\delta^{13}C$ values in ice algae tend to be heavy isotope enriched compared to POM or sediment (Lovvorn et al., 2005; McTigue & Dunton, 2017; North et al., 2014). The peak pulse of organic matter deposition associated with sea ice algae is deposited relatively quickly (Lalande et al., 2021) and is rapidly mixed into the sediment due to bioturbation (North et al., 2014; Zinkann et al., 2022). However, Pacific Arctic benthic macroinvertebrates have longer tissue turnover times with half-lives of about 20 days in Arctic amphipods (Kaufman et al., 2008) and 3 – 15 % uptake of heavy isotope enriched algae over 19 days in Arctic bivalves (McMahon et al., 2006). These benthic macroinvertebrates were collected in July and ice break up typically occurs around April to May in the northern Bering Sea so presumably the heavy isotope enriched $\delta^{13}C$ values of ice algae would still be present to some extent in these samples.

However, if the changes in $\delta^{13}C$ values of the Tellinidae were due to more sea ice algae influence, I would expect to see more heavy isotope enriched $\delta^{13}C$ values of Tellinidae in 2014 than in 2016 – 2017 and 2021, based on the continuing trend of sea ice retreat. The weighted average mean sea ice extent in the northern hemisphere in 2014 was 10.790 million km^2, 10.163 million km^2 in 2016, and 10.292 million km^2 in 2017, and 10.552 million km^2 in 2021 (Fetterer et al., 2017). However, despite higher heat content, higher air temperature and lower ice extent in 2016 and 2017 compared

to 2014 (Thoman et al., 2020), the $\delta^{13}C$ value of the Tellinidae were more heavy isotope depleted in 2014 than in the later years.

These changes could also be due to a change in POM isotopic signatures. POM was only sampled in 2015 and 2016 for the southern Chukchi Sea and 2015 for the northern Bering Sea. Because of the tight coupling between the benthos and water column productivity (Grebmeier et al., 1988), other researchers have found that there is little difference between the sediment and bottom water POM $\delta^{13}C$ and $\delta^{15}N$ values (McTigue & Dunton, 2014; North et al., 2014) which are the two potential food sources for the suspension and deposit feeding Tellinidae. In our study, POM was collected at the chlorophyll maximum and was on average isotopically lighter in both $\delta^{13}C$ and $\delta^{15}N$ (1.6 ‰ and 0.9 ‰, respectively) in the southern Chukchi Sea in 2016 (Table 6). Because Tellinidae can feed on both POM and organic matter in the sediment, a shift in the $\delta^{13}C$ and $\delta^{15}N$ values of the POM could have influenced their isotopic signatures.

In both the southern Chukchi Sea and northern Bering Sea, the TP of Tellinidae was lower in later years. Tellinidae bivalves can both deposit and suspension feed so a decrease in the TP could be due to a switch to suspension feeding. These findings suggest that the temporal differences in Tellinidae $\delta^{13}C$ values and TP are not due to differences in the size distribution of the samples or changes in the isotopic signatures of the sediment (apart from southern Chukchi Sea Tellinidae $\delta^{13}C$ values) but are instead due to diet shifts or changes in a food source that was not tested in this study.

4.5 Do organisms that are thriving have larger trophic niches than those that are declining?

Standard ellipse areas were measured for six families in the northern Bering Sea and southern Chukchi Sea (Figure 19). Pectinariidae, a head-down deposit feeder, in the southern Chukchi Sea had the largest isotopic niche across regions while the predatory polychaete, Nephytidae, had the smallest isotopic niche (Table 11). When I measured the isotopic niche of benthic macroinvertebrate samples in both the northern Bering Sea and southern Chukchi Sea (Pectinariidae, Tellinidae, and Nuculidae), the isotopic niches were larger in the northern Bering Sea. This finding contrasts with the community level where total area was higher for the southern Chukchi Sea than the northern Bering Sea (Table 10). When productivity increases, species tend to have smaller trophic niche size (Lesser et al., 2020; MacArthur & Pianka, 1966). The larger isotopic niches of the species in the northern Bering Sea may be due to less primary productivity in the northern Bering Sea than in the southern Chukchi Sea.

While trends in biomass and abundance over time are beyond the scope of this study, Grebmeier et al (2018) has reported the dominant benthic macroinvertebrates in biomass from 1998 – 2015 in our study regions. Many of the dominant organisms are members of the taxonomic families addressed in this study. In the northern Bering Sea, dominant species include *Ennucula tenuis* (Nuculidae), *Nuculana radiata* (Nuculanidae), *Axiothella catenata* and *Maldane sarsi* (Maldanidae), and *M. calcarea* (Tellinidae). The southern Chukchi Sea stations were mainly dominated by *M.*

calcarea, but *Serripes groenlandicus* (Cardiidae), *E. tenuis* (Nuculidae), *Nephtys ciliata* (Nephtyidae), and *Yoldia* sp. (Yoldiidae) have been the dominant species in certain years and stations.

Among the dominant species in the northern Bering Sea, Tellinidae have the largest isotopic niche space. Goethel et al (2019) analyzed the trends in *M. calcarea* biomass and abundance in the northern Bering Sea and found decreasing trends in *M. calcarea* biomass at SLIP1 and 3 but increasing trends at SLIP4 (Figure 1). This study suggests that a finer scale resolution may be needed to truly determine whether feeding strategies are driving increases or decreases in abundance. Grebmeier et al. (2018) found that the dominant taxa by biomass shifted from nuculanid or nuculid bivalves to maldanid polychetes in the southernmost northern Bering Sea stations (Figure 1; SLIP1, 2, and 3). Maldanidae SEA_B distributions were larger than the Nuculanidae and Nuculidae (81% and 99%, respectively). The more generalist feeding strategy of Maldanidae as determined by SEA_B, may help it outcompete the bivalves (Figure 19; Table 11). The Tu et al., (2015) found that Maldanidae had higher than expected $\delta^{15}N$ values suggesting that they can utilize more refractory material in the northeast Chukchi Sea. Maldanids were also dominant in that study region, and Tu et al. (2015) concluded the success of this polychaete group may be attributed to its ability to utilize refractory material.

In the southern Chukchi Sea, Tellinidae had the largest isotopic niche out of the dominant organisms reported by Grebmeier et al (2018). In comparison to the other organisms measured for isotopic niche, Tellinidae had a higher SEA_B in 90 – 99 % of

the distributions. *M. calcarea* abundance has been increasing in the southern Chukchi Sea at the stations, UTN4 and 5, while *Serripes* spp. increased in abundance from 2015-2017 and then declined dramatically in 2018 and 2019 (Goethel, 2021). Goethel (2021) concluded that these findings may be due to *M. calcarea*'s ability to both suspension and deposit feed while *Serripes* spp. is strictly a suspension feeder. In my study, the Tellinidae SEA_{BS}s were larger than for the strictly deposit feeding bivalves, Nuculidae and Yoldiidae, and the suspension feeding bivalves Cardiidae. These findings support the hypothesis that Tellinidae is utilizing both the organic matter from the water column and the sediment. This ability to feed on multiple food sources may help explain its abundance and ecological importance.

Although I did not measure feeding strategies directly, this analysis provides insight into the general feeding patterns of some dominant benthic macroinvertebrates in the region. With the changing climate, some researchers have suggested that generalist species will be better equipped to adapt to a changing climate (Barton et al., 2019; Kortsch et al., 2015; Ricklefs, 2010). This study suggests that for a small number of benthic macroinvertebrates that are nevertheless important in the Pacific Arctic, larger niche areas may provide competitive advantages.

5 Conclusions and Further Study

My first objective for this study was to determine the differences between food web dynamics and the northern Bering Sea and southern Chukchi Sea. The northern Bering Sea stations had higher $\delta^{15}N$ values in both sediment and benthic

macroinvertebrates than the southern Chukchi Sea. These δ^{15}N value results are consistent with higher rates of denitrification and bacterial reworking in the northern Bering Sea than in the southern Chukchi Sea. The δ^{13}C values were lower in the northern Bering than southern Chukchi Sea. These lower δ^{13}C values are consistent with higher primary production in the southern Chukchi Sea than in the northern Bering Sea. However, benthic macroinvertebrate TP, which accounts for the δ^{15}N values of the sediment, did not differ between locations. This finding suggests that the differences in δ^{13}C and δ^{15}N values of the benthic macroinvertebrates between regions are not due to organisms changing their feeding behavior but are instead due to differences in the δ^{15}N and δ^{13}C values of the basal food resources in the region.

However, these differences could be due to the different bloom phenologies in the region during the time of sampling. The large pulse of organic carbon to the benthos occurs in May for the northern Bering Sea and June for the southern Chukchi Sea (Frey et al., 2015). However, we sampled for both food resources and benthic macroinvertebrates in July. While the southern Chukchi Sea could still be experiencing the productivity from the spring bloom in July, the northern Bering Sea's bloom is largely over by July.

There were also more suspension feeders in the southern Chukchi Sea than in the northern Bering Sea. This finding suggests that organisms in the southern Chukchi Sea could more readily feed directly on organic matter from the water column while in the northern Bering Sea, they relied more heavily on the less labile

sediments. These findings suggest more direct pelagic-benthic coupling in the southern Chukchi Sea than in the northern Bering Sea.

My second objective for this study was to determine whether there were shifts in food web dynamics from 2014 to 2021. My original hypothesis was that there would be more sea ice algae influence in the earlier years than in the later years. I would expect that the $\delta^{13}C$ values would be more positive when ice extent was larger. In both the northern Bering and southern Chukchi Seas, we saw significant differences between years in Tellinidae $\delta^{13}C$ values. In the southern Chukchi Sea, these differences could be attributed to the basal resource (sediment organic matter) $\delta^{13}C$ values, but in the northern Bering Sea, they could not. However, despite a larger ice extent in 2014, 2016, and 2017 than 2021, the Tellinidae $\delta^{13}C$ values were more negative in $\delta^{13}C$ values in earlier years than in later years in the northern Bering Sea. This finding suggests that the differences in sea ice extent between years did not impact the $\delta^{13}C$ values of the Tellinidae. Future studies could use compound-specific stable isotope analysis, DNA metabarcoding, or stomach content analysis to determine why these changes are occurring.

I also found that the Tellinidae bivalves fed at lower trophic levels in 2021 than in earlier years in both the northern Bering and southern Chukchi Sea stations. Tellinid bivalves (mainly *Macoma calcarea* in this study) can both deposit and suspension feed and remain relatively close to the surface (Macdonald, et al., 2010). They rapidly ingest settling algae (North et al., 2014) and are reliant on fresh pulses of phytoplankton (Waga et al., 2021). The lower trophic level of Tellinidae in 2021

compared to the earlier years could be due a switch to suspension feeding with more reliance on the fresh organic matter from the water column rather than the surface sediments.

The final objective was to determine whether organisms that are thriving have larger isotopic niches than those that are declining. We found that the thriving groups were more generalist feeders than the organisms that were declining. This finding helps validate the predictions of mobile generalists outcompeting specialists under climate change scenarios (Bartley et al., 2019; Kortsch et al., 2015).

The limitations of this study can be addressed in future work. Sampling all end-members throughout the bloom and into the summer for $\delta^{13}C$ and $\delta^{15}N$ values would allow for more accurate determinations of trophic position, and laboratory studies of tissue turnover time would also assist in determining appropriate end-member and consumer collection timing. Laboratory studies are also needed to determine accurate TDFs for benthic macroinvertebrates in the Pacific Arctic. Inaccurate TDFs could be causing the lack of heavy isotope enriched $\delta^{13}C$ end-members to account for the enrichment in benthic macroinvertebrate $\delta^{13}C$ values. In the future, larger quantities of similar organisms should be collected across sampling regions to allow for robust temporal analysis. Compound-specific amino acid and fatty acid stable isotope analysis could also be used to determine more specifically the diets of organisms and sea ice algae. With the Arctic warming at a faster rate than the rest of the world, ecosystem studies are imperative to understanding the changing dynamics in the Pacific Arctic region.

6 References

Abrantes, K. G., Barnett, A., & Bouillon, S. (2014). Stable isotope-based community metrics as a tool to identify patterns in food web structure in east African estuaries. *Functional Ecology*, *28*(1), 270–282. https://doi.org/10.1111/1365-2435.12155

Adolfsson, A., Ackerman, M., & Brownstein, N. C. (2019). To cluster, or not to cluster: An analysis of clusterability methods. *Pattern Recognition*, *88*, 13–26. https://doi.org/10.1016/j.patcog.2018.10.026

Alp, M., & Cucherousset, J. (2022). Food webs speak of human impact: Using stable isotope-based tools to measure ecological consequences of environmental change. *Food Webs*, *30*, e00218. https://doi.org/10.1016/j.fooweb.2021.e00218

ArcMap (10.8). (2020). Esri. https://www.esri.com/en-us/arcgis/products/arcgis-desktop/resources

Arrigo, K. R., van Dijken, G., & Pabi, S. (2008). Impact of a shrinking Arctic ice cover on marine primary production. *Geophysical Research Letters*, *35*(19), L19603. https://doi.org/10.1029/2008GL035028

Barnes, C. A., & Thompson, T. G. (1938). Physical and chemical investigations in the Bering Sea and portions of the North Pacific Ocean. *Univ. Wash. Publ. Oceanography*, *3*, 35–79.

Bartley, T. J., McCann, K. S., Bieg, C., Cazelles, K., Granados, M., Guzzo, M. M., MacDougall, A. S., Tunney, T. D., & McMeans, B. C. (2019). Food web

rewiring in a changing world. *Nature Ecology & Evolution*, *3*(3), 345–354. https://doi.org/10.1038/s41559-018-0772-3

Barton, M., Litvin, S., Vollenweider, J., Heintz, R., Norcross, B., & Boswell, K. (2019). Implications of trophic discrimination factor selection for stable isotope food web models of low trophic levels in the Arctic nearshore. *Marine Ecology Progress Series*, *613*, 211–216. https://doi.org/10.3354/meps12893

Batschelet, E. (1981). *Circular statistics in biology*. Academic Press.

Bearhop, S., Adams, C. E., Waldron, S., Fuller, R. A., & Macleod, H. (2004). Determining trophic niche width: A novel approach using stable isotope analysis: Stable isotopes as measures of niche width. *Journal of Animal Ecology*, *73*(5), 1007–1012. https://doi.org/10.1111/j.0021-8790.2004.00861.x

Bekryaev, R. V., Polyakov, I. V., & Alexeev, V. A. (2010). Role of Polar Amplification in long-term surface air temperature variations and modern Arctic warming. *Journal of Climate*, *23*(14), 3888–3906. https://doi.org/10.1175/2010JCLI3297.1

Bluhm, B. A., & Gradinger, R. (2008). Regional variability in food availability for Arctic marine mammals. *Ecological Applications*, *18*(sp2), S77–S96. https://doi.org/10.1890/06-0562.1

Bond, A. L., Jardine, T. D., & Hobson, K. A. (2016). Multi-tissue stable-isotope analyses can identify dietary specialization. *Methods in Ecology and Evolution*, *7*(12), 1428–1437. https://doi.org/10.1111/2041-210X.12620

Brind'Amour, A., & Dubois, S. F. (2013). Isotopic diversity indices: How Sensitive to Food Web Structure? *PLoS ONE*, *8*(12), e84198. https://doi.org/10.1371/journal.pone.0084198

Cabanellas-Reboredo, M., Deudero, S., & Blanco, A. (2009). Stable-isotope signatures ($\delta^{13}C$ and $\delta^{15}N$) of different tissues of *Pinna nobilis* Linnaeus, 1758 (Bivalvia): Isotopic variations among tissues and between seasons. *Journal of Molluscan Studies*, *75*(4), 343–349. https://doi.org/10.1093/mollus/eyp021

Campbell, R. G., Sherr, E. B., Ashjian, C. J., Plourde, S., Sherr, B. F., Hill, V., & Stockwell, D. A. (2009). Mesozooplankton prey preference and grazing impact in the western Arctic Ocean. *Deep Sea Research Part II: Topical Studies in Oceanography*, *56*(17), 1274–1289. https://doi.org/10.1016/j.dsr2.2008.10.027

Casciotti, K. L. (2016). Nitrogen and oxygen isotopic studies of the marine nitrogen cycle. *Annual Review of Marine Science*, *8*(1), 379–407. https://doi.org/10.1146/annurev-marine-010213-135052

Catry, T., Lourenço, P. M., Lopes, R. J., Carneiro, C., Alves, J. A., Costa, J., Rguibi-Idrissi, H., Bearhop, S., Piersma, T., & Granadeiro, J. P. (2016). Structure and functioning of intertidal food webs along an avian flyway: A comparative approach using stable isotopes. *Functional Ecology*, *30*(3), 468–478. https://doi.org/10.1111/1365-2435.12506

Caut, S., Angulo, E., & Courchamp, F. (2009). Variation in discrimination factors ($\Delta^{15}N$ and $\Delta^{13}C$): The effect of diet isotopic values and applications for diet

reconstruction. *Journal of Applied Ecology*, *46*(2), 443–453. https://doi.org/10.1111/j.1365-2664.2009.01620.x

Chang, B. X., & Devol, A. H. (2009). Seasonal and spatial patterns of sedimentary denitrification rates in the Chukchi sea. *Deep Sea Research Part II: Topical Studies in Oceanography*, *56*(17), 1339–1350. https://doi.org/10.1016/j.dsr2.2008.10.024

Clement Kinney, J., Maslowski, W., Osinski, R., Lee, Y. J., Goethel, C., Frey, K., & Craig, A. (2022). On the variability of the Bering Sea Cold Pool and implications for the biophysical environment. *PLOS ONE*, *17*(4), e0266180. https://doi.org/10.1371/journal.pone.0266180

Coachman, L. K., Aagaard, K., & Tripp, R. B. (1975). *Bering Strait: The regional physical oceanography*. University of Washington Press.

Cooper, L. W., & Grebmeier, J. M. (2022). A Chlorophyll Biomass Time-Series for the Distributed Biological Observatory in the Context of Seasonal Sea Ice Declines in the Pacific Arctic Region. *Geosciences*, *12*(8), 307. https://doi.org/10.3390/geosciences12080307

Cooper, L.W. Grebmeier, J. M., Frey, K. E., & Vagle, S. (2019a). Discrete water samples collected from the Conductivity-Temperature-Depth rosette at specific depths, Northern Bering Sea to Chukchi Sea*,* 2016. *Arctic Data Center*. https://doi.org/10.18739/A23B5W875

Cooper, L. W., Grebmeier, J. M., Frey, K. E., & Vagle, S. (2019b). Nutrient, oxygen 18/16 ratio, and chlorophyll data measured from water samples collected

aboard the Sir Wilfred Laurier, Bering and Chukchi Seas, 2014. *Arctic Data Center*. https://doi.org/10.18739/A20K26B4P

Cooper, L. W., Grebmeier, J. M., Frey, K. E., & Vagle, S. (2019c). Nutrient, oxygen 18/16 ratio, and chlorophyll data measured from water samples collected aboard the Sir Wilfred Laurier, Bering and Chukchi Seas, 2015. *Arctic Data Center*. https://doi.org/10.18739/A20000081

Cooper, L. W., Grebmeier, J. M., Larsen, I. L., Egorov, V. G., Theodorakis, C., Kelly, H. P., & Lovvorn, J. R. (2002). Season variation in sedimentation of organic materials in the St. Lawrence Island polynya region, Bering Sea. *Marine Ecology Progress Series*, *226*, 13–26.

Cooper, L. W., Grebmeier, J. M., & Zimmerman, S. (2022). Discrete water samples collected from the Conductivity-Temperature-Depth rosette at specific depths, CCGS Sir Wilfrid Laurier, Northern Bering Sea to Chukchi Sea, 2018. *Arctic Data Center*. urn:uuid:29de9d96-514a-41ed-9151-e0303ccdcb95

Cooper, L. W., Janout, M. A., Frey, K. E., Pirtle-Levy, R., Guarinello, M. L., Grebmeier, J. M., & Lovvorn, J. R. (2012). The relationship between sea ice break-up, water mass variation, chlorophyll biomass, and sedimentation in the northern Bering Sea. *Deep Sea Research Part II: Topical Studies in Oceanography*, *65–70*, 141–162. https://doi.org/10.1016/j.dsr2.2012.02.002

Danielson, S. L., Ahkinga, O., Ashjian, C., Basyuk, E., Cooper, L. W., Eisner, L., Farley, E., Iken, K. B., Grebmeier, J. M., Juranek, L., Khen, G., Jayne, S. R., Kikuchi, T., Ladd, C., Lu, K., McCabe, R. M., Moore, G. W. K., Nishino, S.,

Ozenna, F., … Weingartner, T. J. (2020). Manifestation and consequences of warming and altered heat fluxes over the Bering and Chukchi Sea continental shelves. *Deep Sea Research Part II: Topical Studies in Oceanography*, *177*, 104781. https://doi.org/10.1016/j.dsr2.2020.104781

Dansgaard, W. (1964). Stable isotopes in precipitation. *Tellus*, *XVI*, 1–4.

Delacre, M., Lakens, D., & Leys, C. (2017). Why psychologists should by default use Welch's *t*-test instead of student's *t*-test. *International Review of Social Psychology*, *30*(1), 92. https://doi.org/10.5334/irsp.82

DeNiro, M. J., & Epstein, S. (1981). Influence of diet on the distribution of nitrogen isotopes in animals. *Geochimica et Cosmochimica Acta*, *45*(3), 341–351. https://doi.org/10.1016/0016-7037(81)90244-1

Dunton, K. H., Saupe, S. M., Golikov, A. N., & Schell, D. M. (1989). Trophic relationships and isotopic gradients among artic and subarctic marine fauna. *Marine Ecology Progress Series*, *56*(1/2), 89–97.

Fetterer, F., Knowles, K., Meier, W. N., Savoie, M., & Windnagel, A. K. (2017). Sea Ice Index, Version 3 (Sea Ice Index Monthly Data by Year G02135). *National Snow and Ice Data Cente*r. https://doi.org/10.7265/N5K072F8

Florin, S. T., Felicetti, L. A., & Robbins, C. T. (2011). The biological basis for understanding and predicting dietary-induced variation in nitrogen and sulphur isotope ratio discrimination: Understanding nitrogen and sulphur discrimination. *Functional Ecology*, *25*(3), 519–526. https://doi.org/10.1111/j.1365-2435.2010.01799.x

Fowlkes, E. B., & Mallows, C. L. (1983). A method for comparing two hierarchical clusterings. *Journal of the American Statistical Association*, *78*(383), 553–569.

Frey, K. E., J.C. Cosmiso, L.W. Cooper, J.M. Grebmeier, and L.V. Stock (2021). Arctic Ocean primary productivity: The response of marine algae to climate warming and sea ice decline, pp. 46-57. In: *Arctic Report Card 2021*, T.A. Moon, M.L. Druckenmiller, and R.L. Thoman, eds; DOI: 10.25923/kxhb-dw16.

Frey, K. E., Maslanik, J. A., Kinney, J. C., & Maslowki, W. (2014). Recent variability in sea ice cover, age, and thickness in the Pacific Arctic Region. In J. M. Grebmeier & W. Maslowski (Eds.), *The Pacific Arctic Region: Ecosystem Status and Trends in a Rapidly Changing Environment* (pp. 31–63). Springer Science+Business Media.

Frey, K. E., Moore, G. W. K., Cooper, L. W., & Grebmeier, J. M. (2015). Divergent patterns of recent sea ice cover across the Bering, Chukchi, and Beaufort seas of the Pacific Arctic Region. *Progress in Oceanography*, *136*, 32–49. https://doi.org/10.1016/j.pocean.2015.05.009

Fry, B. (2008). *Stable isotope ecology* (Corr. as of 3. print). Springer.

Fry, B., & Arnold, C. (1982). Rapid $^{13}C/^{12}C$ turnover during growth of brown shrimp (*Penaeus aztecus*). *Oecologia*, *54*(2), 200–204. https://doi.org/10.1007/BF00378393

Fry, B., & Sherr, E. B. (1984). $\delta^{13}C$ measurements as indicators of carbon flow in marine and freshwater ecosystems. *Contributions to Marine Science*, *27*, 13–47.

Galili, T. (2015). dendextend: An R package for visualizing, adjusting and comparing trees of hierarchical clustering. *Bioinformatics*, *31*(22), 3718–3720. https://doi.org/10.1093/bioinformatics/btv428

Gaspar, M. B., Santos, M. N., & Vasconcelos, P. (2001). Weight–length relationships of 25 bivalve species (Mollusca: Bivalvia) from the Algarve coast (southern Portugal). *Journal of the Marine Biological Association of the United Kingdom*, *81*(5), 805–807. https://doi.org/10.1017/S0025315401004623

Goethel, C. L. (2021). *Time-series focused assessments of changing marine bivalve communities in the Bering and Chukchi Seas*. [Doctoral dissertation, University of Maryland, College Park]. https://doi.org/10.13016/pojs-sixs

Goethel, C. L., Grebmeier, J. M., & Cooper, L. W. (2019). Changes in abundance and biomass of the bivalve *Macoma calcarea* in the northern Bering Sea and the southeastern Chukchi Sea from 1998 to 2014, tracked through dynamic factor analysis models. *Deep Sea Research Part II: Topical Studies in Oceanography*, *162*, 127–136. https://doi.org/10.1016/j.dsr2.2018.10.007

Gorokhova, E. (2018). Individual growth as a non-dietary determinant of the isotopic niche metrics. *Methods in Ecology and Evolution*, *9*(2), 269–277. https://doi.org/10.1111/2041-210X.12887

Grebmeier, J. M. (2012). Shifting patterns of life in the Pacific Arctic and sub-Arctic Seas. *Annual Review of Marine Science*, *4*(1), 63–78. https://doi.org/10.1146/annurev-marine-120710-100926

Grebmeier, J. M., Bluhm, B. A., Cooper, L. W., Danielson, S. L., Arrigo, K. R., Blanchard, A. L., Clarke, J. T., Day, R. H., Frey, K. E., Gradinger, R. R., Kędra, M., Konar, B., Kuletz, K. J., Lee, S. H., Lovvorn, J. R., Norcross, B. L., & Okkonen, S. R. (2015). Ecosystem characteristics and processes facilitating persistent macrobenthic biomass hotspots and associated benthivory in the Pacific Arctic. *Progress in Oceanography*, *136*, 92–114. https://doi.org/10.1016/j.pocean.2015.05.006

Grebmeier, J. M., & Cooper, L. W. (1995). Influence of the St. Lawrence Island Polynya upon the Bering Sea benthos. *Journal of Geophysical Research*, *100*, 4439–4460.

Grebmeier, J. M., & Cooper, L. W. (2019a). Benthic macroinfaunal samples collected from the Canadian Coast Guard Ship (CCGS) Sir Wilfrid Laurier, northern Bering Sea to Chukchi Sea, 2012. *Arctic Data Center*. https://doi.org/10.18739/A2736M23F

Grebmeier, J. M., & Cooper, L. W. (2019b). Benthic macroinfaunal samples collected from the Canadian Coast Guard Ship (CCGS) Sir Wilfrid Laurier, northern Bering Sea to Chukchi Sea, 2013. *Arctic Data Center*. https://doi.org/10.18739/A2N29P67H

Grebmeier, J. M., & Cooper, L. W. (2019c). Benthic macroinfaunal samples collected from the Canadian Coast Guard Ship (CCGS) Sir Wilfrid Laurier, northern Bering Sea to Chukchi Sea, 2014. *Arctic Data Center*. https://doi.org/10.18739/A2ZG6G71C

Grebmeier, J. M., & Cooper, L. W. (2019d). Benthic macroinfaunal samples collected from the Canadian Coast Guard Ship (CCGS) Sir Wilfrid Laurier, northern Bering Sea to Chukchi Sea, 2015. *Arctic Data Center.* https://doi.org/10.18739/A28W3827B

Grebmeier, J. M., Cooper, L. W., Feder, H. M., & Sirenko, B. I. (2006b). Ecosystem dynamics of the Pacific-influenced northern Bering and Chukchi Seas in the Amerasian Arctic. *Progress in Oceanography*, *71*(2–4), 331–361. https://doi.org/10.1016/j.pocean.2006.10.001

Grebmeier, J. M., Feder, H. M., & McRoy, C. P. (1989). Pelagic-benthic coupling on the shelf of the northern Bering and Chukchi Seas. II. Benthic community structure. *Marine Ecology Progress Series*, *51*, 253–268.

Grebmeier, J. M., Frey, K., Cooper, L., & Kędra, M. (2018). Trends in benthic macrofaunal populations, seasonal sea ice persistence, and bottom water temperatures in the Bering Strait region. *Oceanography*, *31*(2). https://doi.org/10.5670/oceanog.2018.224

Grebmeier, J. M., McRoy, C. P., & Feder, H. M. (1988). Pelagic-benthic coupling on the shelf of the norther Bering and Chukchi Seas. I. Food supply source and benthic biomass. *Marine Ecology Progress Series*, *48*, 57–67.

Grebmeier, J. M., Overland, J. E., Moore, S. E., Farley, E. V., Carmack, E. C., Cooper, L. W., Frey, K. E., Helle, J. H., McLaughlin, F. A., & McNutt, S. L. (2006a). A major ecosystem shift in the northern Bering Sea. *Science*, *311*(5766), 1461–1464. https://doi.org/10.1126/science.1121365

Gu, B., Schelske, C. L., & Brenner, M. (1996). Relationship between sediment and plankton isotope ratios (δ^{13}C and δ^{15}N) and primary productivity in Florida lakes. *Canadian Journal of Fisheries and Aquatic Sciences*, *53*(4), 875–883. https://doi.org/10.1139/f95-248

Hansen, A. G., Gardner, J. R., Connelly, K. A., Polacek, M., & Beauchamp, D. A. (2018). Trophic compression of lake food webs under hydrologic disturbance. *Ecosphere*, *9*(6). https://doi.org/10.1002/ecs2.2304

Henriksen, K., Blackburn, T. H., Lomstein, B. Aa., & McRoy, C. P. (1993). Rates of nitrification, distribution of nitrifying bacteria and inorganic N fluxes in northern Bering-Chukchi shelf sediments. *Continental Shelf Research*, *13*(5–6), 629–651. https://doi.org/10.1016/0278-4343(93)90097-H

Highsmith, R. C., & Coyle, K. O. (1990). High productivity of northern Bering Sea benthic amphipods. *Nature*, *344*(6269), 862-864.

Hill, V., Ardyna, M., Lee, S. H., & Varela, D. E. (2018). Decadal trends in phytoplankton production in the Pacific Arctic Region from 1950 to 2012. *Deep Sea Research Part II: Topical Studies in Oceanography*, *152*, 82–94. https://doi.org/10.1016/j.dsr2.2016.12.015

Hobson, K. A., & Welch, H. E. (1992). Determination of trophic relationships within a high Arctic marine food web using $\delta^{13}C$ and $\delta^{15}N$ analysis. *Marine Ecology Progress Series*, *84*(1), 9–18.

Holland, S. M. (2019). *Principal Component Analysis.* Department of Geology, University of Georgia, Athens, GA, 30602-2501.

Hoondert, R. P. J., van den Brink, N. W., van den Heuvel-Greve, M. J., Ragas, A. M. J., & Hendriks, A. J. (2021). Variability in nitrogen-derived trophic levels of Arctic marine biota. *Polar Biology*, *44*(1), 119–131. https://doi.org/10.1007/s00300-020-02782-4

Hopkins, B., & Skellam, J. K. (1954). A new method for determining the type of distribution of plant individuals. *Annals of Botany*, *18*(70). 213–227

Hussey, N. E., MacNeil, M. A., Olin, J. A., McMeans, B. C., Kinney, M. J., Chapman, D. D., & Fisk, A. T. (2012). Stable isotopes and elasmobranchs: Tissue types, methods, applications and assumptions. *Journal of Fish Biology*, *80*(5), 1449–1484. https://doi.org/10.1111/j.1095-8649.2012.03251.x

Hutchinson, G. E. (1957). Concluding Remarks. *Cold Spring Harbor Symposia on Quantitative Biology*, *22*(0), 415–427. https://doi.org/10.1101/SQB.1957.022.01.039

Hutchinson, G. E. (1978). *An introduction to population biology*. Yale University Press.

Iken, K., Bluhm, B., & Dunton, K. (2010). Benthic food-web structure under differing water mass properties in the southern Chukchi Sea. *Deep Sea*

Research Part II: Topical Studies in Oceanography, *57*(1–2), 71–85. https://doi.org/10.1016/j.dsr2.2009.08.007

Jackson, A. L., Inger, R., Parnell, A. C., & Bearhop, S. (2011). Comparing isotopic niche widths among and within communities: SIBER - Stable Isotope Bayesian Ellipses in R: Bayesian isotopic niche metrics. *Journal of Animal Ecology*, *80*(3), 595–602. https://doi.org/10.1111/j.1365-2656.2011.01806.x

Jay, C. V., Grebmeier, J. M., Fischbach, A. S., McDonald, T. L., Cooper, L. W., & Hornsby, F. (2014). Pacific walrus (*Odobenus rosmarus divergens*) resource selection in the Northern Bering Sea. *PLoS ONE*, *9*(4), e93035. https://doi.org/10.1371/journal.pone.0093035

Jiguet, F., Julliard, R., Thomas, C. D., Dehorter, O., Newson, S. E., & Couvet, D. (2006). Thermal range predicts bird population resilience to extreme high temperatures. *Ecology Letters*, *9*(12), 1321–1330. https://doi.org/10.1111/j.1461-0248.2006.00986.x

Jolliffe, I. T. (2002). *Principal Component Analysis* (2nd ed.). Springer-Verlag.

Karlson, A. M. L., Reutgard, M., Garbaras, A., & Gorokhova, E. (2018). Isotopic niche reflects stress-induced variability in physiological status. *Royal Society Open Science*, *5*(2), 171398. https://doi.org/10.1098/rsos.171398

Kassambara, A. (2021). *_rstatix: Pipe-friendly framework for basic statistical tests_*[R package version 0.7.0]. https://CRAN.R-project.org/package=rstatix

Kassambara, A., & Mundt, F. (2020). *factoextra: Extract and Visualize the Results of Multivariate Data Analyses* (R package version 1.0.7). https://CRAN.R-project.org/package=factoextra

Kaufman, L., & Rousseeuw, P. J. (2005). *Finding groups in data: An introduction to cluster analysis*. John Wiley & Sons.

Kaufman, M. R., Gradinger, R. R., Bluhm, B. A., & O'Brien, D. M. (2008). Using stable isotopes to assess carbon and nitrogen turnover in the Arctic sympagic amphipod *Onisimus litoralis*. *Oecologia*, *158*(1), 11–22. https://doi.org/10.1007/s00442-008-1122-y

Kędra, M., Cooper, L. W., Zhang, M., Biasatti, D., & Grebmeier, J. M. (2019). Benthic trophic sensitivity to on-going changes in Pacific Arctic seasonal sea ice cover – Insights from the nitrogen isotopic composition of amino acids. *Deep Sea Research Part II: Topical Studies in Oceanography*, *162*, 137–151. https://doi.org/10.1016/j.dsr2.2019.01.002

Kendall, M. G. (1975). *Rank Correlation Methods* (4th Edition). Charles Griffin.

Kortsch, S., Primicerio, R., Fossheim, M., Dolgov, A. V., & Aschan, M. (2015). Climate change alters the structure of arctic marine food webs due to poleward shifts of boreal generalists. *Proceedings of the Royal Society B: Biological Sciences*, *282*(1814), 20151546. https://doi.org/10.1098/rspb.2015.1546

Kruskal, W. H., & Wallis, W. A. (1952). Use of ranks in one-criterion variance analysis. *Journal of the American Statistical Association*, *47*(260), 583–621. https://doi.org/10.1080/01621459.1952.10483441

Kuiper, J. J., van Altena, C., de Ruiter, P. C., van Gerven, L. P. A., Janse, J. H., & Mooij, W. M. (2015). Food-web stability signals critical transitions in temperate shallow lakes. *Nature Communications*, *6*(1), 7727. https://doi.org/10.1038/ncomms8727

Lalande, C., Grebmeier, J. M., McDonnell, A. M. P., Hopcroft, R. R., O'Daly, S., & Danielson, S. L. (2021). Impact of a warm anomaly in the Pacific Arctic region derived from time-series export fluxes. *PLOS ONE*, *16*(8), e0255837. https://doi.org/10.1371/journal.pone.0255837

Lamb, A. L., Wilson, G. P., & Leng, M. J. (2006). A review of coastal palaeoclimate and relative sea-level reconstructions using δ^{13}C and C/N ratios in organic material. *Earth-Science Reviews*, *75*(1–4), 29–57. https://doi.org/10.1016/j.earscirev.2005.10.003

Layman, C. A., Araujo, M. S., Boucek, R., Hammerschlag-Peyer, C. M., Harrison, E., Jud, Z. R., Matich, P., Rosenblatt, A. E., Vaudo, J. J., Yeager, L. A., Post, D. M., & Bearhop, S. (2012). Applying stable isotopes to examine food-web structure: An overview of analytical tools. *Biological Reviews*, *87*(3), 545–562. https://doi.org/10.1111/j.1469-185X.2011.00208.x

Layman, C. A., Arrington, D. A., Montaña, C. G., & Post, D. M. (2007). Can stable isotope ratios provide for community-wide measures of trophic structure? *Ecology*, *88*(1), 42–48.

Lebrun, M., Vancoppenolle, M., Madec, G., & Massonnet, F. (2019). Arctic sea-ice-free season projected to extend into autumn. *The Cryosphere*, *13*(1), 79–96. https://doi.org/10.5194/tc-13-79-2019

Lesser, J. S., James, W. R., Stallings, C. D., Wilson, R. M., & Nelson, J. A. (2020). Trophic niche size and overlap decreases with increasing ecosystem productivity. *Oikos*, *129*(9), 1303–1313. https://doi.org/10.1111/oik.07026

Levene, H. (1960). Robust tests for equality of variances. In I. Olkin & H. Hotelling (Eds.), *Contributions to Probability and Statistics: Essays in Honor of Harold Hotelling* (pp. 278–292). Stanford University Press.

Levine, S. (1980). Several measures of trophic structure applicable to complex food webs. *Journal of Theoretical Biology*, *83*(2), 195–207. https://doi.org/10.1016/0022-5193(80)90288-X

Lewis, K. M., van Dijken, G. L., & Arrigo, K. R. (2020). Changes in phytoplankton concentration now drive increased Arctic Ocean primary production. *Science*, *369*(6500), 198–202. https://doi.org/10.1126/science.aay8380

Lindsay, R., & Schweiger, A. (2015). Arctic sea ice thickness loss determined using subsurface, aircraft, and satellite observations. *The Cryosphere*, *9*(1), 269–283. https://doi.org/10.5194/tc-9-269-2015

Lovvorn, J. R., Cooper, L. W., Brooks, M. L., De Ruyck, C. C., Bump, J. K., & Grebmeier, J. M. (2005). Organic matter pathways to zooplankton and benthos under pack ice in late winter and open water in late summer in the north-central Bering Sea. *Marine Ecology Progress Series*, *291*, 135–150. https://doi.org/10.3354/meps291135

MacArthur, R. H., & Pianka, E. R. (1966). On optimal use of a patchy environment. *The American Naturalist*, *100*(916), 603–609.

Macdonald, T. A., Burd, B. J., Macdonald, V. I., & van Roodselaar, A. (2010). *Taxonomic and feeding guild classification for the marine benthic macroinvertebrates of the Strait of Georgia, British Columbia* (Canadian Technical Report of Fisheries and Aquatic Sciences No. 2874; p. iv + 63).

Maechler, M., Rousseeuw, P. J., Struyf, M., & Hornik, K. (2022). *cluster: Cluster Analysis Basics and Extensions*. https://CRAN.R-project.org/package=cluster

Mann, H. B. (1945). Nonparametric tests against trend. *Econometrica*, *13*(3), 245. https://doi.org/10.2307/1907187

Martínez del Rio, C., & Carleton, S. A. (2012). How fast and how faithful: The dynamics of isotopic incorporation into animal tissues: Fig. 1. *Journal of Mammalogy*, *93*(2), 353–359. https://doi.org/10.1644/11-MAMM-S-165.1

Martiny, A. C., Pham, C. T. A., Primeau, F. W., Vrugt, J. A., Moore, J. K., Levin, S. A., & Lomas, M. W. (2013). Strong latitudinal patterns in the elemental ratios of marine plankton and organic matter. *Nature Geoscience*, *6*(4), 279–283. https://doi.org/10.1038/ngeo1757

Mateo, M. A., Serrano, O., Serrano, L., & Michener, R. H. (2008). Effects of sample preparation on stable isotope ratios of carbon and nitrogen in marine invertebrates: Implications for food web studies using stable isotopes. *Oecologia*, *157*(1), 105–115. https://doi.org/10.1007/s00442-008-1052-8

Matich, P., Bizzarro, J. J., & Shipley, O. N. (2021). Are stable isotope ratios suitable for describing niche partitioning and individual specialization? *Ecological Applications*, *31*(6). https://doi.org/10.1002/eap.2392

McCarthy, M. A. (2007). *Bayesian methods for ecology*. Cambridge University Press.

McCutchan, Jr., J. H., Lewis, Jr., W. M., Kendall, C., & McGrath, C. C. (2003). Variation in trophic shift for stable isotope ratios of carbon, nitrogen, and sulfur. *Oikos*, *102*(2), 378–390.

McMahon, K. W., Ambrose, Jr., W. G., Johnson, B. J., Sun, M.-Y., Clough, L. M., & Carroll, M. L. (2006). Benthic community response to ice algae and phytoplankton in Ny Ålesund, Svalbard. *Marine Ecology Progress Series*, *310*, 1–14.

McTigue, N. D., & Dunton, K. H. (2014). Trophodynamics and organic matter assimilation pathways in the northeast Chukchi Sea, Alaska. *Deep Sea Research Part II: Topical Studies in Oceanography*, *102*, 84–96. https://doi.org/10.1016/j.dsr2.2013.07.016

McTigue, N. D., & Dunton, K. H. (2017). Trophodynamics of the Hanna Shoal Ecosystem (Chukchi Sea, Alaska): Connecting multiple end-members to a

rich food web. *Deep Sea Research Part II: Topical Studies in Oceanography*, *144*, 175–189. https://doi.org/10.1016/j.dsr2.2017.08.010

McTigue, N. D., Gardner, W. S., Dunton, K. H., & Hardison, A. K. (2016). Biotic and abiotic controls on co-occurring nitrogen cycling processes in shallow Arctic shelf sediments. *Nature Communications*, *7*(1), 13145. https://doi.org/10.1038/ncomms13145

Mehta, V., Bawa, S., & Singh, J. (2020). Analytical review of clustering techniques and proximity measures. *Artificial Intelligence Review*, *53*(8), 5995–6023. https://doi.org/10.1007/s10462-020-09840-7

Meier, W. N., Perovich, D., Farrell, S., Haas, C., Hendricks, S., Petty, A. A., Webster, M., Divine, D., Gerland, S., Kaleschke, L., Ricker, R., Steer, A., Tian-Kunze, X., Tschudi, M., & Wood, K. (2021). Sea ice. *NOAA Technical Report OAR ARC*, 21-05. https://doi.org/10.25923/Y2WD-FN85

Minagawa, M., & Wada, E. (1984). Stepwise enrichment of ^{15}N along food chains: Further evidence and the relation between $\delta^{15}N$ and animal age. *Geochimica et Cosmochimica Acta*, *48*(5), 1135–1140. https://doi.org/10.1016/0016-7037(84)90204-7

Moore, S. E., Clarke, J. T., Okkonen, S. R., Grebmeier, J. M., Berchok, C. L., & Stafford, K. M. (2022). Changes in gray whale phenology and distribution related to prey variability and ocean biophysics in the northern Bering and eastern Chukchi seas. *PLOS ONE*, *17*(4), e0265934. https://doi.org/10.1371/journal.pone.0265934

Moore, S. E., & Stabeno, P. J. (2015). Synthesis of Arctic Research (SOAR) in marine ecosystems of the Pacific Arctic. *Progress in Oceanography*, *136*, 1–11. https://doi.org/10.1016/j.pocean.2015.05.017

Moosmann, M., Cuenca-Cambronero, M., De Lisle, S., Greenway, R., Hudson, C. M., Lürig, M. D., & Matthews, B. (2021). On the evolution of trophic position. *Ecology Letters*, *24*(12), 2549–2562. https://doi.org/10.1111/ele.13888

Mueter, F. J., & Litzow, M. A. (2008). Sea ice retreat alters the biogeography of the Bering Sea continental shelf. *Ecological Applications*, *18*(2), 309–320. https://doi.org/10.1890/07-0564.1

Newsome, S. D., Martinez del Rio, C., Bearhop, S., & Phillips, D. L. (2007). A niche for isotopic ecology. *Frontiers in Ecology and Environment*, *5*(8), 429–436.

Nobre, C., & Vagle, S. (2019a). Canada's Three Oceans (C3O) Conductivity, Temperature, Depth (CTD) data collected from the Sir Wilfrid Laurier, Barrow Canyon, Chukchi Sea, 2015. *Arctic Data Center*. https://doi.org/10.18739/A2ZW18S38

Nobre, C., & Vagle, S. (2019b). Canada's Three Oceans (C3O) Conductivity, Temperature, Depth (CTD) data collected from the Sir Wilfrid Laurier, Southern Chukchi Sea, 2014. *Arctic Data Center.* https://doi.org/10.18739/A20V89H3Q

North, C. A., Lovvorn, J. R., Kolts, J. M., Brooks, M. L., Cooper, L. W., & Grebmeier, J. M. (2014). Deposit-feeder diets in the Bering Sea: Potential

effects of climatic loss of sea ice-related microalgal blooms. *Ecological Applications*, *26*(4), 1525–1542.

Parker, P. L. (1964). The biogeochemistry of the stable isotopes of carbon in a marine bay. *Geochimica et Cosmochimica Acta*, *28*(7), 1155–1164. https://doi.org/10.1016/0016-7037(64)90067-5

Perkins, M. J., McDonald, R. A., van Veen, F. J. F., Kelly, S. D., Rees, G., & Bearhop, S. (2014). Application of nitrogen and carbon stable isotopes ($\delta^{15}N$ and $\delta^{13}C$) to quantify food chain length and trophic structure. *PLoS ONE*, *9*(3), e93281. https://doi.org/10.1371/journal.pone.0093281

Peterson, B. J. (1999). Stable isotopes as tracers of organic matter input and transfer in benthic food webs: A review. *Acta Oecologica*, *20*(4), 479–487. https://doi.org/10.1016/S1146-609X(99)00120-4

Peterson, B. J., & Fry, B. (1987). Stable isotopes in ecosystem studies. *Annual Review of Ecology and Systematics*, *18*(1), 293–320. https://doi.org/10.1146/annurev.es.18.110187.001453

Phillips, D. L., Inger, R., Bearhop, S., Jackson, A. L., Moore, J. W., Parnell, A. C., Semmens, B. X., & Ward, E. J. (2014). Best practices for use of stable isotope mixing models in food-web studies. *Canadian Journal of Zoology*, *92*(10), 823–835. https://doi.org/10.1139/cjz-2014-0127

Post, D. M. (2002). Using stable isotopes to estimate trophic position: Models, methods, and assumptions. *Ecology*, *83*(3), 703–718. https://doi.org/10.1890/0012-9658(2002)083[0703:USITET]2.0.CO;2

Post, D. M., Layman, C. A., Arrington, D. A., Takimoto, G., Quattrochi, J., & Montaña, C. G. (2007). Getting to the fat of the matter: Models, methods and assumptions for dealing with lipids in stable isotope analyses. *Oecologia*, *152*(1), 179–189. https://doi.org/10.1007/s00442-006-0630-x

Quezada-Romegialli, C., Andrew L. Jackson, & Harrod, C. (2019). *tRophicPosition: Bayesian trophic position calculation with stable isotopes* (R package version 0.7.7). https://CRAN.R-project.org/package=tRophicPosition

R Core Team. (2022). *R: A language and environment for statistical computing*. R Foundation for Statistical Computing. https://www.R-project.org/

Ricklefs, R. E. (2010). Evolutionary diversification, coevolution between populations and their antagonists, and the filling of niche space. *Proceedings of the National Academy of Sciences*, *107*(4), 1265–1272. https://doi.org/10.1073/pnas.0913626107

Rooney, N., & McCann, K. S. (2012). Integrating food web diversity, structure and stability. *Trends in Ecology & Evolution*, *27*(1), 40–46. https://doi.org/10.1016/j.tree.2011.09.001

Sánchez, F., & Olaso, I. (2004). Effects of fisheries on the Cantabrian Sea shelf ecosystem. *Ecological Modelling*, *172*(2–4), 151–174. https://doi.org/10.1016/j.ecolmodel.2003.09.005

Schlacher, T. A., & Connolly, R. M. (2014). Effects of acid treatment on carbon and nitrogen stable isotope ratios in ecological samples: A review and synthesis.

Methods in Ecology and Evolution, *5*(6), 541–550. https://doi.org/10.1111/2041-210X.12183

Schlitzer, R. (2022). *Ocean Data View*. https://odv.awi.de

Schumacher, J. D., Aagaard, K., Pease, C. H., & Tripp, R. B. (1983). Effects of a shelf polynya on flow and water properties in the northern Bering Sea. *Journal of Geophysical Research*, *88*(C5), 2723. https://doi.org/10.1029/JC088iC05p02723

Shapiro, S. S., & Wilk, M. B. (1965). An analysis of variance test for normality (complete samples). *Biometrika*, *52*(3–4), 591–611. https://doi.org/10.1093/biomet/52.3-4.591

Siddon, E. C., Zador, S. G., & Hunt, G. L. (2020). Ecological responses to climate perturbations and minimal sea ice in the northern Bering Sea. *Deep Sea Research Part II: Topical Studies in Oceanography*, *181–182*, 104914. https://doi.org/10.1016/j.dsr2.2020.104914

Stabeno, P., Kachel, N., Ladd, C., & Woodgate, R. (2018). Flow patterns in the Eastern Chukchi Sea: 2010–2015. *Journal of Geophysical Research: Oceans*, *123*(2), 1177–1195. https://doi.org/10.1002/2017JC013135

Stoker, S. W. (1978). *Benthic invertebrate macrofauna of the Eastern Continental shelf of the Bering and Chukchi Seas* [Doctoral dissertation, University of Alaska Fairbanks]. http://hdl.handle.net/11122/5290

Stuecker, M. F., Bitz, C. M., Armour, K. C., Proistosescu, C., Kang, S. M., Xie, S.-P., Kim, D., McGregor, S., Zhang, W., Zhao, S., Cai, W., Dong, Y., & Jin, F.-F.

(2018). Polar amplification dominated by local forcing and feedbacks. *Nature Climate Change*, *8*(12), 1076–1081. https://doi.org/10.1038/s41558-018-0339-y

Syväranta, J., Lensu, A., Marjomäki, T. J., Oksanen, S., & Jones, R. I. (2013). An empirical evaluation of the utility of convex hull and standard ellipse areas for assessing population niche widths from stable isotope data. *PLoS ONE*, *8*(2), e56094. https://doi.org/10.1371/journal.pone.0056094

Takimoto, G., & Post, D. M. (2013). Environmental determinants of food-chain length: A meta-analysis. *Ecological Research*, *28*(5), 675–681. https://doi.org/10.1007/s11284-012-0943-7

Tamelander, T., Søreide, J. E., Hop, H., & Carroll, M. L. (2006). Fractionation of stable isotopes in the Arctic marine copepod *Calanus glacialis*: Effects on the isotopic composition of marine particulate organic matter. *Journal of Experimental Marine Biology and Ecology*, *333*(2), 231–240. https://doi.org/10.1016/j.jembe.2006.01.001

Tanaka, T., Guo, L., Deal, C., Tanaka, N., Whitledge, T., & Murata, A. (2004). N deficiency in a well-oxygenated cold bottom water over the Bering Sea shelf: Influence of sedimentary denitrification. *Continental Shelf Research*, *24*(12), 1271–1283. https://doi.org/10.1016/j.csr.2004.04.004

Thoman, R. L., Bhatt, U. S., Bieniek, P. A., Brettschneider, B. R., Brubaker, M., Danielson, S. L., Labe, Z., Lader, R., Meier, W. N., Sheffield, G., & Walsh, J. E. (2020). The record low Bering Sea ice extent in 2018: Context, impacts,

and an assessment of the role of anthropogenic climate change. *Bulletin of the American Meteorological Society*, *101*(1), S53–S58. https://doi.org/10.1175/BAMS-D-19-0175.1

Tibshirani, R., Walther, G., & Hastie, T. (2001). Estimating the number of clusters in a data set via the gap statistic. *Journal of the Royal Statistical Society*, *63*(2), 411–423.

Tieszen, L. L., Boutton, T. W., Tesdahl, K. G., & Slade, N. A. (1983). Fractionation and turnover of stable carbon isotopes in animal tissues: Implications for $\delta^{13}C$ analysis of diet. *Oecologia*, *57*(1/2), 32–37.

Tu, K., Blanchard, A., Iken, K., & Horstmann-Dehn, L. (2015). Small-scale spatial variability in benthic food webs in the northeastern Chukchi Sea. *Marine Ecology Progress Series*, *528*, 19–37. https://doi.org/10.3354/meps11216

van de Schoot, R., Depaoli, S., King, R., Kramer, B., Märtens, K., Tadesse, M. G., Vannucci, M., Gelman, A., Veen, D., Willemsen, J., & Yau, C. (2021). Bayesian statistics and modelling. *Nature Reviews Methods Primers*, *1*(1), 1. https://doi.org/10.1038/s43586-020-00001-2

Vaudo, J., & Heithaus, M. (2011). Dietary niche overlap in a nearshore elasmobranch mesopredator community. *Marine Ecology Progress Series*, *425*, 247–260. https://doi.org/10.3354/meps08988

Villamarín, F., Jardine, T. D., Bunn, S. E., Marioni, B., & Magnusson, W. E. (2018). Body size is more important than diet in determining stable-isotope estimates

of trophic position in crocodilians. *Scientific Reports*, *8*(1), 2020. https://doi.org/10.1038/s41598-018-19918-6

Waga, H., Hirawake, T., & Grebmeier, J. M. (2020). Recent change in benthic macrofaunal community composition in relation to physical forcing in the Pacific Arctic. *Polar Biology*, *43*(4), 285–294. https://doi.org/10.1007/s00300-020-02632-3

Waga, H., Hirawake, T., & Nakaoka, M. (2021). Influences of size structure and post-bloom supply of phytoplankton on body size variations in a common Pacific Arctic bivalve (Macoma calcarea). *Polar Science*, *27*, 100554. https://doi.org/10.1016/j.polar.2020.100554

Walsh, J. J., McRoy, C. P., Coachman, L. K., Goering, J. J., Nihoul, J. J., Whitledge, T. E., Blackburn, T. H., Parker, P. L., Wirick, C. D., Shuert, P. G., Grebmeier, J. M., Springer, A. M., Tripp, R. D., Hansell, D. A., Djenidi, S., Deleersnijder, E., Henriksen, K., Lund, B. A., Andersen, P., … Dean, K. (1989). Carbon and nitrogen cycling within the Bering/Chukchi Seas: Source regions for organic matter effecting AOU demands of the Arctic Ocean. *Progress in Oceanography*, *22*(4), 277–359. https://doi.org/10.1016/0079-6611(89)90006-2

Warry, F. Y., Reich, P., Cook, P. L. M., Mac Nally, R., Thomson, J. R., & Woodland, R. J. (2016). Nitrogen loads influence trophic organization of estuarine fish assemblages. *Functional Ecology*, *30*(10), 1723–1733. https://doi.org/10.1111/1365-2435.12647

Weigand, A. C., Lange, D., & Rauschenberger, M. (2021). How can small data sets be clustered?. *Mensch und Computer 2021-Workshopband*. https://doi.org/10.18420/MUC2021-MCI-WS02-284

Wood, H. L., Spicer, J. I., Lowe, D. M., & Widdicombe, S. (2010). Interaction of ocean acidification and temperature; the high cost of survival in the brittlestar *Ophiura ophiura*. *Marine Biology*, *157*(9), 2001–2013. https://doi.org/10.1007/s00227-010-1469-6

Woodgate, R. A. (2005). Revising the Bering Strait freshwater flux into the Arctic Ocean. *Geophysical Research Letters*, *32*(2), L02602. https://doi.org/10.1029/2004GL021747

Woodgate, R. A. (2018). Increases in the Pacific inflow to the Arctic from 1990 to 2015, and insights into seasonal trends and driving mechanisms from year-round Bering Strait mooring data. *Progress in Oceanography*, *160*, 124–154. https://doi.org/10.1016/j.pocean.2017.12.007

Woodgate, R. A., Stafford, K., & Prahl, F. (2015). A synthesis of year-round interdisciplinary mooring measurements in the Bering Strait (1990–2014) and the RUSALCA years (2004–2011). *Oceanography*, *28*(3), 46–67. https://doi.org/10.5670/oceanog.2015.57

Wright, K., YiLan, L., & RuTong, Z. (2022). *clustertend: Check the Clustering Tendency* [R package version 1.6]. https://CRAN.R-project.org/package=clustertend

Wyllie-Echeverria, T., & Wooster, W. S. (1998). Year-to-year variations in Bering Sea ice cover and some consequences for fish distributions. *Fisheries Oceanography*, *7*(2), 159–170. https://doi.org/10.1046/j.1365-2419.1998.00058.x

Zheng, Z., Wei, H., Luo, X., & Zhao, W. (2021). Mechanisms of persistent high primary production during the growing season in the Chukchi Sea. *Ecosystems*, *24*(4), 891–910. https://doi.org/10.1007/s10021-020-00559-8

Zhuang, Y., Jin, H., Cai, W., Li, H., Qi, D., & Chen, J. (2022). Extreme nitrate deficits in the Western Arctic Ocean: Origin, decadal changes, and implications for denitrification on a Polar marginal shelf. *Global Biogeochemical Cycles*, *36*(7). https://doi.org/10.1029/2022GB007304

Zinkann, A.-C., Wooller, M. J., Leigh, M. B., Danielson, S., Gibson, G., & Iken, K. (2022). Depth distribution of organic carbon sources in Arctic Chukchi Sea sediments. *Deep Sea Research Part II: Topical Studies in Oceanography*, *199*, 105076. https://doi.org/10.1016/j.dsr2.2022.105076